REGULATION OF TOLL-LIKE RECEPTOR 9 BY THE HEAT SHOCK PROTEIN GP96 AND PROTEOLYTIC CLEAVAGE

A Dissertation

Presented to the Faculty of the Graduate School

of Cornell University

In Partial Fulfillment of the Requirements for the Degree of

Doctor of Philosophy

by

James Christopher Brooks

May 2012

REGULATION OF TOLL-LIKE RECEPTOR 9 BY THE HEAT SHOCK PROTEIN GP96 AND PROTEOLYTIC CLEAVAGE

James Christopher Brooks, Ph. D.

Cornell University 2012

Toll-like receptors (TLRs) represent the innate immune system's first line of defense against invading pathogens. TLRs are germline encoded type I transmembrane proteins that recognize pathogen associated molecular patterns (PAMPs) which tend to define broad classes of pathogens. TLRs exhibit both surface and intracellular localization. This global cellular distribution of receptors facilitates detection of PAMPs expressed on the surface of foreign organisms or encapsulated within them. In the case of nucleic acid-sensing TLRs, this distribution is also a regulatory mechanism, protecting the host from harmful response to self-nucleic acids. TLR9 primarily detects microbial DNA, however, when self-DNA is in complex with HMGB1, anti-nuclear antibodies, or an antimicrobial peptide such as LL37, it is delivered to TLR9 in endosomes and can elicit inflammatory pathology.

In this dissertation, I investigated the roles that the heat shock protein gp96 and proteolytic cleavage play in regulating TLR9 trafficking and signaling. gp96 was known to be essential for proper folding of TLRs, including TLR9, in the endoplasmic reticulum. However, treatment with a novel gp96 inhibitor, WS13, suppressed CpG

DNA induced NF-κB activation, MAP kinase ERK phosphorylation, and TNF-α secretion, indicating additional roles for gp96 in TLR9 biology. TLR9 and gp96 were found associated in the lysosomes of stably transfected HEK293 cells. Inhibition of gp96 caused proteolytic cleaveage of TLR9 to an 80 kD form identical in molecular weight to the proposed mature form of this receptor, however, signaling was inhibited under these conditions. Furthermore, proteolytic cleavage is not universal among all cell types. Induction of proteolytic cleavage in HEK293 cells, which do not normally generate the 80 kD mature form of TLR9, inhibited CpG DNA-induced NF-κB activation. A retroviral construct analogous to the mature form of TLR9 failed to reconstitute CpG DNA induced responses in HEK293, macrophages and dendritic cells. This inability to respond to CpG DNA correlates with an inability to traffic outside the ER compartment.

In summary, this dissertation explores the regulation of TLR9 signaling by gp96 and proteolytic cleavage. Better understanding of the mechanisms which regulate TLR9 signaling may result in new drug targets for the treatment of autoimmune diseases.

BIOGRAPHICAL SKETCH

James Christopher Brooks was born on May 13th, 1983 in Philadelphia, Pennsylvania. He attended Red Creek Jr/Sr High School in central New York where his interest in the biological sciences began thanks to a very talented teacher named Dr. Henry Spang. James graduated ranked 6th in his class in May of 2001 and moved on to attend college at the Rochester Institute of Technology. While there he was exposed to many great educators and fell in love with the field of immunology while on his way to graduating in 2005 with a B.S. in biotechnology. James came to Cornell to pursue a Ph.D. in immunology in the summer of 2005 and joined the lab of Dr. Cynthia Leifer early in 2006. While in Dr. Leifer's lab he has studied the regulation of TLR9 by the heat shock protein gp96 and proteolytic cleavage and earned his Ph.D. in early 2012.

This thesis is dedicated to my wife Erika whose constant love and support helped me to achieve my goals; and to my daughter Hannah who has taught me the true meaning of strength and determination.

ACKNOWLEDGMENTS

I would like to thank my family for their support and patience during my graduate education. This process has affected everyone in my life at some point and I would be remiss to not thank them for helping me pick myself up and push through the difficult times to achieve my goals. I don't think my wife (then girlfriend) Erika had any idea what she was getting herself into when I told her that I was going to pursue my Ph.D. but she stood by me and married me anyway. She has always helped me keep things in perspective and never let me forget who I am.

I would like to thank my advisor Dr. Cynthia Leifer who pushed me to be the best that I could be. Cindy has a way of making you want to be better and she never let me doubt that I earned the right to be at this institution and be awarded a Ph.D. The rest of the Leifer Lab, past and present, has always been a great group of people to work with. Jody Cameron has been equal parts therapist and friend for me over the years. Dr. Bill Rose was an amazing source of advice and information as well as a friend and sympathetic ear in our efforts to find gainful employment. Dr. Chia-hsin Ju was the best comrade in arms that I could have asked for during our time at Cornell and I will always have fond memories of our time in the Leifer Lab with both her and everyone else.

There are too many people and too little space to thank everyone individually but I remember, and appreciate, everything that everyone has done to help me over the last 7 years, so thank you all.

TABLE OF CONTENTS

LIST OF FIGURES

LIST OF TABLES

CHAPTER 1:

INTRODUCTION*

***** Portions reprinted from Cynthia A. Leifer and James C Brooks "Regulation of Nucleic Acid Sensing Toll-like Receptors in Systemic Lupus Erythematosus", **Systemic Lupus Erythematosus**. Edited by Hani Almoallim. Intech ISBN 978-953-307-868-7. *Copyright 2011*.

Innate Immunity

The mammalian immune system is an amazing product of evolution with the ability to theoretically recognize every possible antigen that could be expressed by a pathogen. The recombination of genes allows for the generation of T cell receptors or antibodies with a multitude of specificities, and this is known as the adaptive immune system. As with all things in life there are consequences, and the major consequence of utilizing a system as intricate and precise as the adaptive immune system is the amount of time that is necessary to generate a response through it. The response via the adaptive immune system upon primary exposure to an antigen reaches its peak at seven to ten days. When the generation time of most pathogens can be measured in minutes to hours, the host would be overwhelmed by the sheer number of microbes it must control before the adaptive immune response could be fully engaged. The solution to this problem is a second arm of the immune system termed the innate immune system. The innate immune system responds to the threat of a pathogen immediately and serves as a method of controlling pathogens until the adaptive immune system is able to sufficiently respond.

While the adaptive immune system utilizes B and T cell receptors and antibodies as its main methods of pathogen recognition, the innate immune system utilizes pattern recognition receptors (PRRs). These PRRs are germline encoded receptors that recognize conserved structures that are generally required for survival, termed pathogen associated molecular patterns (PAMPs). This germline encoding of receptors utilized by the innate immune system is in contrast to the adaptive immune system, which relies on recombination of genes to generate specificity. The fact that PAMPs are often critical for the survival of the pathogen reduces the likelihood that the pathogen will mutate them in order to avoid immune recognition. The cells of the innate immune system respond not only via direct killing of pathogens but also by secreting cytokines and chemokines important for the activation and recruitment of the cells of the adaptive immune system. One such class of PAMPs recognized by the innate immune system is nucleic acids.

Toll-like Receptors

Toll-like receptors (TLRs) are a family of innate immune receptors that directly detect molecular structures and initiate signaling. Engagement of TLRs initiates innate immune responses that promote microbial killing and antigen presentation to educate T cells and B cells. At least 10 different TLRs recognize various microbial structures such as lipopeptides (TLR1, TLR2, and TLR6) (1,2), lipopolysaccharide (TLR4) (3), bacterial flagellin (TLR5) (4), double stranded RNA (dsRNA, TLR3) (5), single stranded RNA (ssRNA, TLR7, TLR8) (6), and single stranded DNA (ssDNA, TLR9) (7). TLRs are type I transmembrane receptors with C-termini facing the cytoplasm of the cell and ectodomains either at the cell surface or in the lumen of intracellular compartments. The

cytoplasmic domain has homology with the IL-1 and IL-18 receptors and has been called the Toll/IL-1-like receptor domain (TIR). The three-dimensional structures of two TLR cytoplasmic TIR domains have been solved and are globular with many surfaces for protein-protein interactions (8). The TIR domain associates with several adapter proteins that initiate signal transduction. These adapters include myeloid differentiation factor 88 (MyD88), and TIR-domain-containing adapter-inducing interferon-β (TRIF, also known as MyD88 adapter-like, MAL), which promote production of proinflammatory cytokines and type I interferons. The ectodomain is composed of a series of leucine rich repeats that form a curved solenoid (Figure 1.1). Alignment studies predicted a model structure for the ectodomains of TLRs (9), which was supported by crystallographic studies (10-15). TLRs are expressed on a wide variety of cell types including B cells, T cells, dendritic cells, macrophages, and intestinal epithelial cells, although different cell types have unique repertoires of TLR expression (16). For example, human plasmacytoid dendritic cells express the nucleic acid-sensing TLRs, TLR7 and TLR9.

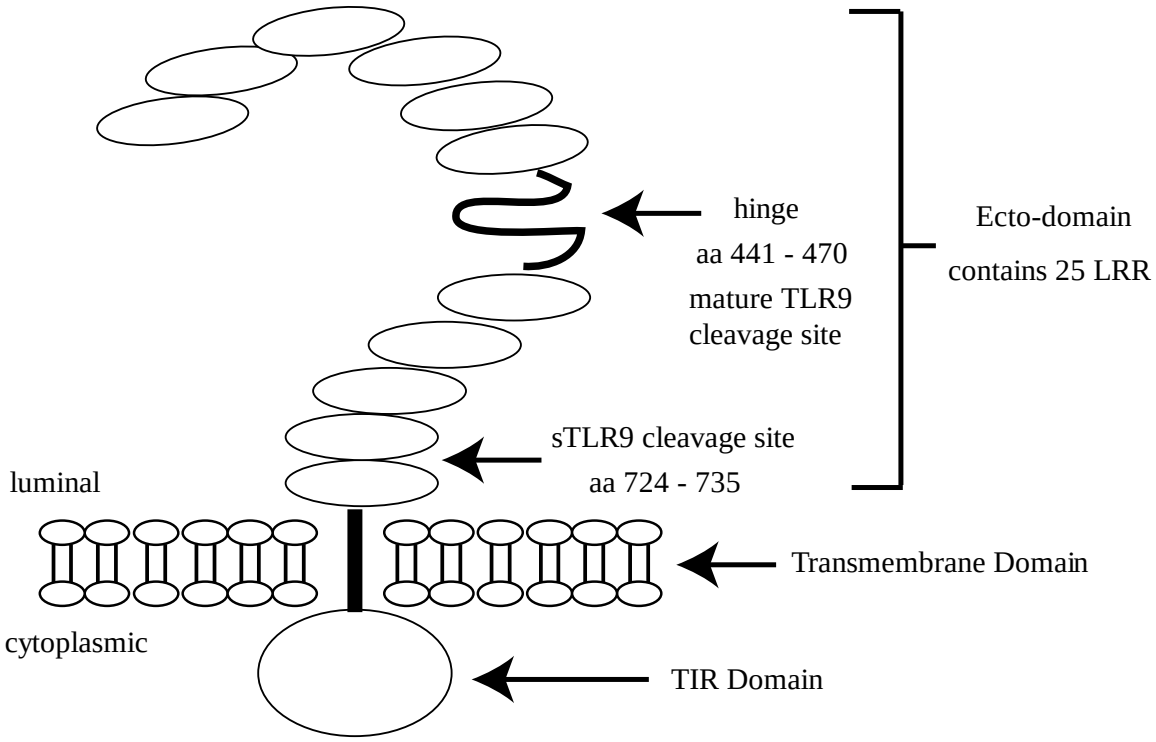

Figure 1.1. Model of TLR9 structure. TLR9 is composed of a lumen-facing ecto-domain made of 25 leucine-rich repeats (LRR), a transmembrane domain, and a cytosolic TIR domain used to bind and transduce signals through adaptor proteins. The ecto-domain contains two known sites of proteolytic cleavage, one between aa 441 and 470 and a second between aa 724 and 735 resulting in mature TLR9 and soluble TLR9, respectively.

Nucleic Acids as PAMPs

Response to DNA, the response is dependent on a 5'-cytosine-guanosine-3' dinucleotide (CpG). The cytosine must be unmethylated, and is active when surrounded by specific bases, which together form the CpG motif (17). These CpG motifs are rare in vertebrate DNA due to reduced frequency of the CG dinucleotide (CpG suppression) and increased frequency of cytosine methylation (18-20). CpG motifs are present and functional in bacterial DNA, in plasmid DNA produced in bacteria, and in synthetic DNA. Variation of sequence and physical structure of synthetic DNAs have resulted in characterization of least four types of CpG oligodeoxynucleotides each with different activity on cells. Three are stimulatory, and one is inhibitory (21-23). Inhibitory DNAs do not require a CpG motif and the mechanism of inhibition has not been clearly defined (21,24,25). A recent report indicates that these inhibitory DNAs may function through preferentially binding to the mature form of TLR9 to inhibit the binding of stimulatory DNA (26). However, it seems unlikely that the mechanism can be contributed solely to competition as the response of RAW 264.7 macrophages to stimulatory DNA was inhibited by fifty percent by a ten-fold lower concentration of inhibitory DNA (27). Type A CpG DNAs (also called D) induce robust type I interferon production, while type B CpG DNAs (also called K) induce B cell proliferation and proinflammatory cytokine production (22). Type C CpG DNAs have properties of both type A and type B CpG DNAs and thus induce both types of cellular responses (28).

Regardless of their class, CpG DNAs require endocytosis and acidification of endosomes for activity. Blockade of uptake by immobilization of the CpG DNA on beads inhibits the

B cell proliferative activity of synthetic CpG DNAs (29). Inhibition of endosomal acidification blocks CpG DNA-induced cytokine release by macrophages (30). Furthermore, cellular activation by CpG DNA initiates on endosomes (31). Vertebrate DNAs are poorly internalized, which contributes to their poor stimulatory activity. However, vertebrate DNA is stimulatory when in complex with proteins such as high mobility group box 1 (HMGB1), the antimicrobial peptide LL37, or anti-DNA antibodies (32-34). Whether the CpG DNA induces proinflammatory cytokines or type I interferon also depends on the endosomal compartment where the DNA is retained (35). Honda and colleagues demonstrated that different types of DNA are trafficked to and retained within different endosomal compartments in plasmacytoid dendritic cells. For example, the type I interferon inducing CpG DNAs (type A) rapidly co-localized with FITC-dextran, a marker for early endosomes, but failed to co-localize with lysosomal markers (35). In contrast, rapid localization with lysosomal markers correlated with proinflammatory cytokine production induced by type B CpG DNAs (35). In another study the outcome of cellular responses to the DNA types could be swapped by changing the physical and chemical properties of the DNA (36). Multimerization of type B CpG DNAs, so that their physical structure resembled type A CpG DNAs, caused them to be retained in early endosomes and induce A-type responses. Response of B cells was also dependent on CpG DNA type and delivery mechanism (37). These studies strongly correlated location of DNA detection with cellular outcome and suggested that manipulation of localization and receptor recognition could change the outcome of cellular response.

At concentrations of CpG DNA used by many investigators, uptake occurs by fluid phase

endocytosis. Uptake of CpG DNA reached a plateau at 2 hours, was slowed at low temperature, and was inhibited by known endocytosis inhibitors such as sodium azide and cytochalasin B (38). Yet, at lower concentrations, uptake was significantly more efficient, which indicated that the CpG DNA was internalized by receptor-mediated endocytosis. Using radiolabeled cells, multiple groups demonstrated specific DNA binding proteins that likely assisted in internalization and trafficking of CpG DNA to the correct endosomal compartment where it encountered TLR9 (38,39). However, the identity of these receptors remains unknown. During the internalization process, CpG DNA transits though both early and late endosomes, which is important because, as mentioned above, CpG DNAs trigger different cellular outcomes depending on the compartment where signaling initiates.

Internalization of both CpG and host DNA is facilitated by several host proteins such as high mobility group protein 1 (HMGB-1), the antimicrobial peptide LL37, and antibodies. The cationic antimicrobial peptide LL37 was highly elevated in the skin of patients with psoriasis (33). LL37 formed a stable complex with host DNA, and induced a TLR9-dependent, DNase-sensitive, type I interferon response from human plasmacytoid dendritic cells. The nuclear factor HMGB1 is retained within cells under normal conditions, but cell death and inflammation releases HMGB1, which formed a stable complex with host DNA. Association of CpG DNA-A with HMGB1 dramatically enhanced production of type I interferon (32). In fact, HMGB1 was found in immune complexes with host DNA. Immune complexes from Systemic Lupus Erythematosus (SLE) patient serum were enriched in CG content within the DNA, consistent with

increased presence of potential stimulatory motifs (40).

Nucleic acid-sensing TLRs detection of self-ligands

Complexes with DNA bound to anti-idiotype B cell receptors (rheumatoid factor) and to Fc receptors to mediate internalization (34,41). Synergistic cytokine production and autoantibody induction by enhanced uptake of DNA-containing immune complexes likely contributes to the induction and propagation of anti-nucleic acid antibody production so frequently observed in SLE. Altogether, these studies demonstrate that while host DNA alone is not very immunostimulatory, association with a variety of different proteins, present in disease states, promotes endosomal uptake where the DNA can associate with TLRs and induce pathologic interferon responses. By either mechanism the uptake was very efficient and delivered the complexes to the endosomal compartment.

When the stimulatory activity of CpG DNA was first described, it was thought to represent microbial DNA and that self-DNA was non-stimulatory. This was due to the requirement for the central CG dinucleotide, unmethylation of the C, and the selectivity for surrounding bases. These arguments held for many years, however, the mammalian genome has the potential to induce TLR9-mediated responses (42,43). Many studies, including the ones reviewed below, have been focused on understanding what regulates TLR9 mediated responses and why self-DNA is not normally detected. However, recent studies suggest that TLR9 signaling is important for normal responses like wound repair (44-46).

Cells go to great lengths to assure that DNA is not released into the extracellular milieu when they die by condensing and digesting their DNA during apoptosis. However, necrosis and neutrophil extracellular trap (NET) formation intentionally releases DNA that can induce inflammatory responses (47-49). Interestingly, SLE neutrophils were primed by high type I interferon levels in vivo, and in response to immune complexes, the neutrophils from SLE patients generated NETs that had a high content of DNA, LL37 and HMGB1. These proteins protected the DNA from degradation and facilitated internalization, and thereby increased the inflammatory potential of the host DNA. Therefore, since it is purposefully released under certain conditions, there must be other regulatory mechanisms to avoid response to host DNA. DNase is present in serum and in the extracellular environment and degrades potentially stimulatory host DNA. DNase deficient mice were born healthy but develop lupus-like disease at about six months of age (50). Heterozygous mice have increased serum concentrations of anti-nuclear antibodies, and increased glomerulonephritis. However, in homozygous DNase-deficient mice, these SLE parameters were even higher. Mutations in DNase have been identified in SLE patients (51), and, together, these studies suggest that DNase is an important enzyme to prevent response to host DNA.

Interestingly, recent studies have shown that detection of self-DNA may be a normal biological process, and is, in fact, critical for wound healing (45,46). In the absence of TLR9, full thickness biopsy wound healing was delayed, and application of CpG DNA, in wild-type mice, enhanced healing in a TLR9 dependent manner (45). These data suggest that TLR9 plays an important role in wound healing. In a different model, tape stripping-induced epidermal injury caused plasmacytoid dendritic cell and neutrophil

infiltration (44). This response was accompanied by production of type I interferon, and was dependent on the signaling adapter molecule MyD88. Treatment of wild-type mice with a TLR7-TLR9 inhibitor reduced the response, implicating these TLRs in the process. In lupus-prone mice, the same tape-stripping procedure led to chronic wounds with a type I interferon signature that resembled SLE skin lesions. Therefore, detection of DNA and RNA by TLR9 and TLR7 is important for normal wound healing. Dysregulation of this pathway in SLE likely contributes to autoimmune inflammation, especially in the skin, and is a potential target for therapeutic intervention.

Compartmentalization of TLR9

Infectious agents replicate in various locations outside and inside cells. Bacteria and viruses are internalized into endosomes, and some can escape into the cytoplasm. Therefore, positioning of TLRs is important for detecting components of microbes in the varied locations where they can reside. Some TLRs, such as TLR2, TLR4, and TLR5, are expressed at the cell surface to detect ligands expressed on the surface of bacteria (lipopolysaccharide, TLR4; lipopeptides, TLR2; and flagellin, TLR5). However, nucleic acids, such as DNA and RNA, are encapsulated within bacteria and viruses, and are only released upon internalization into endosomes. To accommodate this, nucleic acid sensing TLRs are localized intracellularly. For example, TLR9 is primarily found in the endoplasmic reticulum (ER) of resting cells (52,53) where it colocalizes with ER, and not endosomal, markers. Since detection of DNA occurs in endosomes, these data suggest that that there is an induced trafficking event that leads to TLR9 entry into this compartment (53). The unique compartmentalization of nucleic acid-sensing TLRs has

been proposed as a major regulatory mechanism to prevent response to host DNA (54). Fusion of the ectodomain of TLR9 with the transmembrane domain and cytoplasmic tail of TLR4 created a protein that localized to the cell surface. This change in localization endowed the TLR9 ectodomain with the ability to respond to host DNA (54). These data support a model where TLR9 is specifically trafficked intracellularly to avoid access to the extracellular milieu, thereby preventing recognition of host DNA.

Trafficking of TLR9 through the Golgi to localize in the endolysosomes

While TLR9 predominantly resides in the ER it must traffic to the endosomal compartment where it encounters endocytosed CpG DNA (52,53). Normally, transmembrane or secreted proteins synthesized in the ER traffic through the Golgi to access the cell surface or intracellular endosomes. However, TLR9 was found to be sensitive to endoglycosidase H (endo H) treatment, which indicated that TLR9 had not reached the Golgi (52). In 2009 Chockalingam et al., showed that Brefeldin A inhibited TLR9 response to CpG DNA (55). Since Brefeldin A is a small molecule that inhibits transport of proteins from ER to Golgi, TLR9 signaling appeared to be dependent on Golgi trafficking.

When proteins traffic through the Golgi, the high mannose glycans are processed to hybrid forms that are still cleaved by Endo H; therefore, highly specific lectins were used to determine whether TLR9 had glycan modifications indicative of Golgi transit (55). Lectins are plant proteins that selectively recognize carbohydrate structures. For example, *Datura stramonium* (DS) lectin specifically recognizes "Galβ1→4GlcNac" structures

present only on proteins that have been processed by Golgi resident enzymes. DS lectin bound to TLR9, which confirmed that TLR9 trafficked through the Golgi during synthesis (55). TLR9 immunoprecipitated from the lysosomal compartment of HEK293 cells also bound DS lectin, and co-immunoprecipitated with the signaling adapter MyD88 (55). These data indicated that lysosomal TLR9 had transited through the Golgi and contributed to signaling.

Proteins that regulate intracellular localization and trafficking

Several proteins are critical for TLR9 trafficking both out of the ER and to the endosomal compartment (Figure 1.2): UNC93B1, adapter protein 3 (AP3), a protein associated with TLR4 (PRAT4A), Slc15a4, and glycoprotein 96 (gp96, also known as glucose regulated protein 94 (gp94). Wild-type mice exposed to recessive N-ethyl-N-nitrosourea-induced mutagenesis were screened for the ability to respond to TLR ligands and revealed a mouse line that lacked response to TLR3, TLR7, and TLR9 ligands. These mice had a single point mutation (H412R) in UNC93B1 (56). In dendritic cells from these mice, TLR7 and TLR9 did not localize to the endosomal compartment (57). Interestingly, UNC93B1 seems to play opposing roles in regulation of TLR7 and TLR9 (58). Reconstitution of UNC93B1 deficient cells with UNC93B1 containing a single point mutation (D34A) resulted in hyperresponsivenss to TLR7, yet hyporesponsiveness to TLR9, ligands. Therefore, the role of UNC93B1 in regulation of nucleic acid sensing TLRs is clearly important, and interfering with UNC93B1 function has different effects on signaling by different TLRs.

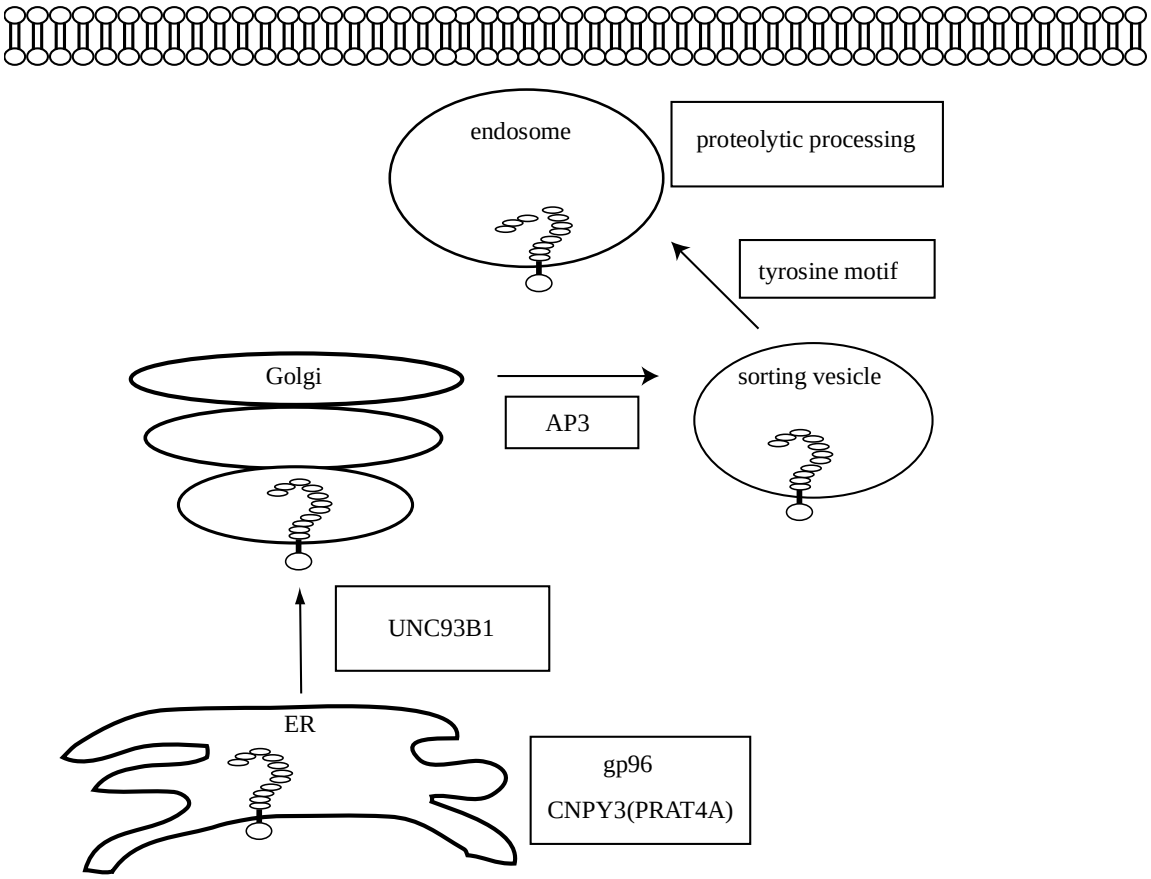

Figure 1.2. Regulation of TLR9 trafficking. After synthesis in the ER, TLR9 associates with gp96. TLR9 traffics out of the ER to the Golgi in a manner dependent on gp96, PRAT4A, and UNC93B1. TLR9 traffics from the Golgi to a sorting vesicle in an AP3 dependent manner where it is then sorted to the endosomal compartment via a cytoplasmic tyrosine motif. In the endosomal compartment TLR9 is proteolytically processed either active or negative regulatory forms that modulate TLR9 signaling.

Two ER luminal proteins, glycoprotein 96 (gp96) and protein associated with TLR4 (PRAT4A), are essential for TLR9 exit from the ER. PRAT4A, also known as CNPY3, associated with TLR9, which depended on methionine 145 of PRAT4A (59). In the absence of PRAT4A, TLR9 did not access endosomes, and PRAT4A deficient cells lacked response through all TLRs, except TLR3 (60). The heat shock protein gp96, also called glucose-regulated protein 94 (grp94), and endoplasmin or ERP94, is the ER paralog of cytoplasmic heat shock protein 90 (Hsp90) (61-63). Similar to what is observed for other Hsps, gp96 expression is induced by the accumulation of misfolded proteins and it both binds to and hydrolyzes ATP (64,65). gp96 is essential for the proper folding of a variety of substrate proteins that include TLRs, integrins and immunoglobulins (66-70). Consistent with its role as a housekeeping protein, embryos of gp96 deficient mice only survive 5.5 days (71). gp96 directly associated with TLR9 and was required for B cell and macrophage response to CpG DNA (72). A pre-B cell line with a frame-shift mutation in gp96 was 10,000 times less sensitive to LPS then the non-mutant line, which was due to a lack of TLR4 on the cell surface (73). This study suggested that gp96 regulated trafficking of TLRs. Further studies using a mouse with macrophage specific knockout of gp96 showed that gp96 is essential for TLR9 trafficking and signaling, and was in fact a chaperone for all TLRs except TLR3 (66,72). In 2011 Liu et al., demonstrated that gp96 and PRAT4A directly interact to form a multimeric complex with TLR9 (67). This TLR9-gp96-PRAT4A multimeric complex was found to be essential for proper TLR9 folding and function, as its disruption either by shRNA or point mutation resulted in post-translational inactivation of TLR9 (67). Furthermore, co-

immunoprecipiation studies revealed that the interaction between TLR9 and gp96 was dependent on the presence of PRAT4A (67). Taken together, the data presented by Liu et al., demonstrated that PRAT4A is a cochaperone of gp96 thus explaining the phenocopy of TLR9 defects in both gp96 knockout and PRAT4A null mice (59,67,72,74).

Cytoplasmic proteins are also important for TLR9 trafficking. Plasmacytoid DCs from AP3 deficient mice failed to induce a type I interferon response after CpG DNA stimulation despite normal IL-12 production (75). AP3 is a cytosolic protein that associates with endosomes and sorts transmembrane proteins from the endosomal compartment to lysosome-related organelles (76). In the absence of AP3, TLR9 did not colocalize with markers for lysosome-related organelles (75). This group suggested that it was these lysosome-related organelles that were critical for induction of type I interferons (75). However, this conclusion contradicts previously published studies showing that initiation of signaling that results in type I interferon production occurs on early endosomes (35,36). In a separate study using the same AP3 deficient mice, both proinflammatory and type I interferon production were lost (77). Therefore, AP3 is important for TLR9-induced cytokine production, but its exact role in TLR9 biology remains unclear.

Recent data have shown that TLR9 signaling also depends on Slc15a4, a twelve-spanning transmembrane oligopeptide transporter that localizes to the endolysosomal compartment (77,78). Cells from Slc15a4 deficient mice lack response to nucleic acid sensing TLRs (77). Again, the specific role of Slc15a4 remains unknown, but may involve

endolysosomal transport of TLR9 or a TLR9-associated protein required for TLR9 function.

Specific motifs in TLR9 that regulate localization and trafficking

Localization of TLRs is regulated by sequences in their transmembrane domains and cytoplasmic tails. Fusion of N-terminal segments of TLR4 to the transmembrane and cytoplasmic tails of various TLRs resulted in distinct localizations of the chimeric proteins (79). For example, TLR4 by itself localized to the cell surface, and fusion of TLR4's ectodomain with the transmembrane and cytoplasmic tail of TLR1, TLR2, TLR5, or TLR6 resulted in similar localization (79). In contrast, when TLR4 was fused to the transmembrane and cytoplasmic tail of any of the nucleic acid-sensing TLRs, the resulting chimeric receptor was not detected at the cell surface (79). Further studies using different approaches identified different motifs in TLR9 responsible for this localization (54,80). TLR9's ectodomain fused to TLR4's transmembrane and cytoplasmic domains localized to the cell surface (54). Despite being localized to the cell surface the chimera retained the ability to respond to CpG DNA, yet was resistant to endosomal acidification inhibitors which normally inhibit TLR9 signaling (54,81,82). Interestingly, co-immunoprecipitation studies using chimeric proteins revealed that TLR9 associates with UNC93B1 via the transmembrane domain and this may explain, in part, the requirement for this association in TLR9 signaling (83).

In contrast, the Leifer lab in collaboration with the Segal lab identified a specific localization motif in the cytoplasmic tail of TLR9 (80). In this study, the ectodomain of

the IL-2 receptor alpha chain, which normally localized to cell surface, was fused to the transmembrane and cytoplasmic tail of different TLRs (80). A fusion with the TLR4 transmembrane and cytoplasmic tail localized to the cell surface; however, a fusion with the same regions of TLR9 did not express at the cell surface (80). Truncation analysis revealed that deletion of all but four amino acids of the cytoplasmic tail generated a protein that was robustly expressed at the cell surface, ruling out a contribution of the transmembrane domain to intracellular localization. It is unclear why these two studies showed opposite requirements for TLR9 transmembrane domain. Regardless, additional truncations and mapping identified a 14 amino acid motif that was important for TLR9 intracellular localization. Follow-up studies showed that mutation of a critical tyrosine (888) within this motif abolished proinflammatory cytokine production. Interestingly, this mutant maintained normal interferon responses suggesting that this motif is required for trafficking TLR9 to the compartment selectively required for induction of proinflammatory cytokines (84). It remains to be determined if this motif is necessary for association with AP3 or other regulatory proteins.

Proteolytic regulation of TLR9

In addition to trafficking to specific endocytic compartments, several recent studies have demonstrated that TLR9 is proteolytically processed in endosomes and that this processing regulates TLR9 function (82,85-88). The ectodomain of TLR9 contains 25 leucine rich repeats. LRR1-14 and LRR15-29 are interrupted by a region predicted to have very little secondary structure, often referred to as the hinge (9). The first described proteolytic event was mapped to this hinge region through a mass spectrometric approach

(87). The form of TLR9 generated encompasses one-half of the ectodomain and all of the transmembrane and cytoplasmic tail. This proteolytic event is inhibited by endosomal acidification inhibitors and by broad-spectrum cathepsin inhibitors (86,87). Additional studies with specific cathepsin inhibitors, and in cathepsin deficient mice, did not reveal a unique cathepsin responsible for the cleavage. This proteolytically cleaved form of TLR9 was reported to be the mature, active form of TLR9 responsible for recognition of CpG DNA (86,87). It was demonstrated that this mature form of TLR9 was able to bind CpG DNA (26,86,87). Furthermore, a retroviral construct encoding the mature form of TLR9 was sufficient to reconstitute CpG DNA induced TNF-α production in $TLR9^{-/-}$ bone marrow derived dendritic cells (87). An independent study, showed an additional proteolytic event (88). While this study did not reveal the precise location of the proteolysis, a specific enzyme, asparagine endopeptidase was shown to be important for this cleavage. A more recent study suggested that stepwise processing of TLR9 is required to attain fully functional proteolytically processed TLR9 (82). Interestingly, knockdown of either PRAT4A (CNPY3) or gp96 by shRNA targeting resulted in a loss of proteolytic processing of TLR9, and suggested that these chaperones are required for TLR9 to access endosomes (67). The Leifer lab recently showed that TLR9 is also proteolytically processed at a completely different position to generate a negative regulator of TLR9 signaling (85). This proteolytic event resulted in generation of an intact ectodomain separated from the transmembrane domain and cytoplasmic tail. This soluble form of TLR9 bound to CpG DNA, associated with full length TLR9, and inhibited responses by the full-length receptor in a dominant negative manner (85). In contrast to the proteolytic cleavage events which generate mature TLR9, we showed that

generation of soluble TLR9 occurred in cells expressing endogenous TLR9 (85). Soluble TLR9 is likely important in regulating TLR9 responses since intestinal epithelial cells poorly responded to CpG DNA and abundantly generate soluble TLR9 (85) (Figure 1.3). Therefore, correlative studies on TLR9 in different pathological conditions must account for the complexity of TLR9 post-translational modification.

Brief Outline of Dissertation Research

The global cellular distribution of TLRs facilitates detection of molecular structures expressed on the surface of foreign organisms or encapsulated within them (16), and in the case of nucleic acid-sensing TLRs, this distribution is also a regulatory mechanism, protecting the host from harmful response to self-nucleic acids such as DNA (54). However, when self-DNA is in complex with HMGB1, anti-nuclear antibodies, or an antimicrobial peptide such as LL37, it is delivered to TLR9 in endosomes and can elicit inflammatory pathology (32-34,89-92).

Based on the studies discussed above, we hypothesized that both the ER resident heat shock protein gp96 and proteolytic cleavage play critical roles in regulating the response of TLR9 to CpG DNA. In the first half of **Chapter 3** I describe data showing that gp96 regulates TLR9 stability and conformation. My results show that gp96 remains associated with TLR9 and both proteins traffic to the lysosomal compartment. Pharmacologic interference with the gp96-TLR9 interaction inhibits the response to CpG DNA. This loss in CpG DNA induced signaling is due to the increased proteolytic sensitivity of TLR9 in the absence of gp96, and suggests that TLR9 conformation is gp96 dependent.

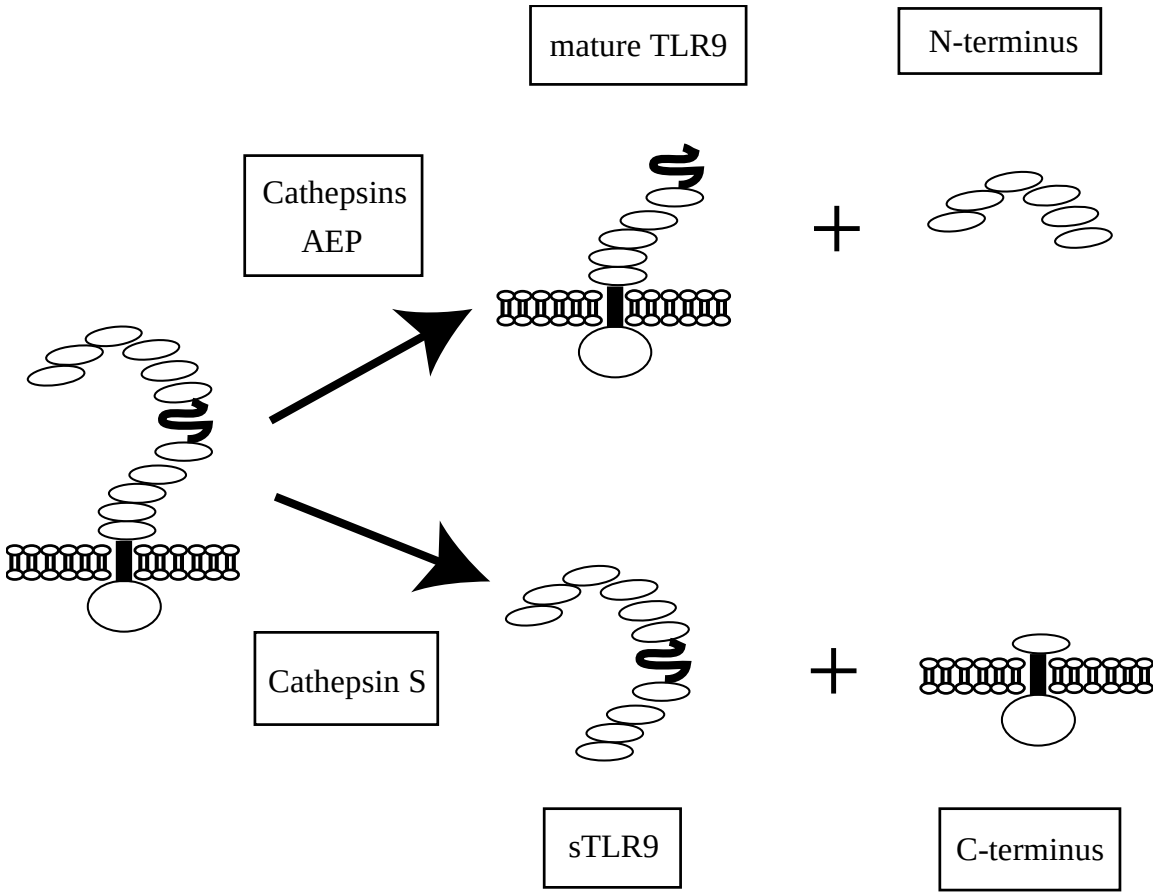

Figure 1.3. Proteolytic cleavage of TLR9. TLR9 undergoes proteolytic processing in two locations in the ectodomain. One cleavage event occurs in the hinge region and is mediated by both cathepsins and AEP; it results in the generation of the proposed active form, mature TLR9, and a remaining N-terminal fragment. An independent cleavage event occurs much closer to the transmembrane domain and generates a soluble negative regulatory form of TLR9 (sTLR9) and a C-terminal fragment.

In the second half of **Chapter 3** I describe data which show that proteolytic cleavage of TLR9 is not necessary or sufficient to support CpG DNA induced signaling events. I provide evidence that generation of the mature form of TLR9 does not directly correlate with response to CpG DNA. A retroviral construct corresponding to the mature form of TLR9 (mTLR9$^{471\text{-}1032}$-HA) fails to exit the ER, serves as a dominant negative to TLR9 signaling, and fails to reconstitute CpG DNA response in any cell type tested. In **Chapter 4** I summarize the data and propose a new model for TLR9 signaling in which gp96 interaction with TLR9 is not solely critical in the ER but is essential for protecting TLR9 from proteolytic cleavage after it traffics outside the ER compartment. Furthermore, proteolytic processing of TLR9 is neither necessary nor sufficient to reconstitute CpG DNA induced signaling in any cell type tested, challenging the current model of obligate proteolytic processing of TLR9 in order to respond to CpG DNA.. These results provide evidence for therapeutically targeting gp96 as a treatment to suppress diseases in which TLR9 signaling plays a role, such as SLE, psoriasis, or rheumatoid arthritis.

CHAPTER 2:

MATERIALS AND METHODS

Reagents and plasmids

The following antibodies and reagents were used: anti-HA for immunoprecipitation (ABM, Richmond, BC, Canada), anti-HA for immunoblotting and anti-HA conjugated to fluorescein isothiocyanate (FITC) (anti-HA FITC) for flow cytometry (Roche Applied Science, Indianapolis, IN, USA), anti-GFP (recognizes YFP) for immunoprecipitation (Invitrogen/Molecular Probes, Carlsbad, CA, USA), anti-GFP for immunoblotting and anti-TNF-α conjugated to allophycocyanin (APC) (anti-TNF-α APC) for flow cytometry (BD Clontech, Mountain View, CA, USA), anti-LAMP-1, anti-Rab 5 and anti-Calnexin (BD-transduction laboratories, San Jose, CA, USA), anti-human gp96 (Santa Cruz Biotechnology, Santa Cruz, CA, USA), anti-phosphorylated and total ERK and p38 (Cell Signaling Technology, Danvers, MA, USA), HRP conjugated anti-mouse, rat and rabbit secondary (Southern Biotech, Birmingham, AL, USA), HRP conjugated anti-goat secondary (Jackson ImmunoResearch Labs, Inc, West Grove, PA, USA), anti-tubulin (eBioscience, San Diego, CA, USA), brefeldin A (eBioscience, San Diego, CA, USA), geldanamycin (Sigma-Aldrich, St. Louis, MO, USA), poly I:C (Calbiochem, San Diego, CA, USA), CpG DNA 10104 5'-TCGTCGTTTCGTCGTTTTGTCGTT-3' and 2006 3′biotin: 5′-TCGTCGTTTTGTCGTTTTGTCGTT-3’ (Eurofins MWG Operon, Huntsville, AL, USA), mouse GM-CSF (Peprotech, Rocky Hill, NJ, USA) All plasmids were prepared using Endo free plasmid maxiprep kits (Qiagen Sciences, MD, USA). WS13, a gp96-specific Hsp90 inhibitor of the purine-scaffold class (93), was synthesized

as previously described (94,95).

Cell culture

Human Embryonic Kidney (HEK) 293 cells (ATCC #CRL-1573), HeLa (ATCC #CCL-2), RAW 264.7 cells (ATCC #TIB-71), and ØNX-Ampho cells (Orbigen, San Diego, CA, RVC-10001) were cultured in Dulbecco's modified Eagle's medium (DMEM) with 2 mM L-glutamine, 50 U ml^{-1} penicillin, 50 µg ml^{-1} streptomycin, 10 mM HEPES, 1 mM sodium pyruvate and 10% low endotoxin FBS. $TLR9^{-/-}$ macrophage cells (NIH Biodefense and Emerging Infections Research Resources Repository #NR-9569) were cultured in Dulbecco's modified Eagle's medium (DMEM) with 2 mM L-glutamine, 10 µg ml^{-1} ciprofloxacin HCl, 10 mM HEPES, 1 mM sodium pyruvate and 10% low endotoxin FBS. 70Z/3 B cells were cultured in Roswell Park Memorial Institute (RPMI) 1640 medium with 2 mM L-glutamine, 50 U ml^{-1} penicillin, 50 µg ml^{-1} streptomycin, 10 mM HEPES, 1 mM sodium pyruvate, 2.5% low endotoxin FBS and 50 µM mercaptoethanol. Cells routinely tested negative for mycoplasma.

DNA cloning

$mTLR9^{471-1032}$-HA was generated by PCR sewing using mTLR9-HA and the mouse IgκB leader sequence from pDisplay (Invitrogen) with the primers as shown in Table 2.1. A 500 base pair (bp) sequence containing the mouse IgκB leader sequence from pDisplay and 5' sequence from mTLR9, along with a 1700 bp sequence encoding 3' sequence from the mouse IgκB leader, amino acids 471-1032 of mTLR9, 3 C-terminal HA tags from mTLR9-HA with an added 5' XhoI site were cloned via PCR. A second PCR

reaction using these two products as templates was performed to "sew" the mouse IgκB leader sequence to the mTLR9 sequence. This second PCR product was digested with EcoRI, which was encoded in the PCR product containing the mouse IgκB leader sequence, and XhoI, then ligated into pcDNA3.1+ or the retroviral vector pBMN-i-GFP and verified by sequencing (Figure 2.1). mTLR9$^{441-1032}$-HA was generated by the same method using the primers as shown in Table 2.1.

HEK293 luciferase reporter assay

The luciferase reporter assay was performed as previously described (55). Briefly, HEK293 cells were transiently transfected using TransIT (Mirus, Madison, WI) with mTLR9-HA, TLR3, mTLR9$^{471-1032}$-HA, or mTLR9$^{441-1032}$-HA, 5x-NF-κB luciferase reporter and empty vector totaling 200 ng/ well of DNA for each well of a 96 well plate. Cells were pretreated for one hour with the indicated concentration of inhibitor or left untreated prior to overnight stimulation with either 1 μM CpG DNA, 5 μg/ml poly I:C or 100 ng/ml LPS. Cells were lysed in Reporter Lysis Buffer (Promega, Madison, WI) and assayed using a Veritas luminometer using luciferase substrate (20 mM tricine, 2.67 mM $MgSO_4 \cdot 7\ H_2O$, 33.3 mM DTT, 100 μM EDTA, 530 μM ATP, 270 μM Acetyl CoA, 132 μg/ml luciferin, 5 mM NaOH, 265 μM magnesium carbonate hydroxide).

Table 2.1. PCR primers used in the generation of mTLR9$^{471-1032}$-HA and mTLR9$^{441-1032}$-HA via PCR stitching

Construct	Forward	Reverse
mTLR9$^{471-1032}$-HA	GGCCCGCCTGGCATTATGCCCAG	CAGGTCCATGGTGAACTTGAA GTTCTTACAGTCACCAGTGGA ACCTGGAACCCAGAGCAGCAG
	CTGCTGCTCTGGGTTCCAGGTTCC ACTGGTGACTGTAAGAACTTCAA GTTCACCATGGAGCTG	TATCTCGAGCTAAGCGTAGTC TGGGACGTCGTATGGG
mTLR9$^{441-1032}$-HA	GGCCCGCCTGGCATTATGCCCAG	CAACAGCTCCTCCTGCTCTGC ATCATCTGCGTCACCAGTGGA ACCTGGAACCCAGAGCAGCAG
	CTGCTGCTCTGGGTTCCAGGTTCC ACTGGTGACGCAGATGATGCAGA GCAGGAGGAGCTGTTG	TATCTCGAGCTAAGCGTAGTC TGGGACGTCGTATGGG

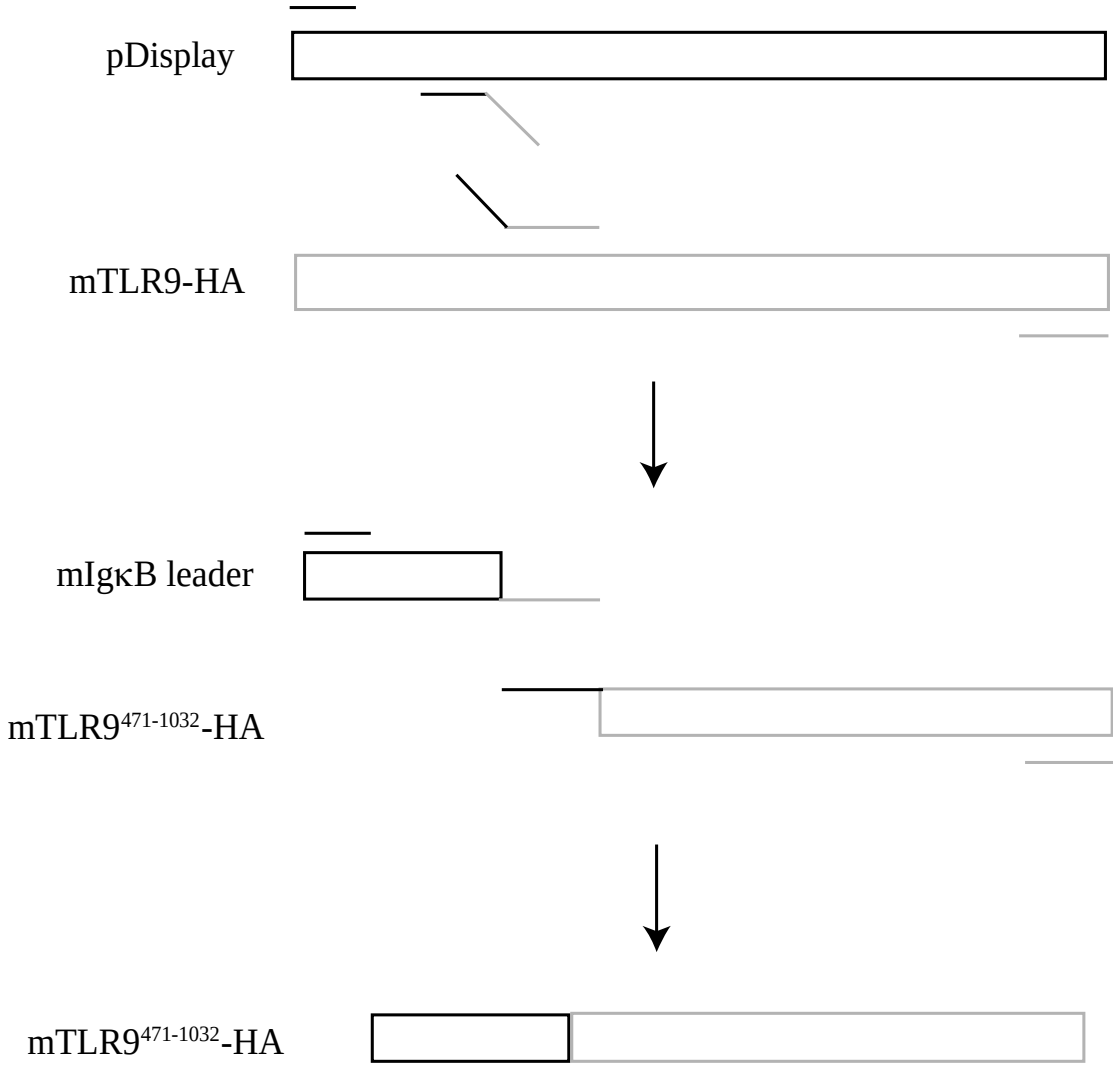

Figure 2.1. Diagram of PCR Sewing Technique. Two initial PCR reactions are performed, the PCR primers at the region to be joined, or "sewn", contains nucleotide sequence from the other product. A third reaction is performed using the products from the initial two reactions as templates the PCR primers corresponding to the region to be sewn are removed from the reaction. The overlapping regions will anneal resulting in one product where the two initial products are "sewn" together.

Retroviral Transduction

Retroviral supernatants were generated by transfecting the ØNX-Ampho cell line with plasmids encoding either mouse TLR9 tagged with hemaglutinin (mTLR9-HA), mTLR9$^{471\text{-}1032}$-HA, mTLR9$^{441\text{-}1032}$-HA or empty vector using Lipofectamine 2000 (Invitrogen, Carlsbad, CA, USA). Retrovirus containing supernatants were harvested 27 and 48 hours later, mixed with 8 μg/mL (final concentration) polybrene (Sigma) and added to RAW 264.7 or TLR9$^{-/-}$ macrophage cells. Following centrifugation at 1811 X g, 32 °C for 90 minutes, the media was changed and cells were incubated for 48 hours at 37 °C.

Organelle fractionation

HEK293 cells stably expressing human TLR9 tagged at the N-terminus with hemaglutinin (HA-hTLR9) (55) were incubated in homogenization buffer (HB: 0.25 M sucrose, 1 mM EDTA, 10 mM Tris, pH 7.4, and protease inhibitor cocktail) on ice for 15 min and homogenized for 20 strokes with a loose fitting 2 ml glass dounce homogenizer, and passed 10 times through a 25G needle attached to a 3 cc syringe. The homogenate was centrifuged at 900 x *g* for 10 min at 4 °C and the postnuclear supernatant was transferred to a fresh tube. The pellet was washed with HB, spun at 4 °C and the combined postnuclear supernatant was centrifuged one additional time at 4 °C. The combined postnuclear supernatant was layered on Percoll in HB (density 1.05 g ml^{-1}) and centrifuged for 60 min at 34 000 x *g* in a 50Ti rotor using a Beckman L-8M ultracentrifuge. Fractions (500 μl each) were collected from the top using an AutoDensi-

Flow IIC gradient unloader (Haake Buchler (Labconoco), Kansas City, MO, USA). Refractive index and protein concentration were tested for each fraction to confirm separation using a Mark II Refractometer (Reichert Scientific Instruments) and the DC-BioRad assay, respectively. Laemmli reduced sample buffer (final concentrations 62.5 mM Tris pH 6.8, 12.5% glycerol, 1% SDS, 0.005% bromophenol blue, 1.7% β-mercaptoethanol) was added to each fraction which were then boiled at 95°C for 5 min and proteins were resolved by SDS-PAGE. After transfer (15V, 35 min in a Trans-Blot SD semi-dry transfer cell (Bio-Rad)), nitrocellulose membranes were immunoblotted for the indicated proteins.

3' biotinylated CpG DNA pulldown

HEK293 cells or HEK293 cells stably expressing hTLR9-YFP (85) were lysed in sample buffer for whole cell lysate control, or lysis buffer and lysates were incubated with 5 μM 3' biotinylated CpG 2006 for one hour at 4°C, followed by affinity purification using streptavidin coated beads (Pierce) for an additional one hour at 4°C. Purified proteins were resolved by SDS-PAGE and transferred to nitrocellulose membranes as described. Membranes were immunoblotted for GFP and gp96.

Co-immunoprecipitation

HEK293 cells transfected with hTLR9-YFP, mTLR9-HA, mTLR9-GFP, $mTLR9^{471-1032}$-HA, $mTLR9^{441-1032}$-HA or empty vector were pretreated as described in the figures then lysed (Lysis buffer: 137 mM NaCl, 20 mM Tris pH 7.4, 1 mM ethylenediaminetetraacetic acid (EDTA), 0.5% Triton X-100, protease inhibitor cocktail (Roche) and 100

μM phenylmethylsulfonyl fluoride) and incubated with anti-TLR9 overnight or anti-HA or anti-GFP for two hours before adding protein A/G sepharose beads and incubating for an additional one hour. After washing three times in lysis buffer, Laemmli reduced sample buffer was added, and samples were boiled. Proteins were resolved by SDS-PAGE and transferred to nitrocellulose membranes. Membranes were immunoblotted as described in the figures. Some membranes were stripped (Restore, Pierce, Rockford, IL) and re-immunoblotted.

Cytokine ELISA

TNF-α production was determined using the mouse TNF-α ELISA MAX Set (BioLegend, San Diego, CA, USA) from supernatants of cells pretreated or not with inhibitors for 2.5 hours then stimulated for 24 hours.

In vitro proteolysis assay

RAW 264.7 cells retrovirally transduced with mTLR9-HA were pretreated with either 2 μM geldanamycin or vehicle control for 2.5 hours. Cells were then lysed in Lysis buffer and incubated at 4 or 24°C for the indicated times. Reactions were terminated with the addition of sample buffer and samples were boiled. Proteins were resolved by SDS-PAGE, transfered to nitrocellulose, and immunoblotted for HA and tubulin.

Densitometric analysis

Quantification of protein bands from radiographic films was performed using ImageJ. The lanes of the Western blot are designated using the rectangular selection tool and a

profile plot is generated with the size of the peaks corresponding to the intensity of the bands in the lane. The base of the peak is then closed off using the straight line tool in order to eliminate the background in the Western blot. Peaks of interest are designated using the wand tool and ImageJ will label each peak with its size, expressed as both the area of the peak itself along with a percentage of the total size of all of the highlighted peaks. Data are then imported into GraphPad Prism for graphing (percentage of total) or additional analysis (calculating RD). Relative densities (RD) are calculated by dividing the areas obtained for different markers as specified in the figures.

Generation of TLR9$^{-/-}$ bone marrow derived macrophage (BMM)

Bone marrow cells were flushed from the femur of a TLR9$^{-/-}$ mouse and cultured in BMM media for five days (DMEM supplemented with 2 mM L-glutamine, 50 U ml^{-1} penicillin, 50 µg ml^{-1} streptomycin, 10% supernatant from L929 cells, and 10% low endotoxin FBS). On days one and three, 1 mL of media was removed and replaced with 1 mL retrovirus-containing supernatants mixed with 8 µg/mL (final concentration) polybrene (Sigma) were added to the cells followed by centrifugation at 1811 X g, 32 °C for 90 minutes. Post centrifugation, 1 mL of the media was removed and replaced with 1 mL fresh BMM media. Differentiation was confirmed by staining the cells with anti-F4/80 phycoerythrin (PE) antibody (Figure 3.15). Fluorescence was measured on a FACS CantoII flow cytometer (BD Biosciences) and analyzed using FlowJo (Tree Star).

Generation of TLR9$^{-/-}$ bone marrow derived dendritic cells (BMDC)

Bone marrow cells were flushed from the femur of a TLR9$^{-/-}$ mouse and cultured in low 2-mercaptoethanol (β-Me) BMDC media for two days RPMI supplemented with 2 mM L-glutamine, 50 U ml^{-1} penicillin, 50 µg ml^{-1} streptomycin, 10% low endotoxin FBS, 20ng/ml GM-CSF and 50 nM β-Me). On days two and four, 1 mL of media was removed and replaced with 1.5 mL retrovirus-containing supernatants mixed with 8 µg/ml (final concentration) polybrene (Sigma) were added to the cells followed by centrifugation at 1811 X g, 32 °C for 90 minutes. Post centrifugation 1.5 mL of the media was removed and replaced with 1 mL fresh high β-Me BMDC media (same as low BMDC media except with 50 µM β-Me). On day six, 1 mL of the media was removed and replaced with 1 mL fresh high β-Me BMDC media. Cells were used on day 7. Differentiation was confirmed by staining the cells with anti-CD11c PE antibody (Figure 3.15). Fluorescence was measured on a FACS CantoII flow cytometer and analyzed using FlowJo.

TLR9 deglycosylation

The TLR9 deglycosylation assay was performed as previously described (55). Lysates from TLR9$^{-/-}$ macrophages or wild-type and gp96 mutant 70Z/3 mouse B cells retrovirally transduced with mTLR9-HA, mTLR9$^{471-1032}$-HA, or mTLR9$^{441-1032}$-HA were divided into three equal portions and were either untreated or treated with endo H or PNGase F according to the manufacturer's instructions (New England Biolabs) overnight at 37°C and the reactions were stopped by adding 6× SDS-PAGE reduced sample buffer and boiling at 95°C for 5 min. The samples were analyzed by immunoblotting for HA.

Intracellular TNF-α Assay

TLR9$^{-/-}$ macrophage, BMM, or BMDC were retrovirally transduced with constructs encoding mTLR9-HA or mTLR9$^{471-1032}$-HA. Cells were then stimulated with 5μM CpG 10104 for 6 hours with the addition of 10μg/mL BFA for the last 4 hours. Cells were fixed with 3% PFA for 15 minutes on ice, then stained with anti-HA FITC and anti-TNF-α APC in 0.1% saponin in PBS with 10% mouse serum for 1 hour on ice. Fluorescence intensity was measured with a FACS CantoII flow cytometer. Data were collected with FACSDiva (BD Biosciences) and analyzed with FlowJo.

70Z/3 NF-κB response assay

Wild-type or gp96 mutant 70Z/3 mouse B cell lines were pretreated for one hour as described in the figures prior to stimulation for 24 hours. GFP expression was measured by flow cytometry using a FACSCalibur cytometer (BD Biosciences) and data analyzed using FlowJo software (Tree Star, Inc).

Lectin blotting

Lysates from wild type or gp96 mutant 70Z/3 mouse B cells retrovirally transduced with mTLR9-HA were immunoprecipitated for HA. Immunoprecipitates were washed with lysis buffer, boiled in sample buffer, and resolved by SDS-PAGE. Following transfer to nitrocellulose, membranes were blocked using 5x Detector Block (KPL) and incubated for 40 minutes with 1.5 μg/mL biotinylated DS lectin (Vector Laboratories, Inc). After 3 washes of 30 minutes each in Tris-buffered saline with 0.1% Tween 20 (TBST), membranes were incubated with avidin-HRP (eBioscience) for 30 minutes. Membranes

were washed an additional 3 times for 60 minutes each with TBST before developing with SuperSignal West Pico substrate (Pierce).

Statistical Analysis

Results are expressed as mean and standard deviation. Student's two-tailed t test was used for comparing drug treatments.

SDS-PAGE

Lysates or immunoprecipitates prepared in SDS -PAGE reduced sample buffer are boiled at 95°C for 5 min and loaded into 8 or 10% polyacrylamide gels and electrophoresed in a Mini PROTEAN 3 Cell (Bio-Rad) filled with Running Buffer (25 mM Tris, 192 mM glycine, 0.1% SDS) at 150V for 1-1.5 hours.

Semi-Dry Transfer

After the SDS-PAGE, Whatman paper, nitrocellulose membrane (GE Healthcare) and polyacrylamide gel are soaked in Transfer buffer (25 mM Tris, 40 mM glycine, 20% methanol) then assembled on a Trans-blot SD semi-dry transfer cell (Bio-Rad) in a stack with Whatman paper on bottom, then the nitrocellulose membrane, polyacrylamide gel and more Whatman paper on top. The transfer cell is closed and the transfer is run at 15V for 35 minutes.

Immunoblotting

After transfer nitrocellulose membranes are blocked in either 4% milk in 1x PBS + 0.1%

Tween-20 (PBS-T, anti-HA, anti-GFP), 5% milk in 1x TBS + 0.1% Tween-20 (TBS-T, MAP kinase antibodies), or Detector Block (anti-gp96) for 1 hour. Membranes are then incubated with primary antibody for 2hr (PBS-T + 1:20 block, anti-HA and anti-GFP) or overnight (5% bovine serum albumin in TBS-T, MAP kinase antibodies or Detector Block, anti-gp96). Membranes are washed 3x in TBS-T or PBS-T and incubated with secondary antibody for 1 hour washed an addition 3x, developed with chemiluminescent substrate and visualized on x-ray film.

CHAPTER 3:

RESULTS

TLRs are responsible for recognizing PAMPs and initiating immune responses. TLR9 is responsible for recognizing CpG DNA (7,96). Regulation of TLR9 is critical as there is little difference between microbial DNA and host DNA. A portion of this regulation occurs at the level of the DNA itself with the frequency of CG dinucleotide repeats being suppressed in the mammalian genome (CpG suppression) and most of those present being cytosine methylated (18-20). However, a large portion of the regulation occurs at the level of the TLR9 protein itself through mechanisms such as localization/trafficking, associating proteins, and proteolytic cleavage (54,60,72,73,82,83,86-88). When TLR9 regulation is subverted, the result is often autoimmune disease or inflammatory pathologies (32-34,89-92). Based on the studies cited above I hypothesized that TLR9 association with gp96 is critical to maintain TLR9 conformational stability and prevent proteolytic degradation. Furthermore, I hypothesized that proteolytic cleavage of TLR9 is not sufficient for response to CpG DNA. Instead, proteolytic cleavage may be a mechanism primarily used by highly phagocytic cells, like macrophages, to degrade TLR9 and prevent recognition of self DNA from apoptotic cells.

One ER protein responsible for regulating TLR9 access to endosomes is gp96 (66,67,72,73). This Hsp regulates intracellular trafficking of both integrins and TLRs (66). Although deficiency in gp96 is embryonic lethal, a mouse pre-B cell line with functionally defective gp96 fails to respond to ligands for TLR1, TLR2 and TLR4

(72,73). Furthermore, macrophage-specific knockout of gp96 abolishes signaling through TLR2, TLR4, TLR5, TLR7 and TLR9 (72). These studies demonstrate the critical function of gp96 in TLR signaling. However, Hsp function is not restricted to trafficking, and it is well established for other Hsps, such as the cytosolic Hsp90, that they may also regulate conformation and ligand binding ability of their client proteins through continuous association (97-99). For gp96, most studies have been conducted using mutant cell lines and gene-deficient mice. By design, these studies were limited to determining phenotype in the absence of functional gp96, and thus they may fail to detect additional chaperoning functions of gp96. Therefore, we hypothesized that gp96 was additionally required to regulate TLR9 conformation, and thus functional activity.

Disruption of the gp96-TLR9 interaction inhibits the TLR9 response to CpG DNA

The heat shock protein gp96 is required for the TLR9 response to CpG DNA (67,72,73). However, in the absence of gp96, TLR9 never gains access to the endosomal compartment as demonstrated by a lack of the 80 kilodalton (kDa) mature form (67). To circumvent this limitation, we asked whether gp96 regulates TLR9 stability and conformation in endosomes using geldanamycin, a benzoquinone ansamycin antibiotic that binds with high affinity to the ATP binding pocket of Hsp90 family members, including gp96. HEK293 cells were transfected with TLR9 and treated with geldanamycin prior to stimulation with the TLR9 ligand CpG DNA. CpG DNA stimulation induced NF-κB activation, and geldanamycin inhibited this response (Figure 3.1A). However, geldanamycin also inhibited background NF-κB activation (Figure 3.1A).

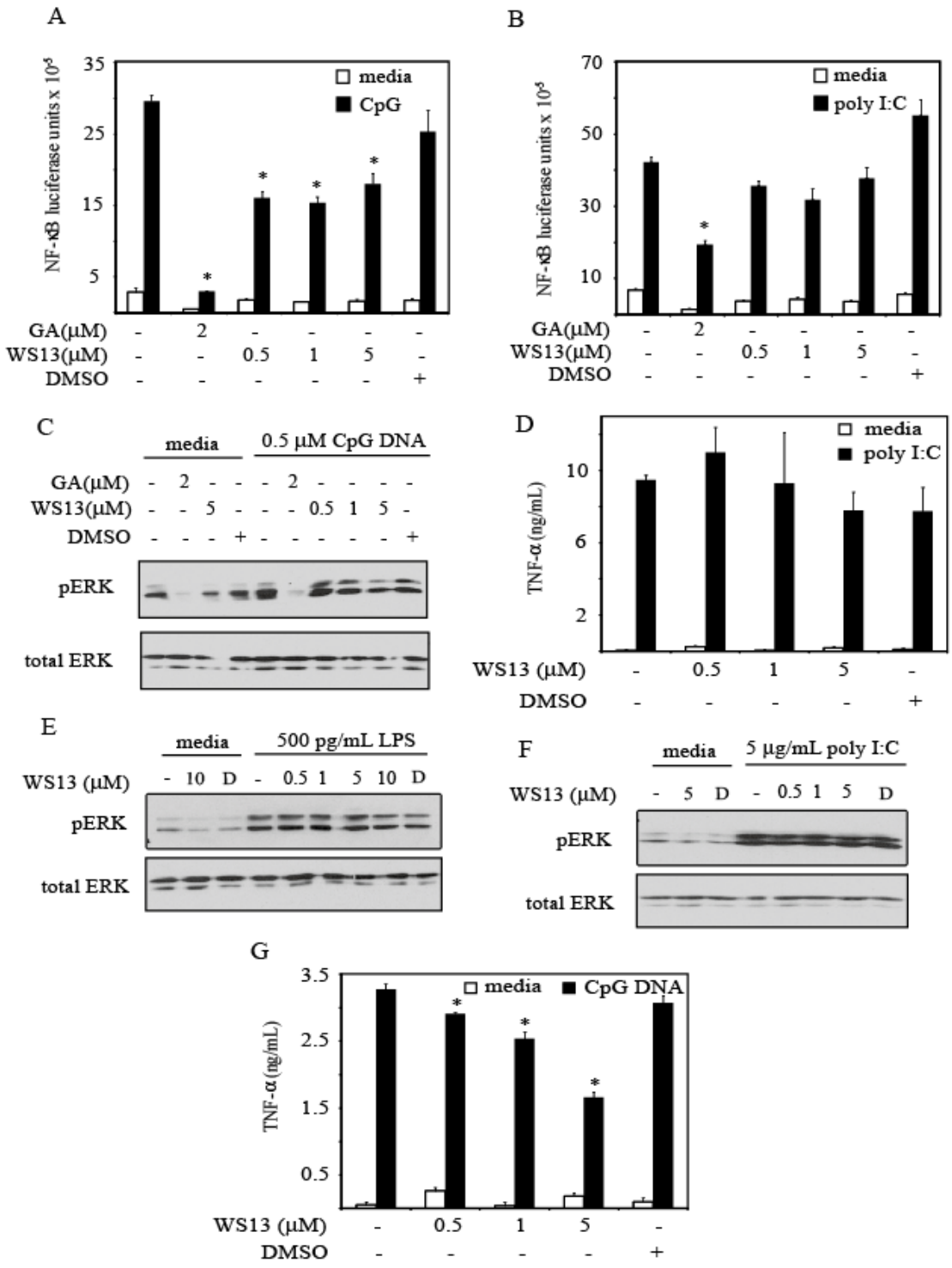
A
NF-κB luciferase units x 10³
35
25
15
5
media
CpG
GA(μM) - 2 - - - -
WS13(μM) - - 0.5 1 5 -
DMSO - - - - - +
B
NF-κB luciferase units x 10³
70
50
30
10
media
poly I:C
GA(μM) - 2 - - - -
WS13(μM) - - 0.5 1 5 -
DMSO - - - - - +
C
media
0.5 μM CpG DNA
GA(μM) - 2 - - - 2 - - - -
WS13(μM) - - 5 - - - 0.5 1 5 -
DMSO - - - + - - - - - +
pERK
total ERK
D
TNF-α (ng/mL)
10
6
2
media
poly I:C
WS13 (μM) - 0.5 1 5 -
DMSO - - - - +
E
media
500 pg/mL LPS
WS13 (μM) - 10 D - 0.5 1 5 10 D
pERK
total ERK
F
media
5 μg/mL poly I:C
WS13 (μM) - 5 D - 0.5 1 5 D
pERK
total ERK
G
TNF-α (ng/mL)
3.5
2.5
1.5
0.5
media
CpG DNA
WS13 (μM) - 0.5 1 5 -
DMSO - - - - +

Figure 3.1 (previous page). Inhibition of gp96 reduces CpG DNA-induced responses. (A, B) HEK293 cells were transfected with an NF-kB-luciferase reporter, TLR9, and TLR3. Cells were pretreated with the indicated concentrations of geldanamycin (GA), WS13, or vehicle control (DMSO) prior to stimulation overnight with (A) 1 μM CpG DNA, or (B) 5 μg/ml poly I:C. Average luciferase activity (n=3) and standard deviation were determined. *P<0.001. Representative of two independent experiments. (C) RAW 264.7 cells were pretreated for 2.5 hours with the indicated concentrations inhibitor or DMSO control and stimulated with 0.5 μM CpG DNA for 30 min. Whole cell lysates were assayed for phosphorylated (pERK) and total ERK by immunoblotting. The two bands detected by the anti-phosphorylated ERK antibody represent ERK 1 (upper band) and ERK 2 (lower band). Representative of three independent experiments (D) RAW 264.7 cells were pretreated with the indicated inhibitors for 2.5 hours and stimulated with 5 μg/ml poly I:C for 24 hours. Secreted TNF-α was determined by ELISA. (E, F) As in (C) except cells were stimulated with (E) 500 pg/mL LPS or (F) 5 μg/ml poly I:C for 30 min. (G) As in (D) except cells were stimulated with 0.5 μM CpG DNA for 24 hrs. *P<0.005. Representative of two independent experiments.

This was likely due to inhibition of cytosolic Hsp90, which was required for many signaling pathways including ERK (100) (Figure 3.1C). In contrast to geldanamycin that binds with similar affinity to both Hsp90 and gp96 (EC_{50}^{Hsp90} = 0.03 μM and EC_{50}^{gp96}=0.026 μM), WS13 is selective for gp96 (EC_{50}^{Hsp90} = 33 μM and EC_{50}^{gp96}=0.16 μM) when tested in an in vitro binding assay against the recombinant proteins (G. Chiosis, personal communication). WS13 also inhibited CpG DNA-induced NF-κB activation at doses based on the Inhibitory Concentration 50 (IC_{50}) of the drug as published by Moulick et al (Figure 3.1A) (101). Importantly, the TLR3 response to poly I:C, which was independent of gp96 (67,72), was not inhibited significantly by WS13, but was significantly inhibited by geldanamycin pretreatment (Figure 3.1B). Since these are membrane permeable drugs, both GA and WS13 will access all gp96 regardless of localization and thus all TLR9 that is bound to gp96. We are measuring the effect of these drugs on TLR9 signaling, and TLR9 signaling initiates from endolysosomes (52,53,55). Therefore, the inhibition that we observe is most likely on TLR9 in the endolysosomal compartment. These studies provide evidence for a specific role for gp96 in TLR9 signaling.

We next asked whether gp96-specific inhibitors blocked endogenous TLR9 responses to CpG DNA. In macrophages, WS13 reduced both CpG DNA-induced ERK phosphorylation (Figure 3.1C) and TNF-α secretion ($p<0.005$, Figure 3.1G) in a concentration dependent manner. However, inhibition of gp96 did not significantly reduce poly I:C-induced (Figure 3.1D and 3.1F) or LPS induced responses (Figure 3.1E and Figure 3.2).

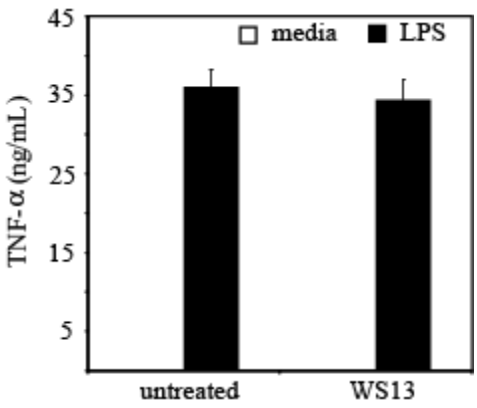

Figure 3.2. LPS induced TNF-α secretion is unaffected by WS13 pretreatment.

RAW 264.7 cells were left untreated or pretreated for 2.5 hours with 2 µM WS13 and stimulated with 100 ng/mL LPS for 24 hrs. Secreted TNF-α was determined by ELISA. Representative of three independent experiments.

Importantly, treatment with the DMSO vehicle did not inhibit CpG DNA-, poly I:C-, or LPS induced NF-κB activation, ERK phosphorylation or TNF-α secretion, indicating that any inhibition observed when using WS13 was from the drug itself and not the DMSO vehicle (Figure 3.1), but the pan-Hsp90 inhibitor geldanamycin blocked all ERK activity (Figure 3.1C). Together, these results indicate that gp96 function is required for TLR9-dependent responses to CpG DNA. It is not surprising that the LPS induced TLR4 response is unaffected by the gp96 specific inhibitor WS13. Published data using a pre-B cell line with a mutant gp96 show that TLR4 is not present on the cell surface and thus not able to respond to LPS (73). However, if these same cells were retrovirally transduced with a constitutively active TLR4 chimera, NF-κB was still activated indicating that in the absence of functional gp96 TLR4 was still folded correctly and its signaling pathway was intact (73). Thus the role of gp96 in TLR4 signaling is to chaperone TLR4 to the cell surface (73). Since our cells have functional gp96, TLR4 will already be expressed on the cell surface before WS13 is administered, and gp96 will no longer be required, so it is expected that signaling will not be affected (Figure 3.1E and 3.2). Thus, unlike TLR4 signaling, gp96 must have additional functions in TLR9 responses although the Leifer lab has shown that TLR9 can be constitutively found outside the ER (55), its response is still inhibited by treatment with WS13 (Figure 3.1A, C, and G).

gp96 is associated with TLR9 after exit from the ER

We next asked whether gp96 association with TLR9 is transient or stable. In 2004 Leifer et al. utilized ^{35}S-methionine to label TLR9 transfected into HeLa cells and was able to

demonstrate that TLR9 protein was reduced by half at 8 hours post labeling (53). This data indicated that eight hours was the half-life of TLR9 protein so we followed TLR9-gp96 association over a similar time course. HEK293 cells stably expressing N-terminally hemaglutinin-tagged human TLR9 (HA-hTLR9) were treated with cycloheximide for various times, and the interaction between TLR9 and gp96 was monitored by co-immunoprecipitation. Cycloheximide binds to the 60S ribosome and stalls translation of protein at the second codon by inhibiting tRNA binding, effectively stopping all protein translation (102,103). Using cycloheximide allowed us to examine one pool of TLR9 throughout the course of the experiment. In our hands the relative density (RD, comparing treated to untreated) of TLR9 was reduced by half at one hour post cycloheximide treatment and this level was stable out to the eight hour time point (Figure 3.3A). gp96 co-immunoprecipitated with TLR9 at a consistent ratio (RD, comparing gp96 to TLR9) regardless of the treatment time and the cycloheximide dose had no effect on the expression of gp96 (Figure 3.4). These data indicated that gp96 remained associated throughout the lifetime of the TLR9 protein.

To determine whether TLR9 and gp96 traffic to the same compartment after TLR9 exits the ER, we performed immunoblot analysis on fractions from HEK293 cells stably expressing N-terminally hemaglutinin-tagged human TLR9. Organelle fractionation resolved early endosomes (Rab5), ER (calnexin) and lysosomes (LAMP-1) (Figure 3.3B). Note that some Rab5 and LAMP-1 overlapped with calnexin-positive ER fractions but $Rab5^{+}LAMP\text{-}1^{-}$ and $Rab5^{-}LAMP\text{-}1^{+}$ fractions were evident. Approximately 6-13% of TLR9 and 37.1% of gp96 was detected in $LAMP\text{-}1^{+}Rab5^{-}$ fractions (Figure 3.3C).

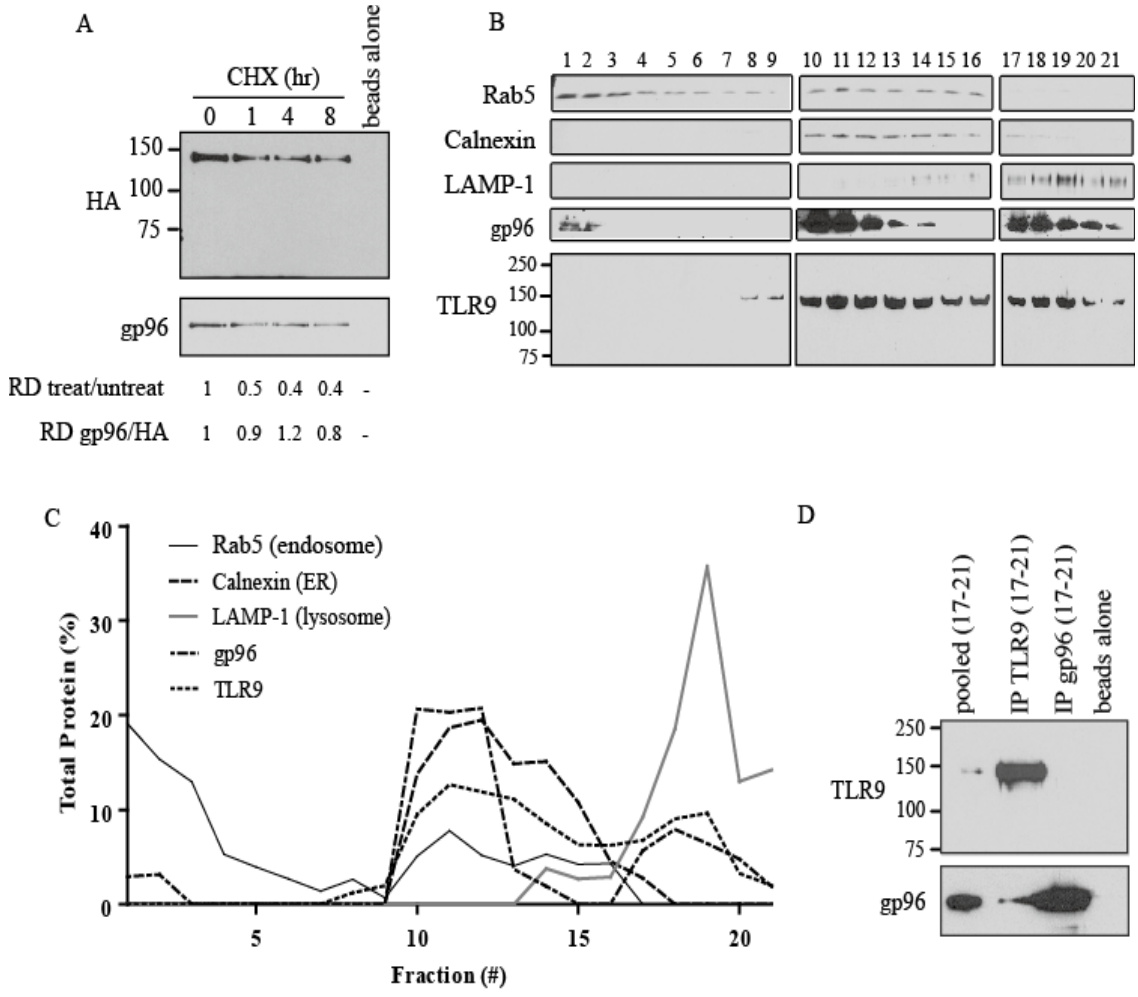
A
CHX (hr)
0 1 4 8
beads alone
150
100
75
HA
gp96
RD treat/untreat 1 0.5 0.4 0.4 -
RD gp96/HA 1 0.9 1.2 0.8 -
B
1 2 3 4 5 6 7 8 9 10 11 12 13 14 15 16 17 18 19 20 21
Rab5
Calnexin
LAMP-1
gp96
250
150
100
75
TLR9
C
Rab5 (endosome)
Calnexin (ER)
LAMP-1 (lysosome)
gp96
TLR9
Total Protein (%)
40
30
20
10
0
5
10
15
20
Fraction (#)
D
pooled (17-21)
IP TLR9 (17-21)
IP gp96 (17-21)
beads alone
250
150
100
75
TLR9
gp96

Figure 3.3 (previous page). Lysosomal TLR9 Binds gp96. (A) HEK293 cells stably expressing N-terminally HA-tagged human TLR9 (HA-hTLR9) were pretreated with 10 μg/ml cycloheximide (CHX) for the indicated times prior to cell lysis and HA immunoprecipitation followed by HA and gp96 immunoblotting. Relative densities (RD) were calculated as described in the methods and data are representative of two independent experiments (B) Sub-cellular fractions from HEK293 cells stably expressing N-terminally HA-tagged human TLR9 (HA-TLR9) were resolved by SDS-PAGE, and immunoblotted for early endosomes (Rab5), ER (calnexin), Lysosomes (LAMP-1), HA (TLR9), and gp96. (C) Densitometric analysis for (B). Each line depicts an individual marker and is represented as percent of total for that marker. (D) Combined LAMP-1 positive fractions (17-21) from (C) were immunoprecipitated for TLR9 and immunoblotted for TLR9 and gp96 Representative of three independent experiments.

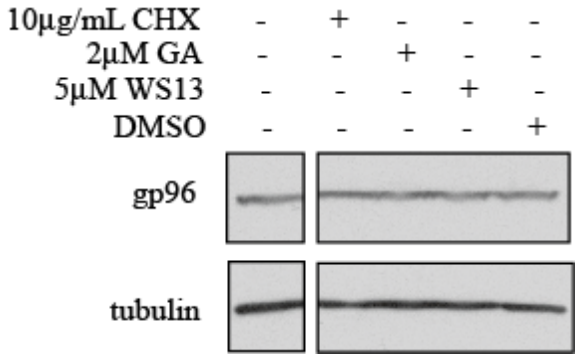

Figure 3.4. gp96 expression is unaffected by drug treatments. HEK293 cells were pretreated with the indicated concentration of drug for either 6 hrs (CHX) or 2.5 hrs (GA and WS13). Whole cell lysates were immunoblotted for gp96 and tubulin.

These results indicate that TLR9 and gp96 both traffic out of the ER to the lysosomal compartment and most likely remain associated. However, given the increased representation of gp96 in these fractions as compared to TLR9, there are likely additional gp96 client proteins in the lysosomal compartment. To confirm that TLR9 and gp96 directly interacted in the lysosomal fractions, the $LAMP1^{+}$ fractions were combined and immunoprecipitated for either TLR9 or gp96. TLR9 was detected in both the total pooled fractions and following TLR9 immunoprecipitation (Figure 3.3D). Similarly, gp96 was detected in the total pooled, and immunoprecipitated fractions, but was also detected in the TLR9 immunoprecipitate (Figure 3.3D). Therefore, gp96 associated with TLR9 in the endolysosomal compartment. It is important to note that we were unable to detect the mature form of TLR9 in these experiments due to the fact that the TLR9 in this experiment was N-terminally tagged and the anti-tag antibody would not detect the mature form as the cleavage event would remove the HA tag from the mature form. However, it is also relevant to note that HEK293 cells poorly proteolytically process TLR9 without co-expression of the ER transmembrane protein UNC93B1 (Figure 3.5).

Inhibition of gp96 has no effect on TLR9 oligomerization

Since dimerization is required for TLR9 signaling (104), we next asked if disruption of the gp96-TLR9 interaction disrupted TLR9 homodimer formation. When HA-hTLR9 and wild-type human TLR9 C-terminally tagged with YFP (hTLR9-YFP) were co-expressed in HeLa cells, immunoprecipitation with antibodies to GFP, which also react to YFP, resulted in the precipitation of both hTLR9-YFP and HA-hTLR9, indicating oligomer formation in the absence of ligand (Figure 3.6).

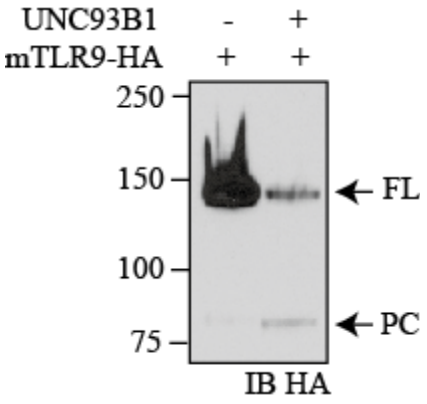

Figure 3.5. HEK293 cells require UNC93B1 to generate mature TLR9. HEK293 cells were transfected with mTLR9-HA plus empty vector or UNC93B1 and lysates were immunoblotted for HA. Arrows indicate full length TLR9 (FL); proteolytically cleaved TLR9 (PC).

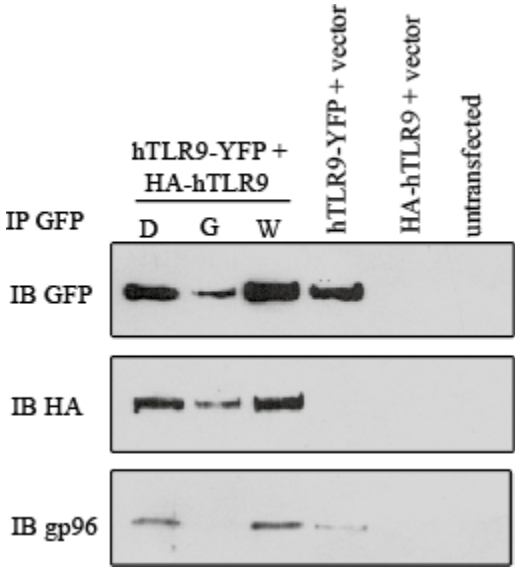

Figure 3.6. Inhibition of gp96 does not affect TLR9 dimer formation. HeLa cells transfected with combinations of human hTLR9-YFP, HA-hTLR9 and vector were pretreated with 2 µM Geldanamycin (GA), 2 µM WS13 (W) or DMSO (D) for 2.5 hours. GFP immunoprecipitates (IP) were assayed for GFP and HA by immunoblotting. One of two similar experiments.

Pretreatment with either geldanamycin or WS13 had no effect on the ability to co-immunoprecipitate HA-hTLR9 with hTLR9-YFP. Therefore, we conclude that gp96 does not regulate TLR9 oligomerization.

gp96 binds CpG DNA independent of TLR9

Our preliminary data suggest that TLR9 and gp96 are still associated outside of the ER in the lysosomal compartment (Figure 3.3). Furthermore, inhibition of gp96 function inhibited CpG DNA induced signaling events (Figure 3.1A, C, and G). Since the TLR9-gp96 interaction is stable we next asked whether TLR9 which had bound CpG DNA still associated with gp96. As expected when lysates from HEK293 cells or HEK293 cells stably expressing hTLR9-YFP were incubated with 5 µM 3' biotinylated CpG, TLR9 was only detected in affinity purifications from TLR9 expressing cells (Figure 3.7). Interestingly, in the non-TLR9 expressing cells, gp96 was purified with the 3'bt CpG DNA indicating that gp96 is capable of direct binding to CpG DNA. Previous published data demonstrated that commercially available purified human Hsp90 was able to bind CpG DNA in an electrophoretic mobility shift assay in a sequence dependent manner (105). Bandholtz et al. demonstrated that Hsp90 preferentially interacted with CpG DNA which was known to be immunostimulatory, while non-stimulatory sequences showed little to no binding (105). We were unable to draw any conclusions from this experiment as the direct binding of gp96 to 3'bt CpG DNA prevents us from addressing whether or not TLR9 which has bound CpG DNA is still associated with gp96.

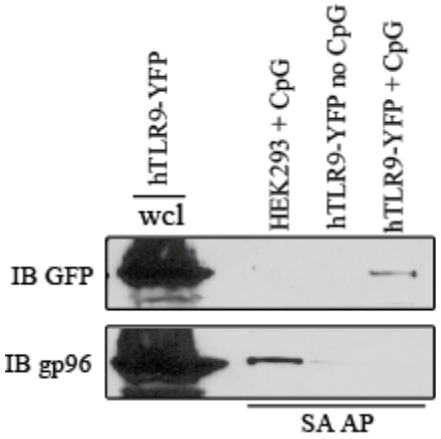

Figure 3.7. gp96 binds CpG DNA independent of TLR9. HEK293 or HEK293 cells stably expressing hTLR9-YFP were lysed and lysates were incubated with 3'biotinylated CpG 2006 (5 µM) for 1 hr at 4°C then affinity purified (AP) with streptavidin (SA) coated beads (SA AP). SA APs were immunoblotted for GFP and gp96.

Inhibition of gp96 alters TLR9 distribution

We next asked whether altered localization of TLR9 accounted for the reduced CpG DNA-induced ERK phosphorylation (Figure 3.1A) and TNF-α secretion (Figure 3.1G) in gp96 inhibitor treated cells. HEK 293 cells stably expressing HA-hTLR9 were treated with vehicle control or geldanamycin. Similar to our previous observations ((55), and Figure 3.3B), untreated cells contained TLR9 in the ER and lysosomal fractions (Figure 3.8A, and 3.8B and 3.8C, white bars). Following treatment with geldanamycin the level of TLR9 in lysosomes was reduced, but there was an increase in TLR9 in lighter density fractions (Figure 3.8A**,** 3.8B and 3.8C, black bars). This new localization might represent accumulation of TLR9 in the Golgi compartment, which localizes between the Rab 5 positive early endosomes and the calnexin positive ER fractions (55), while loss of TLR9 from the lysosomal fractions likely reflects changes in TLR9 conformation and proteolytic degradation as addressed below. These experiments highlight additional chaperoning functions of gp96 outside of chaperoning ER exit.

Proteolytic processing of TLR9 requires gp96

CpG DNA response by TLR9 depends on several events including intracellular trafficking to endosomes, ligand binding, conformational changes and proteolytic processing (52,53,80,86,104). Hsp90 family members, including the ER paralog gp96, regulate client protein conformations and ligand binding. To address whether TLR9 was proteolytically processed in the absence of functional gp96, we used a pair of mouse B cell lines: one wild type (WT) and one functionally deficient for gp96 (mutant, MT) (73).

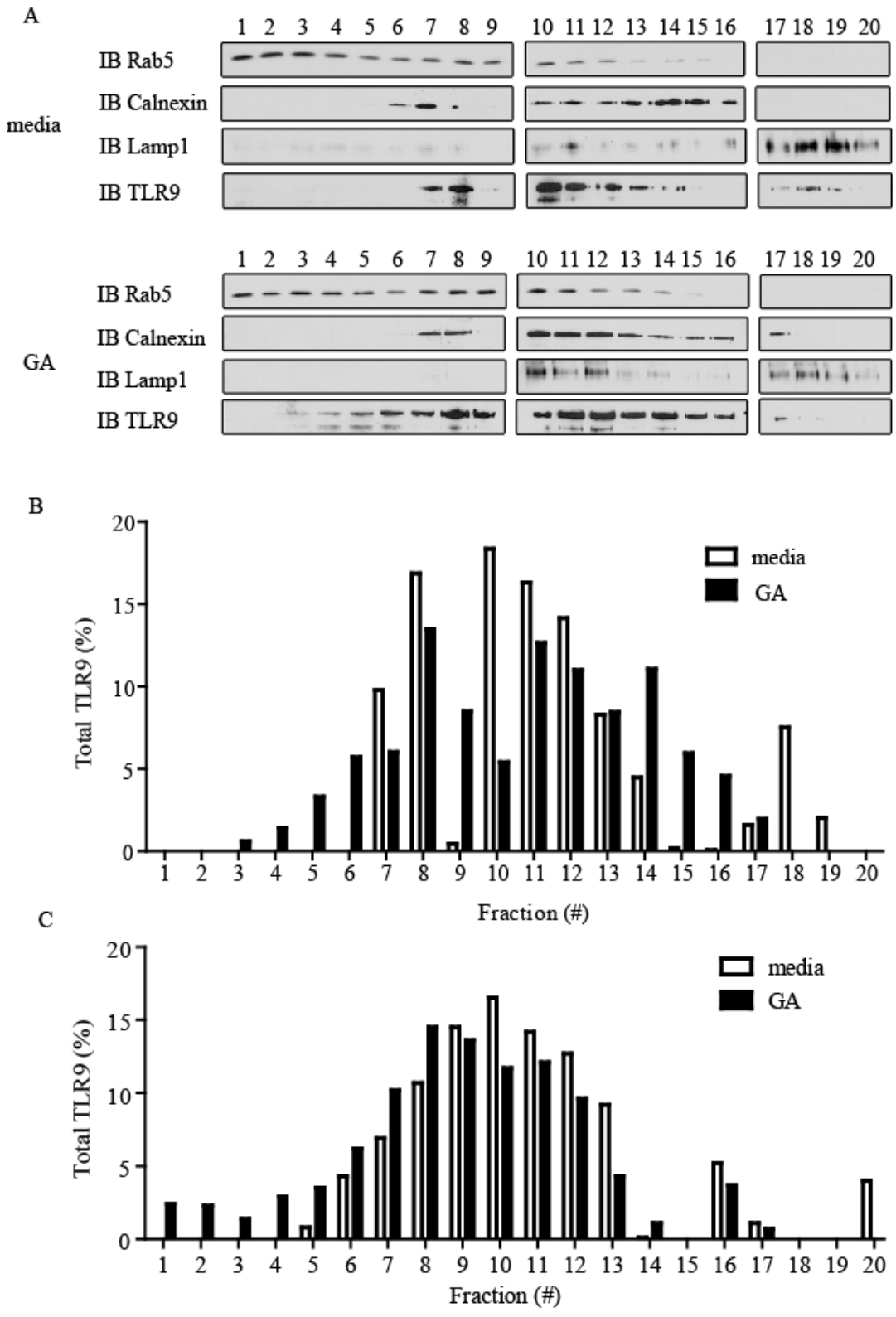
A
media
GA
IB Rab5
IB Calnexin
IB Lamp1
IB TLR9
1 2 3 4 5 6 7 8 9 10 11 12 13 14 15 16 17 18 19 20
B
C
media
GA
Total TLR9 (%)
Fraction (#)

Figure 3.8 (previous page). Inhibition of gp96 changes the localization of TLR9. (A) HEK293 cells stably expressing HA-hTLR9 were either left untreated or treated with 2µM GA for 1 hour, and subcellular fractions were assayed by immunoblotting for early endosomes (Rab5), ER (calnexin), Lysosomes (LAMP-1), and HA (TLR9), (B) Immunoblots for TLR9 from (A) were subjected to densitometric analysis as in and graphed on the same graph. GA, geldanamycin. Data are representative of three independent experiments. (C) Densitometric analysis for a similar experiment as in (B) showing reproducibility of trend for change in localization upon treatment with GA.

Both cell lines contain a stably integrated NF-κB-driven green fluorescent protein (GFP) reporter (NF-κB-GFP). Flow cytometric analysis showed that both cell lines respond to phorbol myristic acid (PMA) stimulation by up-regulating GFP expression (Figure 3.9A). While CpG DNA stimulation induced an increase in GFP expression from the wild type cells, the mutant cells failed to respond (Figure 3.9A). These studies confirm previous findings that gp96 is required for TLR9 response (72). When these cells were retrovirally transduced with hemaglutinin-tagged mouse TLR9 (mTLR9-HA), less total TLR9 protein was immunoprecipitated from gp96 mutant cells. Furthermore, gp96 was co-immunoprecipitated with TLR9 in the wild type cells but not in the gp96 mutant cells (Figure 3.9B). We hypothesized that TLR9 may fail to be properly folded and glycosylated in the absence of functional gp96. However, TLR9-HA showed no difference in sensitivity to endoglycosidase H or PNGase F regardless of gp96 status (Figure 3.9C). Importantly, the level of TLR9 observed in gp96 wild type and mutant cells was similar (Figure 3.9C). Differences in TLR9 levels observed between wild type and mutant cells after immunoprecipitation suggest that TLR9 is subject to post-lysis proteolysis (compare Figure 3.9B to Figure 3.9C). To determine whether lack of proteolytic processing in gp96 mutant cells was due to failure of TLR9 to exit the ER, we tested whether TLR9 expressed glycan modifications characteristic of Golgi processing (55). *Datura stramonium* (DS) lectin binds to hybrid and complex glycan residues, which only occur on proteins that have reached the Golgi compartment (55). DS lectin bound to mTLR9-HA from wild type, but only weakly to mTLR9-HA from gp96 mutant cells (Figure 3.9D).

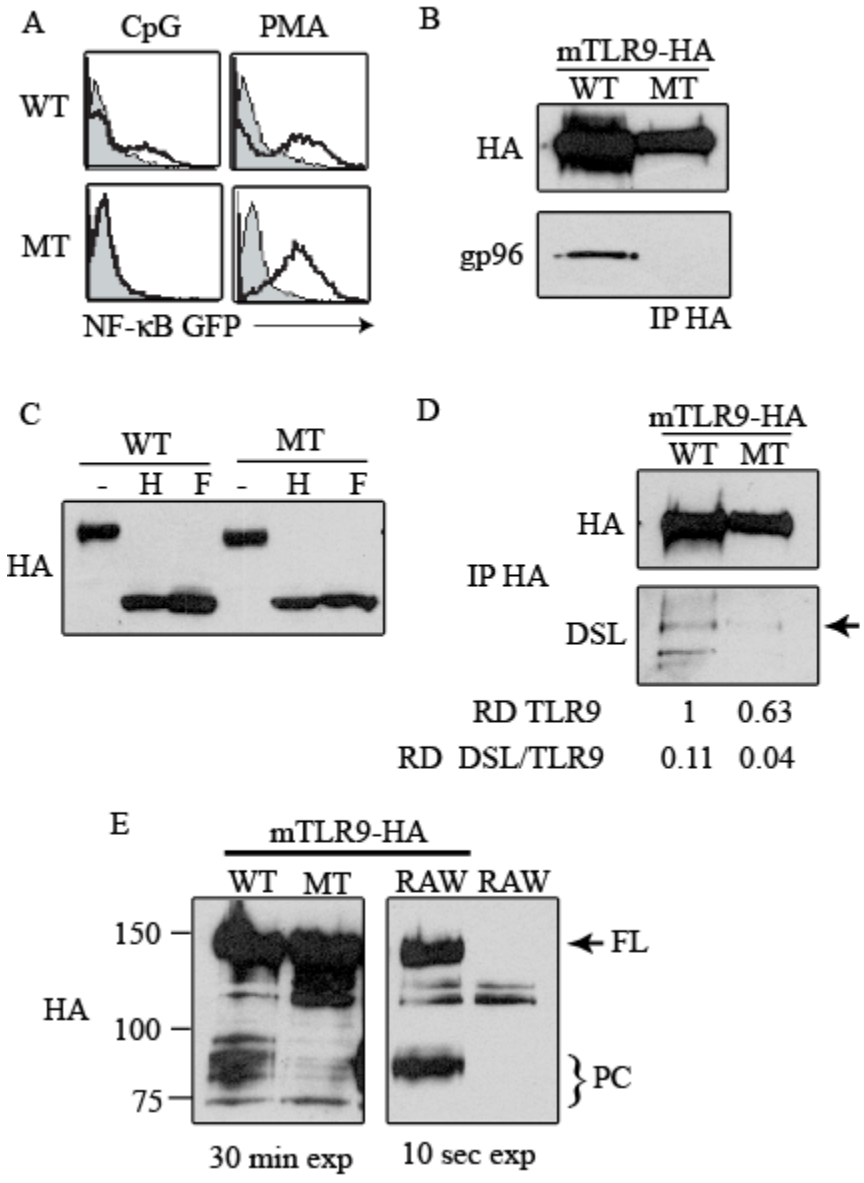
A
CpG
PMA
WT
MT
NF-κB GFP
B
mTLR9-HA
WT MT
HA
gp96
IP HA
C
WT
MT
- H F - H F
HA
D
mTLR9-HA
WT MT
HA
IP HA
DSL
RD TLR9 1 0.63
RD DSL/TLR9 0.11 0.04
E
mTLR9-HA
WT MT
RAW RAW
150
100
75
HA
FL
PC
30 min exp
10 sec exp

Figure 3.9 (previous page). Proteolytic processing of TLR9 requires gp96. (A) Wild type (WT) and gp96 mutant (MT) cells were stimulated with 1 μM CpG or 50 ng/mL PMA for 24 hours and expression of an NF-κB driven green fluorescent protein (GFP) reporter was measured by flow cytometry (open histograms). Shaded histograms, untreated. One of three similar experiments. (B) WT and gp96 mutant (MT) cells were retrovirally transduced with mouse TLR9-HA (mTLR9-HA). HA immunoprecipitates were analyzed for HA and gp96 expression by immunoblotting. (C) RAW 264.7 cells were transduced with TLR9-HA and lysates were either left untreated (-) or treated with endoH (H) or PNGase F (F) prior to SDS-PAGE and immunoblotting for HA. (D) As in (B) except immunoprecipitates analyzed for HA by immunoblotting and binding of *Datura stramonium* lectin (DSL) by lectin blotting. Relative densities (RD) were calculated as described in the methods. (E) WT, gp96 mutant B cells and RAW 264.7 (RAW) cells were left untransduced or transduced with TLR9-HA and analyzed for HA by immunoblotting. Two different exposure times (10 Seconds for RAW 264.7 and 30 minutes for WT and gp96 mutant B cells) are shown due to the increased expression of both full length TLR9 and p80 in RAW 264.7 cells. IP, immunoprecipitation; FL, full length; PC, proteolytically processed TLR9; p80, 80 KDa form. One of three similar experiments.

Since TLR9 does not associate with mutant gp96 and only partially acquires glycans indicative of ER exit in cells lacking functional gp96, we next asked if TLR9 was proteolytically processed in gp96 mutant cells. Both full length TLR9 and three bands running at approximately 80 kilodalton were detected in lysates from wild type cells transduced with mTLR9-HA (Figure 3.9E). However, less TLR9 was expressed by the gp96 mutant cells and little mature TLR9 was detected; compare RD of TLR9 and TLR9/DSL (Figure 3.9E). Interestingly, the level of mature TLR9 in wild type mouse B cells (Figure 3.9E, WT) was significantly less than that present in mouse macrophages (Figure 3.9E, RAW, note the exposure times were different: B cells 30 minutes; macrophages 10 seconds). Therefore, although proteolytic processing was not as robust in B cells, in the absence of functional gp96, TLR9 was still proteolytically processed.

Disruption of the gp96-TLR9 interaction enhances TLR9 proteolytic sensitivity

Since TLR9 remained associated with gp96, and pharmacologic inhibition of gp96 inhibited TLR9 signaling, we next asked whether inhibition of gp96 induced proteolysis of TLR9. We utilized both geldanamycin and WS13 as they inhibit gp96 through different mechanisms. In HEK293 cells stably expressing hTLR9-YFP pretreated with geldanamycin, little to no gp96 was co-immunoprecipitated with TLR9 (Figure 3.10A). In contrast, WS13 does not disrupt association of gp96 with client proteins (106) thus TLR9 and gp96 were co-immunoprecipitated even in the presence of WS13 (Figure 3.10A). RAW 264.7 macrophages were retrovirally transduced with C-terminally HA tagged mouse TLR9. As expected, both full length TLR9 and the mature form were detected in HA immunoprecipitates.

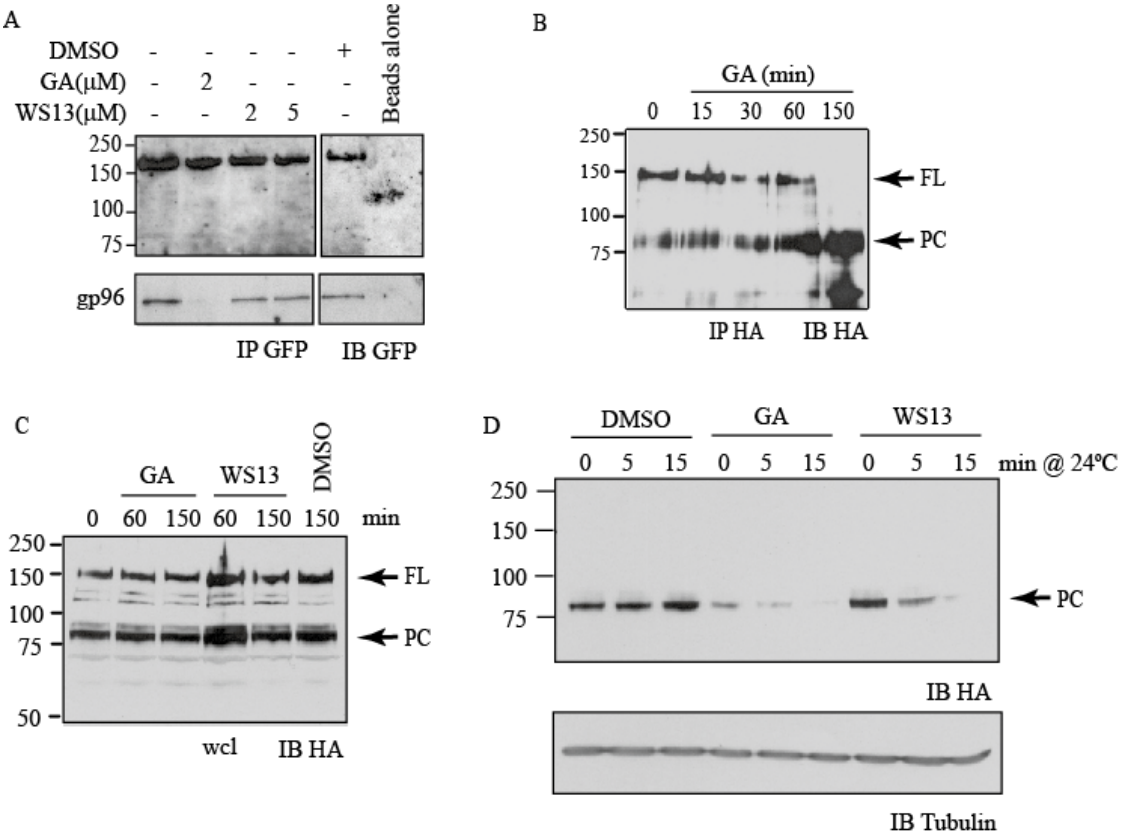
A
DMSO - - - - +
GA(μM) - 2 - - -
WS13(μM) - - 2 5 -
Beads alone
250
150
100
75
gp96
IP GFP
IB GFP
B
GA (min)
0 15 30 60 150
250
150
100
75
FL
PC
IP HA
IB HA
C
GA
WS13
DMSO
0 60 150 60 150 150 min
250
150
100
75
50
FL
PC
wcl
IB HA
D
DMSO
GA
WS13
0 5 15 0 5 15 0 5 15 min @ 24ºC
250
150
100
75
PC
IB HA
IB Tubulin

Figure 3.10 (previous page). Inhibition of gp96 increases TLR9 sensitivity to proteolytic digestion. (A) HEK293 cells stably expressing human TLR9-YFP (hTLR9-YFP) were treated with DMSO or the indicated concentrations of geldanamycin (GA) or WS13 for 1 hour. Cells were lysed and immunoprecipitated for GFP, or with no antibody (beads alone), and immunoblotted for GFP and gp96. Representative of two independent experiments. (B) RAW 264.7 cells were transduced with C-terminally HA-tagged mouse TLR9 (mTLR9-HA) and treated with 2 μM geldanamycin (GA) for the indicated times. HA immunoprecipitates (IP) were assayed by immunoblotting (IB) for HA. FL, full length TLR9; PC, proteolytically cleaved TLR9. Representative of three similar experiments. (C) As in (B) except cells lysed in sample buffer (wcl) were assayed by immunoblotting (IB) for HA and some cells were pretreated with vehicle control (DMSO). Representative of two similar experiments. Arrows indicate full length TLR9 (FL); proteolytically cleaved TLR9 (PC) (D) RAW 264.7 cells were transduced with TLR9-HA and pretreated with either vehicle control (DMSO), 2 μM geldanamycin (GA), or 2 μM WS13 for 2.5 hours. Lysates were prepared as for IP and incubated at 24°C for the indicated times and assayed by immunoblotting (IB) for HA and tubulin. PC, proteolytically cleaved TLR9. Representative of two similar experiments.

Treatment with geldanamycin for one hour decreased the abundance of full length TLR9 protein, yet increased an 80-kDa form, in immunoprecipitates (Figure 3.10B). Additional proteolytic fragments were detected after two and a half hours of geldanamycin treatment (Figure 3.10B, band lower than p80). Since proteolysis can occur in vitro during immunoprecipitation, we also examined the effect of GA and WS13 on TLR9 proteolysis in transduced RAW 264.7 cell whole cell lysates. In contrast to the increased proteolysis observed in the immunoprecipitates (Figure 3.10C), when cells were directly lysed in sample buffer, and the whole cell lysates were assayed by immunoblotting for TLR9, there was no reduction in full length TLR9, or increase in the 80-kDa form, in geldanamycin treated cells (Figure 3.10C). Therefore, the proteolysis we observed occurred during the immunoprecipitation step. We interpret these data to mean that upon treatment with geldanamycin, a condition where gp96 is dissociated, TLR9 has an increased sensitivity to proteases. This is despite the inclusion of a cocktail of broad protease inhibitors. Increased sensitivity to proteases could reflect a change in TLR9 conformation. To test whether inhibition of gp96 had an effect on TLR9 proteolytic sensitivity, we performed an in vitro proteolysis assay. Lysates were prepared from mTLR9-HA retrovirally transduced RAW 264.7 cells treated with GA, where gp96 dissociates from TLR9, and WS13, where gp96 dissociation does not occur yet gp96 function is inhibited. Lysates were incubated at 24°C for five or 15 minutes. In lysates from DMSO treated cells, the abundance of a control protein, tubulin, and the abundance of TLR9 protein were not significantly reduced during the 15-minute incubation at 24°C (Figure 3.10D). In geldanamycin or WS13 treated cells tubulin levels were maintained while the 80-kDa form of TLR9 was dramatically reduced, even in the lysates not

incubated at 24°C, 0 min time point (Figure 3.10D). Interestingly, this enhancement of proteolysis required lysis of the cells which indicates that TLR9 does not normally come into contact with this particular protease in large quantities. However it is possible that this enhancement in TLR9 proteolysis does occur *iv vivo* at a reduced frequency and by lysing the cells we are simply enhancing the process. Therefore, we conclude that gp96 function was required to protect TLR9 from proteolysis and potentially maintain TLR9 conformational stability.

TLR9 cleavage is not necessary for response to CpG DNA in fibroblasts

My results up to this point demonstrate that while inhibition of gp96 induces proteolytic cleavage of TLR9 (Figure 3.10B and D) it in turn inhibits CpG DNA induced signaling events (Figure 3.1A, C, and G). These results do not support the current dogma of TLR9 biology that states that TLR9 is obligately proteolytically cleaved prior to signaling (86,87). This proteolytic event occurrs between aa 741-770 and resulted in an 80 kD version of TLR9 reported to be the mature, and active form of the protein (86,87). This mature form of TLR9 is found in abundance in the phagosomes of macrophages. If proteolytic cleavage were required, then treatment of cells with geldanamycin, which induces sensitivity to proteolytic cleavage and results in cleavage to an 80 kD form of TLR9, similar in size to the mature form (Figure 3.10B), should enhance signaling, not inhibit it, as I have observed (Figure 3.1A, C, and G). Taken together, these data led me to question the role of proteolytic cleavage in TLR9 signaling.

Previous data showed that fibroblast cell lines such as MEFs do not robustly

proteolytically cleave TLR9 to the mature form without the presence of UNC93B1 (86). However, these cells respond to CpG DNA in the apparent absence of mature 80 kD TLR9 (86). Co-transfection of UNC93B1 along with TLR9 into a fibroblast cell line causes an increase in the mature form of TLR9 (Figure 3.5) along with increased response to CpG DNA (86). Co-transfection with increasing concentrations of UNC93B1 plasmid did not result in a dose dependent increase in TLR9 response to CpG DNA. Instead, we observed an increase in TLR9 response to CpG DNA at a 2:1 ratio of TLR9 plasmid to UNC93B1 plasmid followed by a decrease in TLR9 response as the concentration of UNC93B1 plasmid increased relative to TLR9 plasmid (Figure 3.11A). This suggests that proteolytic cleavage is not necessary for TLR9 signaling in all cell types. We next asked if the proteolytic fragment is sufficient for signaling on its own. A C-terminally hemaglutinin (HA) tagged fragment of TLR9 encompassing residues 471-1032 (mTLR9$^{471\text{-}1032}$-HA) was readily detected when expressed in HEK293 cells (87) (Figure 3.11B and C). However, this form did not reconstitute a response to CpG DNA in HEK293 cells (Figure 3.11D), and addition of UNC93B1 or stimulation with higher doses of CpG DNA did not restore response (Figure 3.12A and B). The inability of mTLR9$^{471\text{-}1032}$-HA to respond to CpG DNA could be due to a defect in its trafficking outside the ER compartment and this will be discussed in a later figure. From this data we conclude that the mature form of TLR9 alone is insufficient to confer response to CpG DNA and that cleavage does not directly correlate with response to CpG DNA in HEK293 cells.

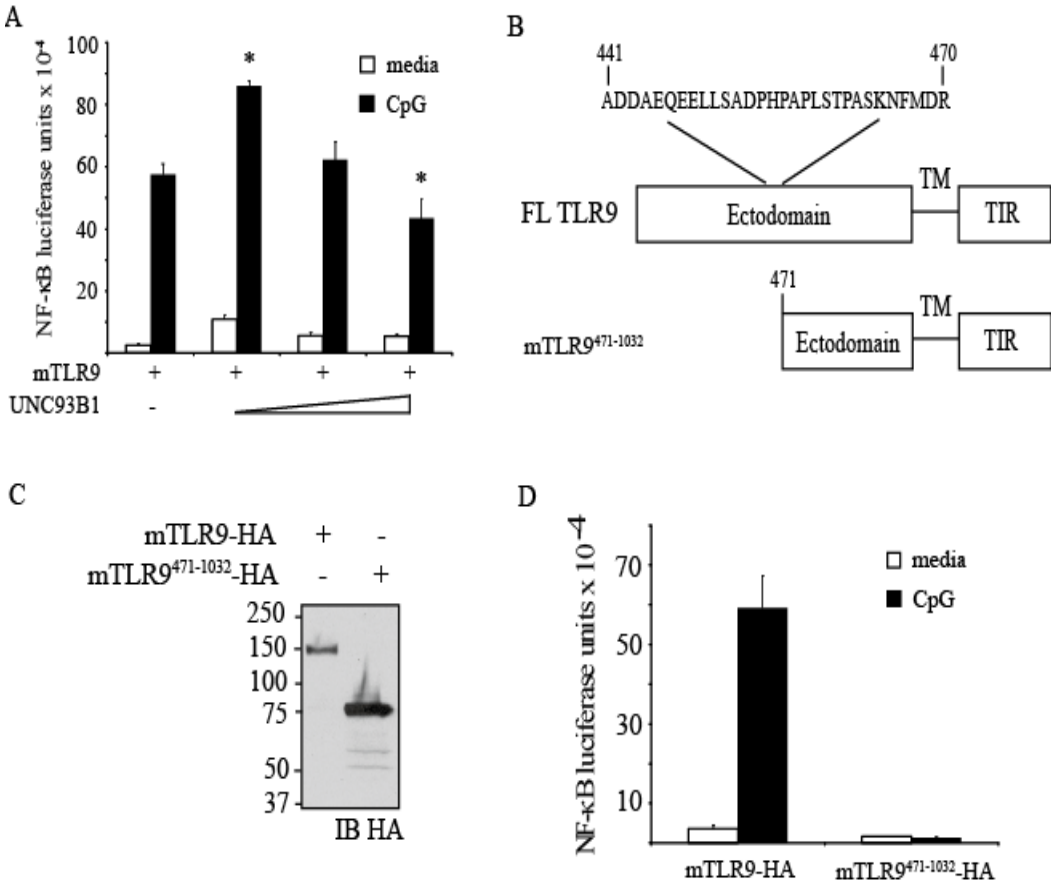
A
NF-κB luciferase units x 10⁻⁴
100
80
60
40
20
media
CpG
*
*
mTLR9 + + + +
UNC93B1 -
B
441
470
ADDAEQEELLSADPHPAPLSTPASKNFMDR
FL TLR9
Ectodomain
TM
TIR
471
mTLR9471-1032
Ectodomain
TM
TIR
C
mTLR9-HA + -
mTLR9471-1032-HA - +
250
150
100
75
50
37
IB HA
D
NF-κB luciferase units x 10⁻⁴
70
50
30
10
media
CpG
mTLR9-HA
mTLR9471-1032-HA

Figure 3.11 (previous page). Cleavage does not correlate with response to CpG DNA in HEK293 cells. (A) HEK293 cells were transfected with an NF-kB-luciferase reporter, TLR9 and increasing concentrations of UNC93B1 (15 ng/row, 30ng/row, or 50ng/row) as shown and stimulated overnight with 1 μM CpG DNA. Average luciferase activity (n=3) and standard deviation were determined. Representative of two independent experiments. (B) Model showing the proposed TLR9 cleavage site and the N-terminus of the mTLR9$^{471\text{-}1032}$-HA construct. (C) HEK293 cells were transfected with mTLR9-HA or mTLR9$^{471\text{-}1032}$-HA and lysates were immunoblotted for HA. Representative of two independent experiments. (D) HEK293 cells were transfected with an NF-kB-luciferase reporter, mTLR9-HA and mTLR9$^{471\text{-}1032}$-HA as shown and stimulated overnight with 1 μM CpG DNA. Average luciferase activity (n=3) and standard deviation were determined. Representative of three independent experiments.

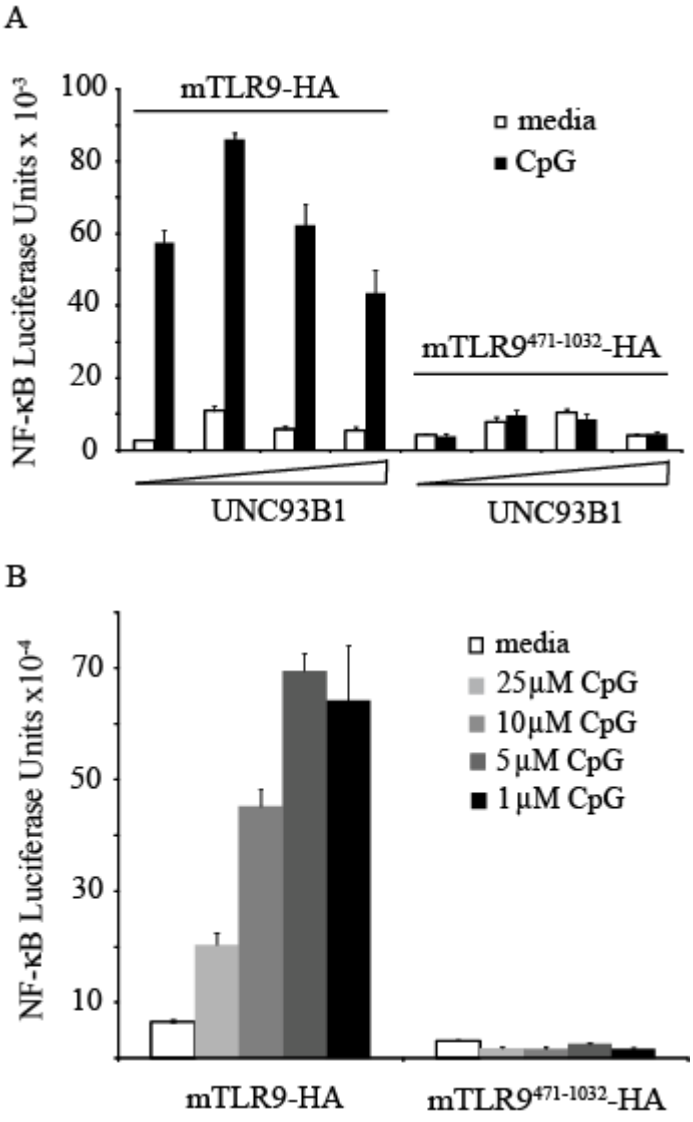
A
NF-κB Luciferase Units x 10-3
100
80
60
40
20
0
mTLR9-HA
media
CpG
mTLR9471-1032-HA
UNC93B1
UNC93B1
B
NF-κB Luciferase Units x10-4
70
50
30
10
media
25μM CpG
10μM CpG
5μM CpG
1μM CpG
mTLR9-HA
mTLR9471-1032-HA

Figure 3.12 (previous page). Defect in mTLR9$^{471\text{-}1032}$-HA signaling cannot be rescued by UNC93B1 or high dose CpG. (A) HEK293 cells were transfected with an NF-kB-luciferase reporter, mTLR9-HA and UNC93B1 or mTLR9$^{471\text{-}1032}$-HA and increasing concentrations of UNC93B1 (15 ng/row, 30ng/row, or 50ng/row) as shown and stimulated overnight with 1 μM CpG DNA. Average luciferase activity (n=3) and standard deviation were determined. Representative of three independent experiments. (B) HEK293 cells were transfected with an NF-κB-luciferase reporter, mTLR9-HA or mTLR9$^{471\text{-}1032}$-HA and stimulated overnight with the indicated concentrations of CpG DNA. Average luciferase activity (n=3) and standard deviation were determined. Representative of two independent experiments.

Co-expression of mTLR9$^{471-1032}$-HA decreases full length TLR9 signaling in HEK293 cells

The Leifer lab has previously shown that a second TLR9 cleavage product, sTLR9, fails to signal on its own and is able to interact with full length TLR9 and inhibit full length TLR9 signaling (85). To determine whether or not mTLR9$^{471-1032}$-HA had a similar function, we next asked whether mTLR9$^{471-1032}$-HA is able to oligomerize with full length mTLR9-GFP. TLR9 is known to exist in preformed homodimers, and dimerization is required for signaling (104). Co-immunoprecipitation analysis revealed that mTLR9$^{471-1032}$-HA was readily detected in immunoprecipitates of mTLR9-GFP (Figure 3.13A). Since mTLR9$^{471-1032}$-HA was unable to respond to CpG DNA (Figure 3.11D) but was able to associate with full length TLR9 (Figure 3.13A) we next asked whether expression of mTLR9$^{471-1032}$-HA could reduce signaling through the full length receptor. Indeed when mTLR9-HA and mTLR9$^{471-1032}$-HA were co-transfected into HEK293 cells we observed a dose dependent decrease in mTLR9-HA response to CpG DNA (Figure 3.13B). From this data we conclude that that mTLR9$^{471-1032}$-HA reduces mTLR9-HA response to CpG DNA in HEK293 cells. These data are inconsistent with mature TLR9 being that active form. The decrease in full length TLR9 response could be due to preferential binding of the CpG DNA to mTLR9$^{471-1032}$-HA thus preventing CpG DNA binding to full length TLR9 dimers. This hypothesis is supported published data demonstrating that the mature form of TLR9 is able to bind CpG DNA (26,86,87). Combined with my data demonstrating that mTLR9$^{471-1032}$-HA does not respond to CpG DNA this would indicate that mTLR9$^{471-1032}$-HA is functioning as a sink for CpG DNA.

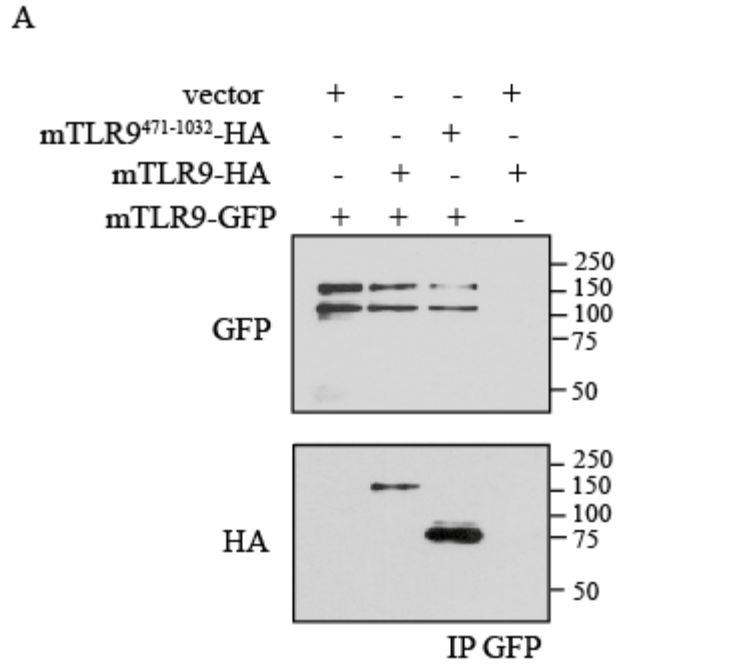
A
vector + - - +
mTLR9471-1032-HA - - + -
mTLR9-HA - + - +
mTLR9-GFP + + + -
GFP
250
150
100
75
50
HA
250
150
100
75
50
IP GFP

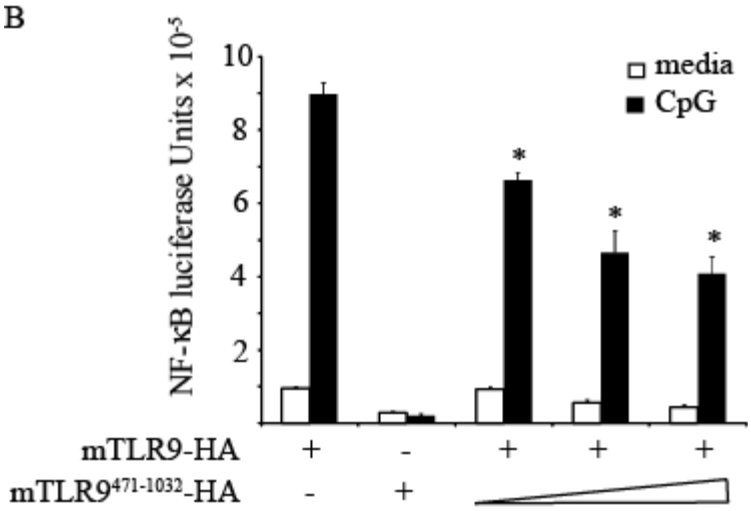
B
NF-κB luciferase Units x 10-5
10
8
6
4
2
media
CpG
*
*
*
mTLR9-HA + - + + +
mTLR9471-1032-HA - +

Figure 3.13 (previous page). mTLR9$^{471-1032}$-HA reduces full length TLR9 signaling in HEK293 cells. (A) HEK293 cells were transfected with constructs encoding, mTLR9-HA, mTLR9-GFP, mTLR9$^{471-1032}$-HA or empty vector (pBMN-i-GFP). Cells were lysed and immunoprecipitated for GFP followed by GFP and HA immunoblotting. Representative of two independent experiments. (B) HEK293 cells were transfected with an NF-κB-luciferase reporter, mTLR9-HA and increasing concentrations (10 ng plasmid/row, 50 ng plasmid/row, or 100ng plasmid/row) of mTLR9$^{471-1032}$-HA then stimulated overnight with 1 μM CpG DNA. Average luciferase activity (n=3) and standard deviation were determined. Representative of two independent experiments.

However, a second possibility is that mTLR9$^{471-1032}$-HA is able to change the localization of full length TLR9 to an intracellular compartment which prevents the recognition of DNA.

mTLR9$^{471-1032}$-HA is not sufficient to reconstitute CpG DNA response in macrophages

Since the precise location of the TLR9 cleavage event is unknown, one explanation for our results is that we generated a fragment that did not correspond to the mature form. Although we generated our fragment using the published primers used to synthesize mature TLR9, which reconstituted response to CpG DNA in TLR9 deficient dendritic cells (87), it was possible that we were lacking an important part of TLR9. Mature TLR9 has been published to lack the entire hinge region (aa 441-470) (87). However, this hinge region may play an important role in the localization of the protein since a construct of TLR9 lacking only this hinge region fails to co-localize with *Aspergillus fumigatus* containing phagosomes and demonstrates reduced response to CpG DNA (87,107). Therefore, we generated a C-terminally HA tagged protein corresponding to residues 441-1032 of TLR9, which contained the hinge region in addition to LRR15 to the C-terminus (mTLR9$^{441-1032}$-HA) (Figure 3.14A). We next asked whether mTLR9$^{471-1032}$-HA or mTLR9$^{441-1032}$-HA reconstituted CpG DNA response in a TLR9$^{-/-}$ macrophage cell line. This line is derived from murine TLR9$^{-/-}$ bone marrow cells on a C57BL/6 background immortalized with the replication deficient retrovirus J2 and was obtained from BEI Resources.

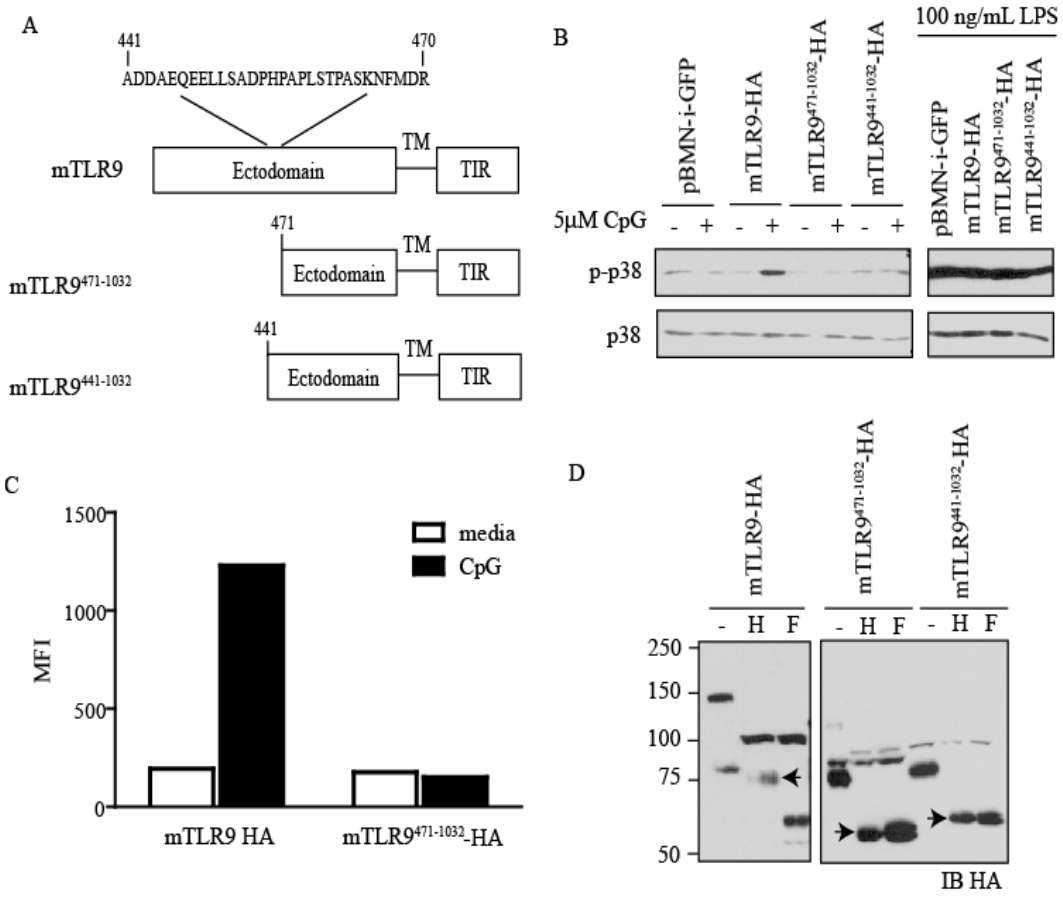
A
441
470
ADDAEQEELLSADPHPAPLSTPASKNFMDR
mTLR9
Ectodomain
TM
TIR
471
mTLR9^471-1032
441
mTLR9^441-1032
B
100 ng/mL LPS
pBMN-i-GFP
mTLR9-HA
mTLR9^471-1032-HA
mTLR9^441-1032-HA
5μM CpG
- + - + - + - +
p-p38
p38
C
1500
1000
500
0
MFI
media
CpG
mTLR9 HA
mTLR9^471-1032-HA
D
mTLR9-HA
mTLR9^471-1032-HA
mTLR9^441-1032-HA
- H F - H F - H F
250
150
100
75
50
IB HA

Figure 3.14 (previous page). mTLR9$^{471-1032}$-HA and mTLR9$^{441-1032}$-HA cannot reconstitute CpG DNA response in a TLR9$^{-/-}$ macrophage cell line due to a defect in ER exit. (A) Model showing the proposed TLR9 cleavage site and the N-terminus of the mTLR9$^{471-1032}$-HA and mTLR9$^{441-1032}$-HA constructs. (B) TLR9-/- macrophages were retrovirally transduced with empty vector, mTLR9-HA, mTLR9$^{471-1032}$-HA, or mTLR9$^{441-1032}$-HA and stimulated for 30 min with media (-) or CpG DNA (+) or LPS. Whole cell lysates were assayed for phosphorylated (p-p38) and total p38 by immunoblotting. (C) Intracellular cytokine staining for TNF-α production by TLR9$^{-/-}$ macrophage retrovirally transduced with vectors encoding mTLR9-HA or mTLR9$^{471-1032}$-HA and stimulated for 6 hr with CpG DNA (5 μM). Brefeldin A (10 μg/mL) was included for the final 4 hr, prior to fixing and staining with anti-HA and anti-TNF-α; TNF-α expression by HA^{+} cells is presented as mean fluorescence intensity (MFI). Representative of two independent experiments. (D) Lysates from TLR9$^{-/-}$ macrophage transduced with retroviral vectors encoding mTLR9-HA, mTLR9$^{471-1032}$-HA, or mTLR9$^{441-1032}$-HA were left untreated (-) or treated with endoglycosidase H (H) or PNGase F (F) and immunoblotted for HA. Arrows indicated endoglycosidase H treated samples. Representative of two independent experiments.

TLR9$^{-/-}$ macrophages were retrovirally transduced to reconstitute the cells with mTLR9-HA, mTLR9$^{471-1032}$-HA or mTLR9$^{441-1032}$-HA, and stimulated with CpG DNA. At 30 minutes post-CpG DNA stimulation, p38 was phosphorylated only in cells reconstituted with wild type TLR9 (Figure 3.14B). However, neither mature TLR9, mTLR9$^{471-1032}$-HA, nor the mature form plus the hinge, mTLR9$^{441-1032}$-HA, were capable of reconstituting signaling, despite all of the cells responding similarly to LPS stimulation due to endogenous TLR4 expression (Figure 3.14B). We conclude that the hinge region of TLR9 is insufficient to rescue the defect in CpG DNA response observed for mature TLR9. TLR9 is synthesized in the ER and must traffic to the endolysosomal compartment in order to encounter its ligand, CpG DNA (31,52,53). One potential explanation for the inability of mTLR9$^{471-1032}$-HA and mTLR9$^{441-1032}$-HA to reconstitute CpG DNA response is that on their own the two proteolytic fragments are unable to access endosomes, and thus CpG DNA. In order to test this we took advantage of the fact that naturally generated mature form displays a partial endoglycosidase H (endo H) resistance, indicating that the sugars present on the protein had been modified in the Golgi (86,87). While proteins are still in the ER they are glycosylated with high mannose structures. As proteins traffic out of the ER these high mannose glycan structures are trimmed and modified in the Golgi apparatus. Naturally generated mature TLR9 displays a partially endo H resistance characteristic of modification in the Golgi (Figure 3.14D, left) (86,87). However, the glycosylations present on the mTLR9$^{471-1032}$-HA and mTLR9$^{441-1032}$-HA constructs are completely endo H sensitive (Figure 3.13D, compare arrows). The molecular weights of all the TLR9 fragments were reduced to the predicted sizes by treatment with PNGase F, an enzyme which will remove all N-linked glycans (Figure

3.14D). Therefore, we conclude that the reason that the mTLR9$^{471-1032}$-HA and mTLR9$^{441-1032}$-HA constructs fail to respond to CpG DNA is that they are unable to access the endosomal compartment.

Only full length TLR9 reconstitutes CpG DNA response in TLR9$^{-/-}$ primary cells

Previously published data shows that mature TLR9 reconstitutes CpG DNA signaling in bone marrow derived dendritic cells from TLR9$^{-/-}$ mice (TLR9$^{-/-}$ BMDC) (87). However, our data suggests that mTLR9$^{471-1032}$-HA is insufficient to reconstitute CpG DNA signalling in HEK293 cells and a TLR9$^{-/-}$ macrophage cell line (Figure 3.11, 3.12 and 3.14). We hypothesized that the disparity between our results could be a result of differences in the cell types used. While we observed that mature TLR9 did not reconstitute signaling in HEK293 cells or a macrophage cell line (Figure 3.11, 3.12, and 3.14), mature TLR9 did reconstitute signaling in primary dendritic cells (87). To test this we generated bone marrow-derived macrophages (BMM) and bone marrow-derived dendritic cells (BMDC) from TLR9$^{-/-}$ mice. Differentiation of these cells was confirmed via staining with anti-F4/80 (macrophage marker) and anti-CD11c (dendritic cell marker). Using our protocol we were able to achieve approximately 85% cell differentiation into BMM and 50% differentiation into BMDC (Figure 3.15). Similar to the result obtained with the TLR9$^{-/-}$ cell line, TLR9$^{-/-}$ BMM retrovirally transduced with mTLR9-HA produced TNF-α when stimulated with CpG DNA (Figure 3.16, top panel), while TLR9$^{-/-}$ BMM retrovirally transduced with mTLR9$^{471-1032}$-HA did not (Figure 3.16, top panel). TLR9$^{-/-}$ BMM responded equally to LPS stimulation through constitutive expression of TLR4 regardless of transduction (Figure 3.16, top panel).

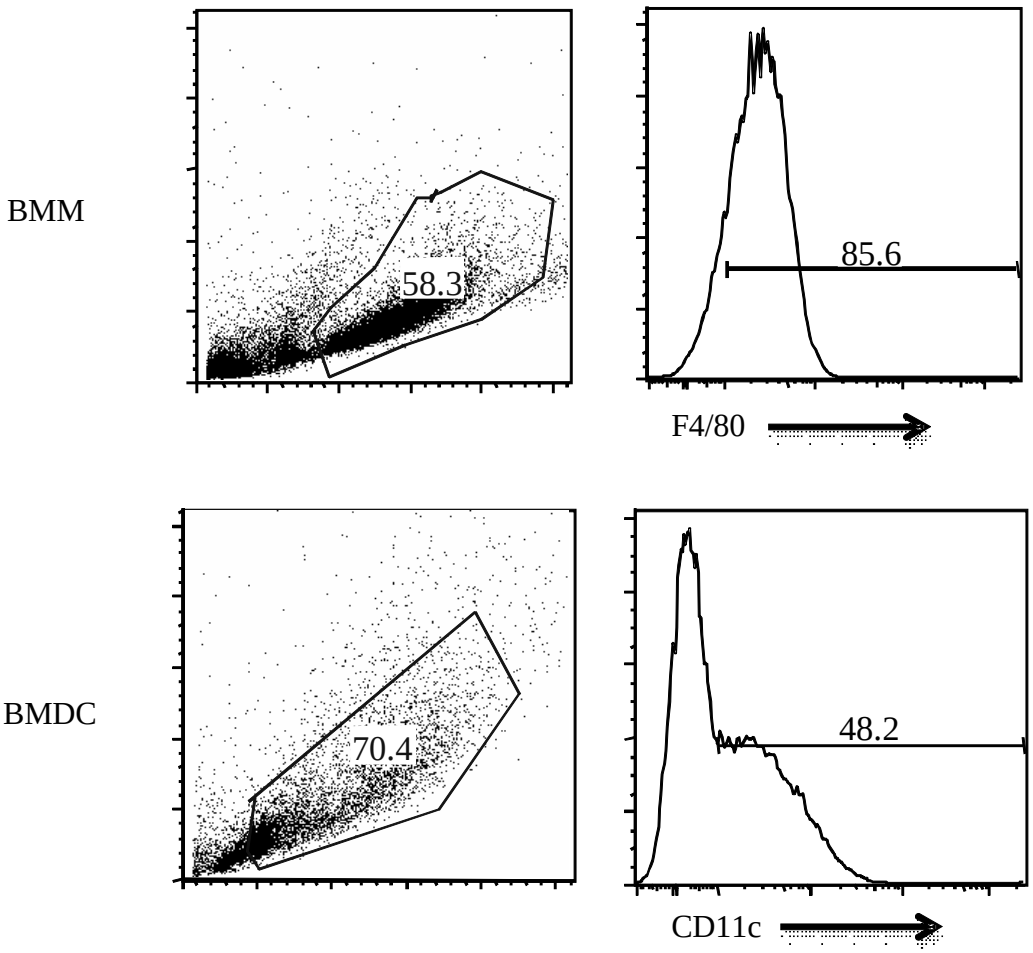

Figure 3.15. Differentiation of TLR9$^{-/-}$ bone marrow cells into macrophage or dendritic cells. TLR9$^{-/-}$ bone marrow cells were treated as described methods to differentiate into bone marrow derived macrophage (BMM) or bone marrow derived dendritic cells (BMDC). Cells were then stained with anti-F4/80 (macrophage marker, top) or anti-CD11c (dendritic cell marker, bottom).

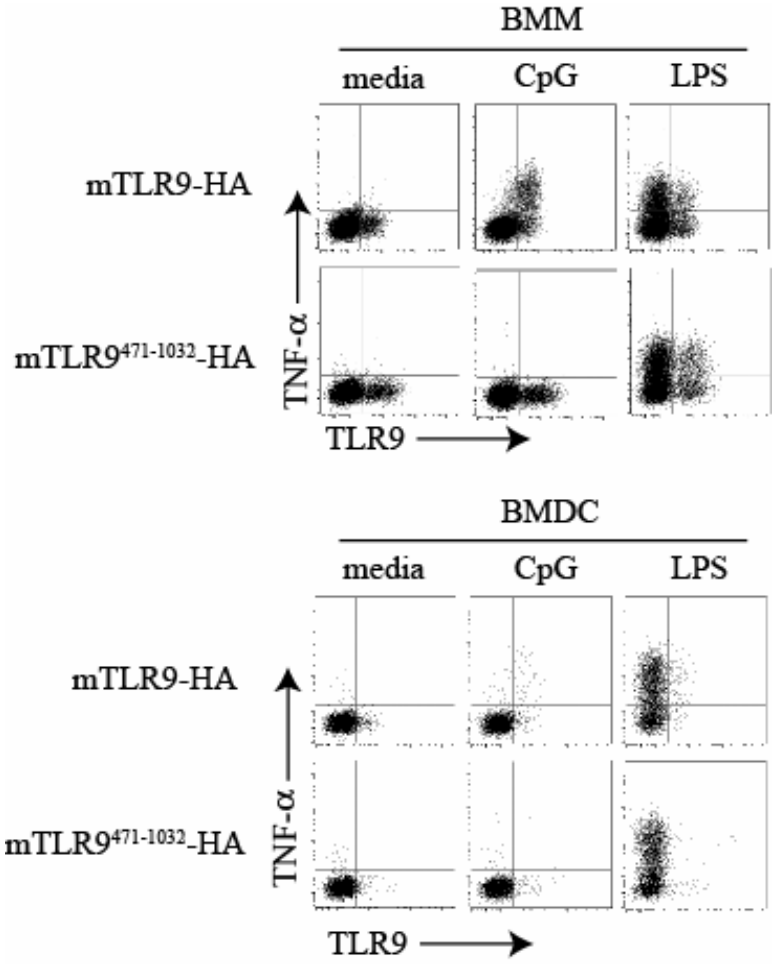

Figure 3.16. mTLR9$^{471-1032}$-HA fails to reconstitute CpG DNA induced signaling in TLR9$^{-/-}$ primary cells. Intracellular cytokine staining for TNF-α production by TLR9$^{-/-}$ BMM (top) and BMDC (bottom) retrovirally transduced with vectors encoding mTLR9-HA or mTLR9$^{471-1032}$-HA and stimulated for 6 hr with CpG DNA (5 μM) or LPS (100 ng/mL). Brefeldin A (10 μg/mL) was included for the final 4 hr, prior to fixing and staining with anti-HA and anti-TNF-α; TNF-α expression by HA^{+} cells is presented as mean fluorescence intensity (MFI).

Our data indicate that mature TLR9 is insufficient to reconstitute CpG DNA induced TNF-α production in $TLR9^{-/-}$ BMM. Published data only demonstrate mature TLR9 functions in $TLR9^{-/-}$ BMDC (87), raising the possibility that the activity of mature TLR9 is unique to dendritic cells. However, this is not the case as $TLR9^{-/-}$ BMDC retrovirally transduced with $mTLR9^{471-1032}$-HA failed to produce TNF-α in response to CpG DNA, while $TLR9^{-/-}$ BMDC retrovirally transduced mTLR9-HA produced TNF-α when stimulated with CpG DNA (Figure 3.15, bottom panel). As was the case with $TLR9^{-/-}$ BMM, $TLR9^{-/-}$ BMDC responded equally to LPS stimulation regardless of transduction through the constitutive expression of TLR4 (Figure 3.16, bottom panel). The data from Figure 3.16 are summarized graphically in Figure 3.17, depicting TNF-α expression as mean fluorescence intensity (MFI) of cells which are stained by anti-HA. From this data we conclude that mature TLR9, $mTLR9^{471-1032}$-HA, is insufficient to reconstitute a CpG DNA response in primary $TLR9^{-/-}$ BMM or BMDC.

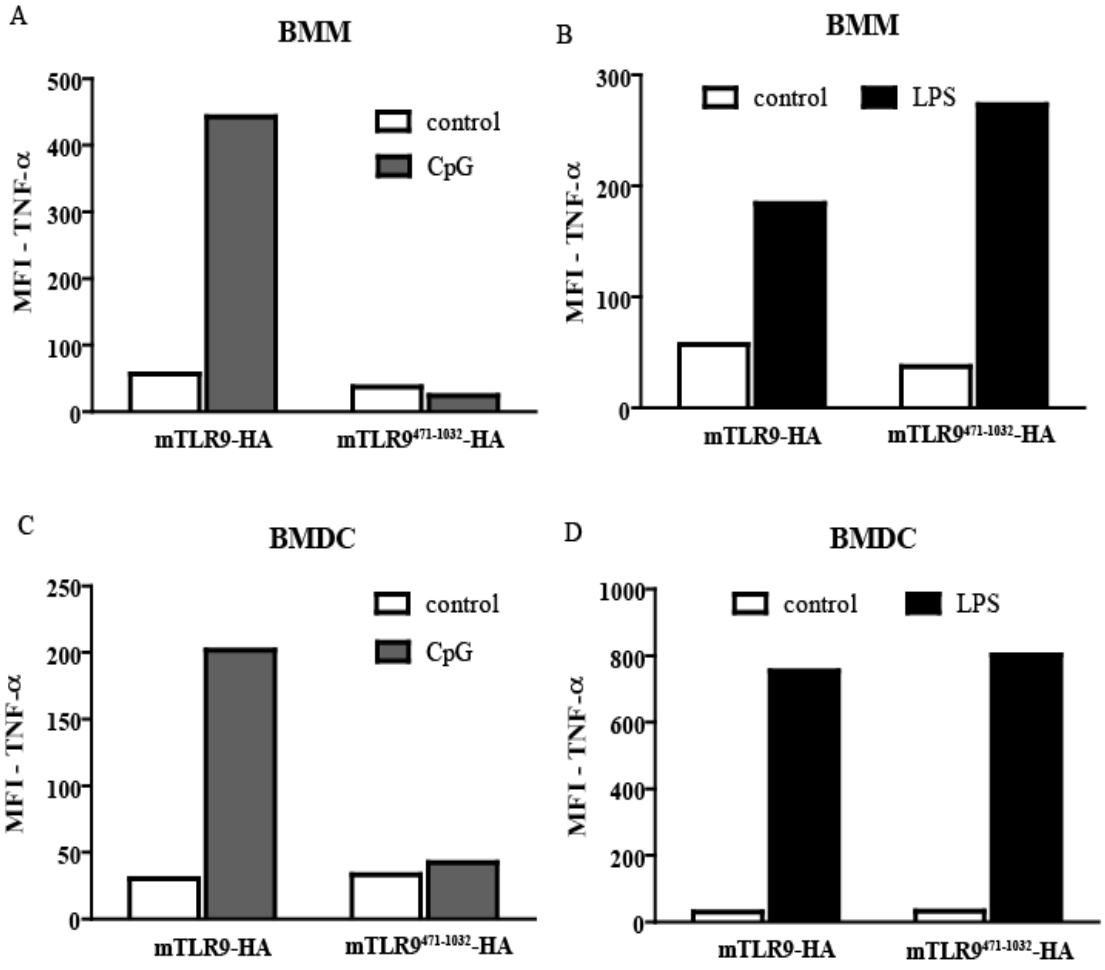

Figure 3.17. CpG DNA induced signaling is not reconstituted by mTLR9$^{471\text{-}1032}$-HA. Graphical representation of the data from Figure 3.16 depicting the MFI of TNF-α staining of TLR9$^{-/-}$ BMM (A and B) and BMDC (C and D) retrovirally transduced with vectors encoding mTLR9-HA or mTLR9$^{471\text{-}1032}$-HA and stimulated for 6 hr with CpG DNA (5 μM, A and C) or LPS (100 ng/mL, B and D).

CHAPTER 4:

DISCUSSION

Summary of findings

TLRs are one of the primary mechanisms utilized by the innate immune system to recognize the threat of, and initiate response to, invading pathogens (108). TLR9, the receptor for CpG DNA, is part of a larger subfamily of TLRs responsible for recognizing nucleic acids (7,96,109). Regulation of nucleic acid sensing TLRs is critical as their ligands are not only expressed by pathogens, but additionally as self. In this thesis I examined two mechanisms of regulating TLR9 function: association with the heat shock protein gp96 (66,67,73) and activation of proteolytic cleavage (82,86-88).

First I examined the role of the heat shock protein gp96 in TLR9 signaling. Published data established a role for gp96 in the folding and ER exit of TLR9. However, this work was conducted using mutant cell lines and cell specific knockouts which would mask any additional role for gp96 in TLR9 signaling beyond the initial protein folding events and subsequent exit from the ER compartment (66,72,73). I have shown that inhibition of gp96 function via a proprietary gp96 specific inhibitor, WS13, reduces TLR9, but not TLR3 or TLR4, response as detected by NF-κB reporter activation, phosphorylation of the MAP kinase ERK, and TNF-α secretion. The interaction between TLR9 and gp96 is sufficiently stable that the two proteins can be co-immunoprecipitated up to eight hours after inhibition of protein synthesis by cycloheximide. Preliminary results indicate that TLR9 and gp96 can be co-immunoprecipitated in the lysosomal compartment of HEK293 cells, however, this result must be confirmed using alternative methods. This stable

association between TLR9 and gp96 most likely protects TLR9 from proteases, as inhibition of gp96 function by pretreatment with WS13 or the commercially available gp96 inhibitor geldanamycin increases the sensitivity of TLR9 to proteolysis. The sensitivity to proteolysis is most likely caused by a conformational change in TLR9 after inhibition of gp96 function that exposes sites on the TLR9 protein that are normally buried, as it is not observed in geldanamycin or WS13 treated cells which are directly lysed in sample buffer.

Inhibition of gp96 function leads to induced proteolysis of TLR9 and generation of a fragment of TLR9 which was 80 kD in size, the same molecular weight as the proposed mature form (86,87). Contrary to what the literature suggests, increased 80 kD fragment generation did not correlate with enhanced response to CpG DNA, but rather a reduction. This contradiction between the published literature and my own results led me to address whether or not the 80 kD mature form of TLR9 is sufficient to reconstitute CpG DNA induced signaling. I have shown that enhancing cleavage of TLR9 in a cell line that does not normally cleave TLR9, HEK293 cells, via co-transfection with the ER transmembrane protein UNC93B1 only increases the magnitude of response to CpG DNA at low concentrations of UNC93B1. Furthermore, expression of mTLR9$^{471\text{-}1032}$-HA alone was insufficient to reconstitute CpG DNA induced signaling in HEK293 cells and when co-expressed with mTLR9, mTLR9$^{471\text{-}1032}$-HA was able to both associate with, and reduces the response of, full length TLR9 to CpG DNA. In cell types that normally generate mature TLR9, such as macrophages or DCs, mTLR9$^{471\text{-}1032}$-HA alone was insufficient to reconstitute CpG DNA induced phosphorylation of the MAP kinase p38,

or TNF-α induction. The inability of mTLR9$^{471-1032}$-HA to reconstitute CpG induced signaling correlates with an inability to traffic outside of the ER compartment as determined through complete sensitivity of mTLR9$^{471-1032}$-HA glycosylations to endo H treatment.

Mechanisms of GA and WS13 and their effect on TLR9 proteolysis and signaling

The two inhibitors used in this study, geldanamycin and WS13, have different mechanisms of gp96 inhibition. In cells pretreated with geldanamycin, little to no gp96 was co-immunoprecipitated with TLR9, while co-immunopreciptation between TLR9 and gp96 was unaffected by WS13 (Figure 3.9A). Crystallographic and biochemical investigations suggest that geldanamycin preferentially interacts with Hsp90 in an apo, open-conformation, that is unfavorable for certain client protein binding (106,110-112). In contrast, PU-H71 and WS13 preferentially associate with an ATP-bound conformation of Hsp90, or for WS13, gp96, which stabilizes client protein/Hsp interaction (113). Thus, while recognizing similar Hsp90 species, WS13 and geldanamycin induce distinct conformations in Hsp90 and/or gp96 upon binding, leading to client protein trapping or release, respectively. Since both inhibitors block CpG DNA-induced signaling (Figure 3.1) and increase TLR9 proteolytic sensitivity (Figure 3.10D), we conclude that the chaperoning activity of gp96 requires both binding to and dissociation from TLR9. Although I attempted to address whether or not CpG DNA associated TLR9 remains associated with gp96, the results were inconclusive because gp96 bound CpG DNA (Figure 3.7). Indeed, gp96 from non-TLR9 expressing cells was affinity purified by 3'biotinylated CpG DNA (Figure 3.7). Previously published data using an electrophoretic

mobility shift assay demonstrated that cytosolic Hsp90 also bound stimulatory CpG DNA sequences (105). Warger et al demonstrated that incubation of the gp96 N-terminus with concentrations of TLR2 or TLR4 ligands too low to activate dendritic cells induced both dendritic cell maturation and proinflammatory cytokine production (114). These data support my result that gp96 itself binds CpG DNA.

Model for gp96 regulation of TLR9 signaling

Our findings have uncovered a new role for the heat shock protein gp96 in the multi-step process of TLR9 maturation and intracellular trafficking as summarized in Figure 4.1. Upon exit from the ER, TLR9 transits through the Golgi apparatus and it is sorted to endolysosomes (52,53,55). Once in the endosomal compartment, TLR9 is proteolytically processed to generate an 80-kDa fragment containing about one-half of the ecto-domain, the transmembrane domain and the cytoplasmic tail (86,87). This form of the receptor is proposed to be the mature form of TLR9 that binds CpG DNA and elicits a cellular response. In the absence of functional gp96, TLR9 is not appropriately trafficked or proteolytically processed (Figure 4.1 “1”) (67,72,73). Therefore, a major function of gp96 is to chaperone TLR9 in the ER, assisting TLR9 in folding, maturation and exit from the ER. The ER-resident protein CNPY3 (PRAT4A) assists gp96 in chaperoning TLRs by coordinating binding of gp96 to its client protein, TLR9 (67). Another chaperone, UNC93B1, is required for TLR9 endosomal translocation (Figure 4.1 “2”) (57). One potential hypothesis to explain the reduced ER exit of TLR9 in the absence of functional gp96 may be that gp96 is required for formation of a TLR9-UNC93B1 complex.

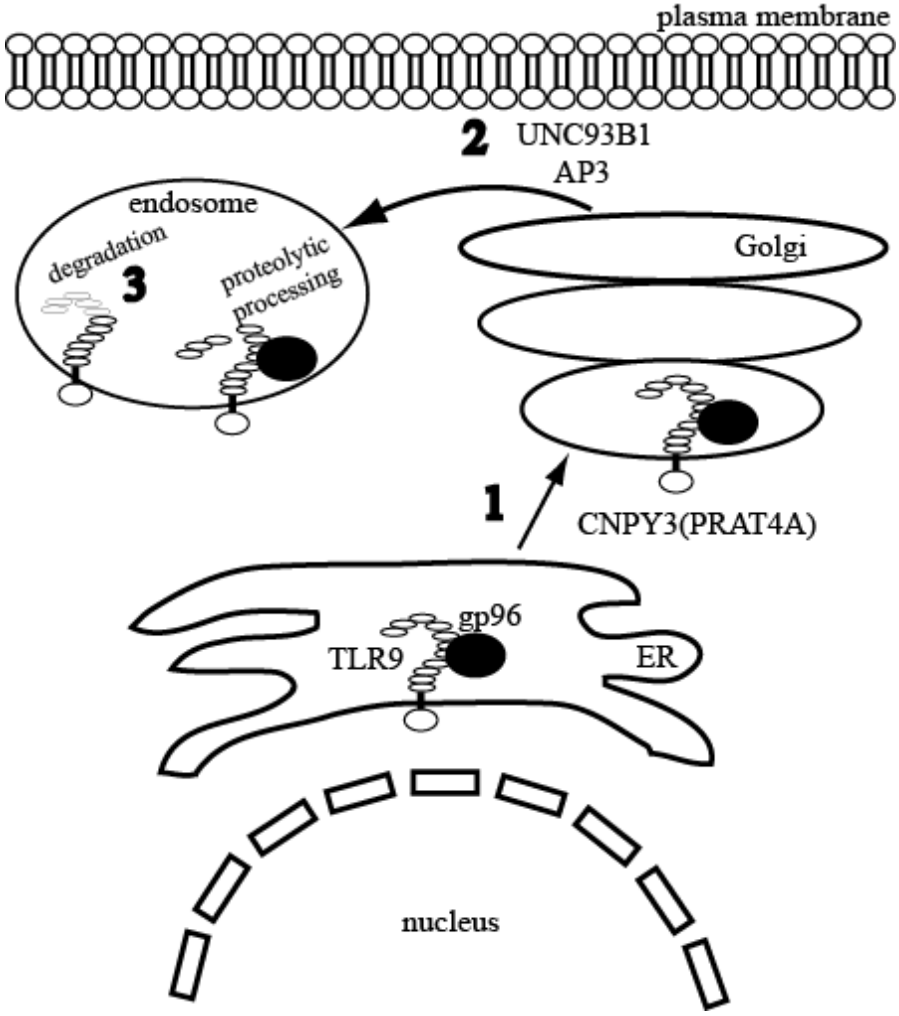

Figure 4.1. Model for TLR9 regulation by gp96. (1) Following synthesis in the ER, TLR9 traffics to the Golgi. In the absence of gp96 or CNPY3 (PRAT4A), TLR9 fails to exit the ER. (2) UNC93B1 associates with TLR9 and is required for TLR9 sorting to endosomes. Endosomal trafficking of TLR9 is also dependent on AP3. Once in endosomes, TLR9 remains associated with gp96 to maintain conformational stability. (3) Based on my studies I propose that in endosomes, TLR9 is protected by gp96 until TLR9 can bind CpG DNA. Disruption of the TLR9-gp96 interaction inhibits signaling and increases TLR9 sensitivity to proteolytic digestion.

Recent data have also implicated adaptor protein 3 (AP3) in the endosomal translocation of TLR9; however, there is disagreement as to the exact role of AP3 in cytokine and interferon production. Sasai et al. demonstrated that plasmacytoid DC from AP3 deficient mice were unable to produce type I interferon in response to CpG DNA while IL-12 production was normal (75). They went on to show that in the AP3 deficient mice TLR9 failed to colocalize with lysosome-related organelles (75) This report contradicts the published literature which states that CpG DNA induced type I interferon production initiates from endosomes while proinflammatory cytokine production initiates from the lysosomal compartment (35). In contrast, Blasius et al showed a global defect in CpG DNA induced cytokine production (both proinflammatory and type I interferon) from the same AP3 deficient mouse strain (77). Here, we have shown that TLR9 and gp96 both traffic to lysosomes and that inhibition of gp96 inhibits signaling and increases sensitivity of TLR9 to proteolysis (Figure 3.1, Figure 3.10, and Figure 4.1 "3").

Potential mechanisms of TLR9 regulation via gp96

There are several potential mechanisms by which gp96 may regulate TLR9. The ecto-domain of TLR9 forms a solenoid of two sets of leucine rich repeats separated by an unordered hinge, and proteolytic processing in endosomes at the hinge generates two fragments, the mature form and the remaining N-terminus (N-ter). Co-immunoprecipitation analysis has revealed that these two cleavage fragments remain associated (87). Therefore one possibility is that gp96 may bridge the mature form and N-ter fragments following proteolytic cleavage. Although the mature form of TLR9 has been proposed to signal in response to phosphorothioate modified synthetic CpG DNAs,

the N-ter also contains ligand-binding domains (115), and may contribute to CG dinucleotide specificity. Therefore, gp96 may be required to bring the different DNA binding domains in close proximity to allow for appropriate ligand binding that could facilitate either qualitative or quantitative modification of the response (discussed in greater detail below). A second possibility is that gp96 may associate with TLR9 that failed to successfully mature and is destined for degradation in lysosomes. However, if gp96 targeted TLR9 to the lysosome for degradation, one would predict that dissociation should prevent proteolysis, not enhance proteolysis as we detected (Figure 3.10B).

The most likely mechanism by which gp96 regulates TLR9 is that gp96 maintains conformational stability of the TLR9 ecto-domain. We showed that treatment of cells with geldanamycin and WS13 increased TLR9 sensitivity to proteolytic processing (Figure 3.10D). In our hands we observe much more mature TLR9 in macrophage lysates than full length TLR9, making detection of the full length protein variable and problematic (Figure 3.10D). However, using our assay we were able to observe a reproducible effect on the proteolysis of the mature form of TLR9 once gp96 was inhibited. Inhibition of gp96 increases the sensitivity of TLR9 to proteolysis (Figures 3.10B and 3.10D).

Previous studies demonstrated that TLR9 undergoes a major conformational change upon ligand binding (104). Using a TLR-Fc fusion protein, Latz et al published that the fusion protein alone demonstrated a circular dichroism (CD) spectrum indicative of a well folded protein (104). When CpG DNA was combined with the fusion protein, they

observed a shift in the CD spectrum consistent with a ligand induced conformational change (104). Latz et al. supported this study using FLIM-FRET analysis. FRET measures radiation-free energy transfer from an excited donor fluorophore to an acceptor fluorophore. Fluorescence lifetime imaging microscopy (FLIM), on the other hand, measures the amount of time required for an excited fluorophore to decay. Using the FLIM-FRET technique, Latz et al. demonstrated that there is a distance of 7.3 nm between the N and C terminus of TLR9, and the addition of CpG DNA reduced the distance by 12%, indicative of a large conformational change in the protein (104). Finally, they utilized a split GFP system consisting of fusing each half of a GFP monomer to TLR9 and then expressing both in the same cell. The two GFP fragments are not fluorescent unless brought into close proximity. Only when CpG DNA was added was GFP fluorescence detected indicating that CpG DNA induced a conformational change in TLR9 (104).

Our data are consistent with gp96 playing a similar role for TLR9 to that of cytoplasmic Hsp90 and its most well studied client proteins, steroid receptors (SR). In this model the TLR9 polypeptide chain would associate with CNPY3 much the same way that the cytosolic SRs first associate with Hsp40, then Hsp70 (116). CNPY3 would assist in the loading of the TLR9 polypeptide chain onto gp96, which will facilitate folding of TLR9. After folding, gp96 would remain associated with TLR9, maintaining TLR9 in a ligand-accessible conformation (97,99). Interestingly, in the case of Hsp90, a protein called p23 associates with the Hsp90-SR complex and blocks Hsp90 in a substrate-binding conformation reinforcing stable association with its SR client (97,117,118). Perhaps

CNPY3 plays a similar role for gp96 in addition to facilitating gp96 binding to its substrates. Alternatively, there may be yet another unidentified protein in the TLR9 complex which will fill this role. Without gp96 function, TLR9 likely unfolds, increasing its sensitivity to proteases, and reducing its ability to bind CpG DNA. This hypothesis will discussed in greater detail below.

Treatment with geldanamycin increases the sensitivity of TLR9 to proteolytic degradation, not proteolytic degradation itself, similar to what is observed for the glucocorticoid and progesterone receptors (119,120). We believe that gp96 is regulating TLR9 function by maintaining its conformational stability and protecting TLR9 from premature proteolytic degradation in the endolysosomal compartment (Figure 4.1 "3"). Premature proteolytic degradation of TLR9 could result in two major outcomes. The first possibility is that the premature proteolytic degradation could result in the mature form of TLR9 being present in an intracellular compartment where it is colocalized with, and can respond to, self-DNA. This is similar to what is observed with the TLR9-4 chimera, which mislocalizes to the cell surface where it detects self-DNA (54). The second possibility is that the premature proteolytic cleavage of TLR9 results in a rapid degradation of TLR9, so that it cannot bind and respond to microbial or self DNA. This would be analagous to the inhibition observed on glucocorticoid or progesterone receptor signaling when cells are treated with geldanamycin (119,120). It is important to note that gp96 itself is destabilized at pH$\leq$5 (121), which would be encountered in lysosomes. This suggests that gp96 would maintain ligand-binding conformation in most endosomes, but when the gp96-TLR9 complex traffics to late endosomes, gp96 will dissociate and TLR9

will be degraded. This is likely a mechanism for TLR9 turnover to maintain low abundance of TLR9 in this compartment.

TLR9-gp96 interaction outside of the ER

Previous studies supported a role for gp96 in ensuring proper folding of TLR9 and exit from the ER compartment. This conclusion was based on the observations that, in the absence of functional gp96, TLRs 1, 2, and 4 were not detected on the cell surface, and there was no generation of mature TLR9 (66,67,72,73). If these were the only roles that gp96 played in TLR9 signaling, one would envision a relatively short term interaction between the two proteins. However, my data demonstrates a stable association between TLR9 and gp96. Combined with my data demonstrating that inhibition of gp96 function induces proteolytic cleavage of TLR9, yet inhibits signaling, I propose that gp96 has additional functions in TLR9 biology once TLR9 has exited the ER. Perhaps TLR9 still exits the ER in the absence of gp96, but once it enters the endosomal compartment, it is rapidly turned over due to an increased sensitivity to proteases. This hypothesis is supported by my data using the gp96 MT B cells which show that although reduced when compared to WT, a very small amount of mature TLR9 is still generated in the MT cells (Figure 3.9E). In addition, DSL binds to a small portion of full length TLR9 from the gp96 MT cells indicating that TLR9 is glycosylated in the Golgi (Figure 3.9D). These data suggest that TLR9 exits the ER in the absence of functional gp96, albeit to a much lesser extent. Although the concept of stable association of gp96 with its client proteins would be novel, it fits well when compared to cytoplasmic Hsp90. Although its chaperone functions are substrate specific Hsp90 is thought to remain associated with its

client proteins to perform two major functions; either protecting its client proteins from proteosome mediated degradation, or maintaining them in a conformation that is conducive to ligand binding (discussed in greater detail below) (97-99,122).

Role of proteolysis in TLR9 signaling

In contrast to the current model where the 80 kD fragment of TLR9 is the mature and active form of the protein (82,86-88), my data suggest that the 80 kD fragment of TLR9 is insufficient in any cell type, and certainly not necessary in others, to reconstitute CpG DNA induced signaling. This is supported by several published studies, as mentioned below (Table 4.1). Despite the ability to respond robustly to CpG DNA in a TLR9 dependent manner, HEK293 cells fail to proteolytically process TLR9 to the mature form (55,80,85,86). More compelling perhaps, is the fact that, in B cells, very little proteolytic cleavage of TLR9 occurs, yet these cells respond to CpG DNA (Figure 3.5 and 3.10). Furthermore, even among the cell types that have been published to robustly cleave TLR9 there seem to be multiple cleavage events. Generation of the mature form of TLR9 was initially observed in macrophage phagosomes and depended on cathepsins (82,86,87). However, in dendritc cells, the processing of TLR9 relies on AEP and generates additional cleavage products (88). A chimeric receptor consisting of the ectodomain of TLR9 and the transmembrane domain of cytoplasmic tail of TLR4 localizes to the plasma membrane and responds to CpG DNA, but it is not proteolytically cleaved (54). Yet, the same group showed that TLR9 fused to a yeast ist2 sequence localized to the plasma membrane, was not cleaved, but now failed to respond to CpG DNA (86).

Table 4.1 Summary of published data demonstrating that proteolytic cleavage of TLR9 does not correlate with signaling

Construct	Proteolytic Cleavage	Signaling	Reference
TLR9	Yes	Yes	(86,87)
TLR9 + Bafilomycin	No	No	(86)
TLR9-4	No	Yes	(54)
TLR9-ist2	No	No	(86)
TLR9 (B cells)	No	Yes	Figure 3.9E
TLR9 (HEK293)	No	Yes	(55,80,85)

Therefore, mislocalization and cleavage does not directly correlate with signaling. Finally, neutralization of endosomal acidification inhibits both proteolytic cleavage in macrophage and response to CpG DNA in macrophage and HEK293 cells (30,31,35,87). In 2004 Rutz et al. utilized recombinant fusion proteins consisting of the ectodomain of murine TLR9 and the Fc portion of human IgG1 (mTLR9ect) in surface plasmon resonance biosensor-based assays to examine the binding between TLR9 and CpG (81). Data from Rutz et al. demonstrated that inhibitors of endosomal acidification such as chloroquine, quinacrine, and bafilomycin A1 inhibit CpG DNA binding to TLR9 (81).

In my hands mTLR9$^{471\text{-}1032}$-HA is insufficient to reconstitute CpG DNA induced signaling in TLR9$^{-/-}$ BMDC (Figure 3.15), this is in contrast to published studies (87). This is despite using published primers to generate the mTLR9$^{471\text{-}1032}$-HA construct and verifying it by sequencing. The experiment was performed the same as previously published with the exception of using a longer stimulation time. Thus I was unable to confirm the only published example of mTLR9$^{471\text{-}1032}$ activity. However, this does not eliminate the possibility that while the mature form of TLR9 may not be sufficient for CpG DNA induced signaling, it may be required. The fact that not all cell types proteolytically cleave TLR9 could merely suggest that mechanisms of regulating TLR9 are not universal among all cell types. This view is supported by the observation that different cell types will produce different cytokines when stimulated with CpG DNA. For example, human pDCs predominantly produce type I interferon when stimulated with CpG DNA while macrophages predominantly produce proinflammatory cytokines (17,36). Data presented in this thesis demonstrate that mature TLR9 is insufficient to

reconstitute CpG DNA induced responses, most likely due to an inability to traffic out of the ER compartment (Figure 3.14). If mature TLR9 is in fact necessary in some cell types my data would suggest that there is an unidentified role for the N-ter in TLR9 biology (explored further below).

Redefining the model of TLR9 trafficking and signaling

The current dogma for the initiation of TLR9 signaling is that the protein is initially folded in the ER in a manner dependent on the co-chaperones gp96 and PRAT4A(CNPY3) (52,53,60,67,72). TLR9 exits the ER via an association with the transmembrane protein UNC93B1 and traffics through the Golgi apparatus to the endolysosomal compartment (55-57,83). Once TLR9 reaches endosomes it is proteolytically processed to a mature and active 80 kD form (82,86-88).

My thesis challenges this model in two ways. First I propose that gp96 has additional functions in TLR9 biology, other than facilitating its folding in the ER. My data using cycloheximide reveals that the TLR9-gp96 interaction is stable, not transient (Figure 3.3A). Using organelle fractionation I have preliminary results showing that both full length TLR9 and gp96 are associated in the lysosomal compartment (Figure 3.3B and C). The Leifer lab previously showed that TLR9 and the TLR signaling adaptor MyD88 are constitutively associated in the lysosome, indicating that this is the pool of TLR9 which is responding to CpG DNA (55). I have also shown that inhibition of gp96 function inhibits TLR9 signaling and increases its sensitivity to proteolytic degradation (Figure 3.5C). Taken together, these data show that gp96 is not just a chaperone responsible for

folding TLR9 in the ER compartment, but that, much like Hsp90, gp96 remains associated with TLR9 and both protecting its client from proteolytic degradation as well as stabilizing it in a ligand binding conformation. The TLR9-gp96 interaction most likely persists to the lysosomal compartment (Figure 3.3B and C) where the CpG DNA induced proinflammatory cytokine production initiates (35). However, if no CpG DNA is present to bind to and stabilize TLR9 the low pH of the lysosomal compartment ($pH \leq 5$) will cause destabilization of gp96 (121) resulting in dissociation from TLR9 and subsequent proteolytic degradation of TLR9. This could be a mechanism to regulate the amount of TLR9 available for CpG DNA binding in the endolysosomal compartment.

The second major area challenged by this thesis is the role of proteolysis in TLR9 signaling. As stated previously, the data present in the literature do not universally support the concept of obligate proteolytic cleavage to activate TLR9 (Table 4.1). My own data demonstrate that mTLR9$^{471-1032}$-HA alone is insufficient to reconstitute CpG DNA induced signaling in fibroblasts, macrophages, or dendritic cells (Figure 3.11, 3.14, and 3.15), contradicting the only published report of mTLR9$^{471-1032}$ function available in the literature (87). My data also show that, on its own, mTLR9$^{471-1032}$-HA fails to exit the ER, and the addition of the TLR9 hinge region fails to rescue mature TLR9 signaling or ER exit (Figure 3.9 B and D). Indeed, when co-expressed with mTLR9-GFP, mTLR9$^{471-1032}$-HA is able to associate with, and reduce the signaling of, mTLR9-HA most likely by preventing it from exiting the ER compartment (Figure 3.8).

In summary, I propose a new model in which interaction between TLR9 and gp96 is both

necessary in the ER to ensure maturation and after ER exit to maintain conformational stability. In the absence of gp96, TLR9 fails to exit the ER or is rapidly degraded once it moves beyond the ER compartment. The TLR9-gp96 interaction is stable over the half-life of TLR9 and both proteins are associated in the lysosomal compartment. Inhibition of gp96 function changes the conformation of TLR9 and enhances sensitivity to proteolysis. Despite generating an 80 kD fragment analogous in size to the mature form, this proteolytic cleavage inhibits signaling. Proteolytic cleavage is not required in all cell types to facilitate CpG DNA induced signaling and the mature form of TLR9 alone is insufficient to reconstitute a response to CpG DNA. However proteolytic cleavage of TLR9 may be required in a smaller subset of cell types, such as macrophages and dendritic cells. It is difficult to conclude this because the inhibitors used to block cleavage and TLR9 signaling also directly block TLR9 binding to CpG DNA (81,82,86). Regardless of the requirement for proteolytic cleavage in TLR9 signaling, I speculate that the TLR9 N-ter plays an important but unidentified role in TLR9 trafficking or coordinating accessory protein binding.

CHAPTER 5:

FUTURE DIRECTIONS

Role of TLR9-gp96 interaction outside the ER

My preliminary results indicate that TLR9 and gp96 are associated in the lysosomal compartment of HEK293 cells (Figure 3.3). While the data are promising, further experiments should be performed to strengthen the co-immunoprecipitation data (Figure 3.3D). One approach would be to perform confocal microscopy on TLR9$^{-/-}$ macrophages retrovirally transduced with full length TLR9. These reconstituted macrophages could be immunostained for TLR9, gp96 and markers for the endosomal or lysosomal compartment (Rab 5 and LAMP-1, respectively), and Pearson's coefficients could be calculated to determine the extent of TLR9-gp96 colocalization in both endosomes and lysosomes. This approach would both add support to the co-immunoprecipitation data but also reproduce the finding in macrophages, which will normally express TLR9.

A second area for future study is the role that gp96 association plays in TLR9 biology outside of the ER compartment. Based upon the data presented in this study, that inhibition of gp96 function inhibits CpG DNA induced TLR9 responses and increases TLR9 sensitivity to proteolysis, I would predict that the function of gp96 is to protect TLR9 from proteolytic degradation and assist TLR9 in binding CpG DNA (Figure 3.1 and 3.10) Organelle fractionation of either gp96 mutant cells or cell specific gp96 knockouts would be useful in confirming the presence of TLR9 outside the ER in the absence of gp96. Similarly it would be interesting to address whether or not gp96

dissociation from TLR9 is required for cleavage to occur. My data on dissociation of gp96 and enhanced proteolysis of TLR9 would argue for this point. One method to address this question would be to first feed or "pulse" cells with ^{35}S-methionine to label all newly synthesized TLR9. The pulsed cells could then be treated with cycloheximide to stop any further protein synthesis, then at fixed time points post cycloheximide treatment, organelle fractionation could be preformed and lysosomes isolated. These lysosomes could be lysed and immunoprecipitated for TLR9 and examined by auto-radiograph for TLR9 and immunoblotting for gp96. The ^{35}S-methionine pulse labeling would allow for the monitoring, or "chasing" of one pool of TLR9 as it traffics out of the ER to the endolysosomal compartment. In addition, immunoprecipitation from LAMP1 positive fractions would explore the TLR9-gp96 interaction specifically in the endolysosomal compartment where proteolytic cleavage occurs (82,86-88). My data demonstrates that inhibiting gp96 function with WS13, which reinforces gp96-client protein interactions, still enhances sensitivity of TLR9 to proteolysis (Figure 3.10D). However, from this experiment, we can not observe the effect on full length TLR9. Additional data presented in this study suggest that full length TLR9 may be stabilized when cells are treated with WS13, which would suggest that dissociation of gp96 is required for generation of mature TLR9 (Figure 3.10A, compare WS13 treated to GA treated)**.** In the context of the pulse-chase experiment outlined above I would predict that the TLR9, which had been proteolytically cleaved, would not be associated with gp96. Although I attempted to address whether or not TLR9 that had bound CpG DNA was still bound to gp96, no conclusions could be drawn due to the fact that gp96 was able to bind CpG DNA in the absence of TLR9 (Figure 3.7). Another approach would be to attempt to

purify TLR9 from gp96 MT B cells using 3'biotinylated CpG DNA. This experiment would directly address whether or not TLR9 is able to bind to CpG DNA in the absence of gp96.

Using gp96 inhibitors as therapeutics

Hsps have a long history as therapeutic targets for the treatment of diseases, most notably Hsp90 in cancer (123-128). Hsp inhibitors also demonstrate therapeutic promise through their immunosuppressive effects. For example, Hsp90 inhibitors halt disease progression in models of rheumatoid arthritis (129,130). However, targeting Hsp90 remains challenging, as many client proteins depend on its chaperoning function. Thus, inhibition of Hsp90 function may have far reaching effects on many normal cellular processes and be highly toxic with many adverse side effects. For example, inhibition of Hsp90 via geldanamycin results in suppressed ERK, glucocorticoid receptor, and progesterone receptor signaling (100,119,120) Furthermore, in the case of geldanamycin and its derivatives, the drugs themselves display dose-limiting liver toxicity (131). gp96, on the other hand, has a much smaller repertoire of known client proteins, making it a more attractive therapeutic target.

gp96 may be immunologically active when detected extracellularly. A transgenic mouse with constitutive expression of gp96 at the cell surface via a cytomegalovirus promoter-driven construct (96tm-Tg) developed systemic lupus erythematosus (SLE) like disease at >20 weeks of age (132). This SLE-like disease was characterized by both IgA and IgG immune complex deposition in the glomeruli of the kidney resulting in

glomerulonephritis and enhanced DC activation (132). Disease was also dependent on the TLR signaling adaptor MyD88 as lethally irradiated 96tm-Tg mice reconstituted with MyD88$^{-/-}$ bone marrow failed to develop any SLE-like disease (132). These data suggest that gp96 itself can be recognized as a "danger signal" by the immune system when detected outside of the cell and this recognition occurs via a TLR. Published data also show an increased expression of gp96 in the synovial fluid of human patients with rheumatoid arthritis (133). Previous data have also shown that inhibition of TLR9 signaling protected mice from both autoimmune arthritis and autoimmune encephalomyelitis (134). These results, taken together with my data demonstrating that specific inhibition of gp96 inhibits TLR9 signaling, lend support to the idea of using the gp96 specific inhibitor WS13 as a means to control autoimmune diseases in which TLR9 plays a role, such as SLE. While the exact role that TLR9 plays in SLE remains unclear, TLR9 deficient mice have reduced anti-DNA antibodies, but enhanced disease (91). A specific role for TLR9 in B cell responses to DNA containing immune complexes was supported by studies using a mouse expressing a transgenic "rheumatoid factor" receptor (explored in further detail below). In vitro stimulation with immune complexes that included DNA, such as anti-nucleosome complexes, induced proliferation of the transgenic B cells while non-nucleic acid complexes, such as BSA-anti-BSA complexes, did not. The response was DNase sensitive and dependent on MyD88 and uptake of the immune complexes into the endosomal compartment (34).

Since constant suppression of TLR function would be detrimental to the host in terms of general immune function and pathogen recognition it would not be ideal to administer

gp96-specific inhibitors daily. However, one could imagine a treatment regimen in which gp96-specific inhibitors are only administered during disease reactivation to manage symptoms. It would be beneficial to test WS13 as a therapeutic in a mouse model of autoimmune disease such as the AM14 transgenic mice. The B cells of AM14 transgenic mice constitutively express an immunoglobulin heavy chain which when combined with the Vκ8 light chain yields a B cell receptor specific for mouse IgG2a antibodies, also called rheumatoid factor (RF) (135). This mouse model of SLE is more comparable to the human disease since these RF positive B cells only constitute a small portion of the total circulating B cell population (135-137). The main advantage of the AM14 transgenic model is that it allows for controlled administration of the autoantigen-immune complexes, for example, IgG2a antibody in complex with DNA to induce disease. The AM14 model allows for induction of autoimmune disease in the presence or absence of WS13, different time courses and dosages could also be explored. Since WS13 treatment inhibits TLR9 signaling, and TLR9 signaling plays a role in SLE disease progression, I would hypothesize that treatment with WS13 would result in a less severe disease. However, the role that TLR9 plays in SLE is unclear with the published literature demonstrating a more dominant role being played by TLR7 (91,138). Although given that TLR7 and TLR9 are structurally very similar and seem to share common regulatory mechanisms, like proteolytic cleavage and the requirement for UNC93B1, perhaps WS13 will also inhibit TLR7 dependent responses (9,56,57,82,83,86). This question could be addressed by pretreating RAW 264.7 macrophages with WS13 or DMSO control and the stimulating with the TLR7 ligand loxoribine. Supernatants from the stimulated cells could then be collected and assayed for the presence of the cytokine TNF-α by ELISA.

Alternatively, after the WS13 or DMSO treated cells are stimulated with loxoribine, brefeldin A could be added to prevent secretion of cytokines. The brefeldin A treated cells could be fixed, permeabilized and immunostained with antibodies to TNF-α to be assayed by flow cytometery.

A second caveat to using WS13 as a therapeutic is the possibility of infection. Even though other TLRs will be localized to the correct compartments to respond to ligand and thus won't need gp96 function any longer, treatment with WS13 will inhibit the newly synthesized TLRs from trafficking to the correct compartment. This inhibition will eventually result in global signaling defects through most TLRs, and the opportunity for invasion by pathogens. Nevertheless, using WS13 to manage symptoms in autoimmune diseases such as SLE is just one potential regimen for using gp96 specific inhibitors as immunotherapeutics.

The role of the N-terminal portion of TLR9

My data indicate that there is a yet unidentified role for the TLR9 N-ter that is removed when the mature form of TLR9 is generated (Figure 1.3). Inspection of the TLR9 N-ter sequence reveals that there are potential DNA binding domains present in this portion of TLR9 which is removed when the mature form of TLR9 is generated (115). Since the TLR9 N-ter can be detected, via co-immunoprecipitation, in association with the mature form of TLR9, the N-ter could modify the response of mature TLR9, either qualitatively or quantitatively (87) The synthetic CpG DNA utilized by most researchers is phophorothioate modified because this form of DNA more stable in vitro and in vivo

(139). However, naturally occurring CpG DNA bears a phosphodiester modification (17). Current studies have examined the role of the mature form of TLR9 in response only to synthetic, phosphorothioate modified CpG DNA, not the more physiologically relevant phosphodiester modified CpG DNA (87,140-142). This is an important caveat because it the sequence specificity of the CpG hexamer motif (GACGTT for mouse and GTCGTT for human) is lost when the DNA backbone is phosphorothioate modified (22,81,139).

Stimulatory CpG DNAs can be grouped into three main categories based on the type of response they induce. The first, class A, is characterized by induction of type I interferon production while class B CpG DNA induces B cell maturation and proinflammatory cytokine production (22). The third class, class C CpG DNA, displays properties of both class A and class B (28). More recently, a fourth class of stimulatory CpG DNA has been described. This class, called class P CpG DNA, functions similarly to class C CpG DNA in that it is able to induce both type I interferon and proinflammatory cytokine production. However, through the addition of a second pallindromic CpG sequence, P class CpG DNA induce higher type I interferon, as well as proinflammatory cytokine, production at a lower concentration than C class CpG DNA (143). Published studies on mature TLR9 function have only been conducted using class B CpG DNA and assaying for proinflammatory cytokine production, not class A CpG DNA and induction of type I interferons. I propose to reconstitute TLR9 deficient cells with either full length TLR9 or mature TLR9, both with and without the hinge, and assay these cells for their ability to respond to different classes of CpG DNA (A, B, C, or P) and different backbone compositions (phosphodiester or phosphorthioate).

It would also be informative to use the mTLR9$^{471\text{-}1032}$-HA and mTLR9$^{441\text{-}1032}$-HA constructs that I have generated and attempt to restore response to CpG DNA by providing the TLR9 N-ter. This could be done either in *cis*, in the same vector via and internal ribosomal entry site, or in *trans*, on two separate vectors (Figure 4.2). I expect that providing the N-ter in cis or trans, on two separate plasmids, will reconstitute function in both mTLR9$^{471\text{-}1032}$-HA and mTLR9$^{441\text{-}1032}$-HA constructs. On their own both mTLR9$^{471\text{-}1032}$-HA and mTLR9$^{441\text{-}1032}$-HA remain sensitive to endoglycosidase H which I interpret to mean that the two constructs fail to exit the ER compartment. I hypothesize that the TLR9 N-ter is essential for ER exit. Since the N-ter retains the ability to associate with mature TLR9 post cleavage when the two products are expressed in the same cell they should be able to associate, traffic out of the ER, and respond to ligand (87). In addition I expect that the N-ter will modify the response to CpG DNA by defining specificity to both the various physical and chemical structures of DNA and the different classes of CpG DNA. Using retroviral transduction to perform these experiments in different cell types will also address the requirement for proteolytic cleavage in different cell types. The main caveat to this study is the assumption that the two constructs of TLR9, mTLR9$^{471\text{-}1032}$-HA and mTLR9$^{441\text{-}1032}$-HA, will be able to associate with the TLR9 N-ter. Published data demonstrates that mature TLR9 and the TLR9 N-ter associate by co-immunoprecipitation analysis. (87).

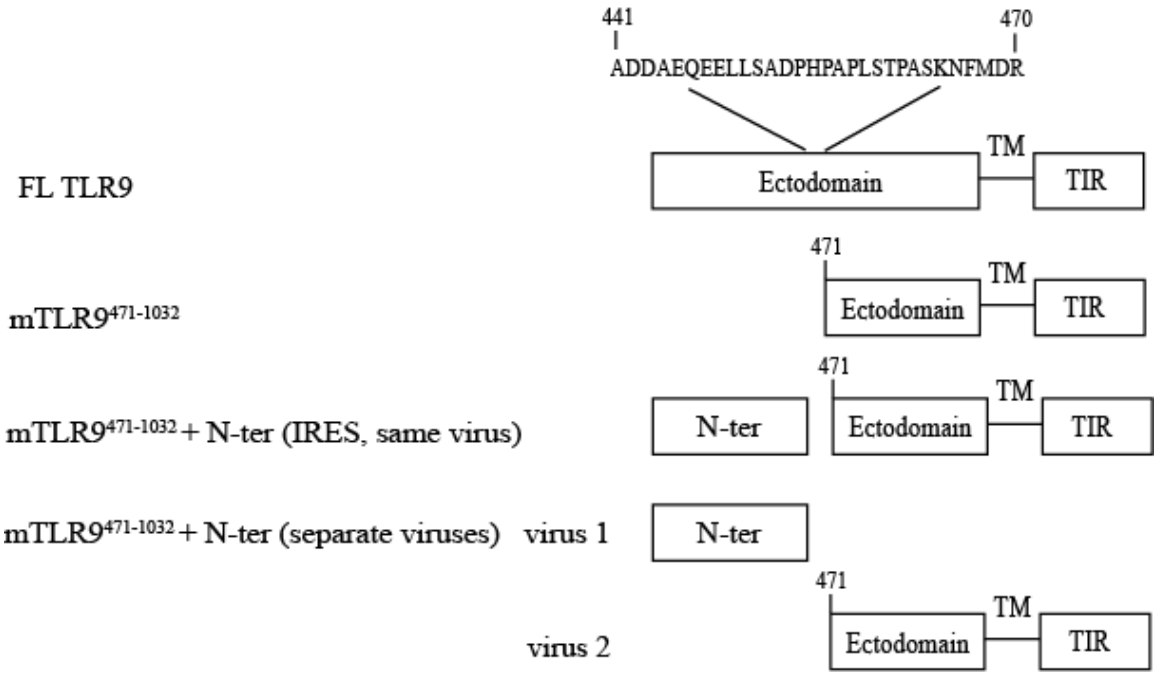

Figure 5.1. System for determining the role of N-ter in TLR9 signaling. TLR9$^{-/-}$ cells (macrophages and dendritic cells) will be retrovirally transduced with plasmids encoding full length (FL) TLR9, mature TLR9 (mTLR9$^{471-1032}$), mature TLR9 + N-ter on the same vector via an internal ribosome entry site (IRES), or on separate vectors. Retrovirally transduced cells can then be assayed for the ability to respond to CpG DNA of different class (A, B, or C) and chemistry (phosphorothioate and phosphodiester).

However, this is when the two fragments are generated from full length TLR9 in a macrophage, so we do not know if the two fragments will associate when expressed independently from a retroviral vector. Co-immunoprecipitation analysis of the retroviral constructs will confirm that mTLR9$^{471\text{-}1032}$-HA and mTLR9$^{441\text{-}1032}$-HA associate with TLR9 N-term.

Another possibility is that the N-ter coordinates binding of a chaperone essential for exit from the ER. Our data suggest that mTLR9$^{471\text{-}1032}$-HA fails to acquire endogycosidase H resistance, an indicator of trafficking through the Golgi (Figure 3.9D). I interpret this to mean that the mTLR9$^{471\text{-}1032}$-HA construct does not exit from ER compartment. Previous studies have shown that in the absence of two ER resident chaperones, gp96 and CNPY3, TLR9 fails to exit the ER compartment. Therefore, failure to associate with either protein is an attractive hypothesis to explain the inability of the mTLR9$^{471\text{-}1032}$-HA construct to exit the ER (67,72). A third ER resident protein, UNC93B1, has previously been shown to be critical for TLR9 exit from the ER, and its localization to, and cleavage in, endosomes (57,83,86). However, unlike gp96 and CNPY3, UNC93B1 is a transmembrane protein and interacts with TLR9 via its transmembrane domain (83). The proteolytic cleavage event in TLR9 that generates the mature form occurs in the ectodomain, leaving the transmembrane domain of the protein intact and unaltered (86,87). Since the transmembrane domain is unaltered there should be no deficiency in association of mTLR9$^{471\text{-}1032}$-HA with UNC93B1 making this an unlikely explanation for the inability of mTLR9$^{471\text{-}1032}$-HA to exit the ER. However, the TLR9 N-ter could be important for coordinating binding of UNC93B1 directly, or through an additional

protein that in turn allows UNC93B1 to bind to TLR9. Published data demonstrate that TLR9 lacking only the hinge region, fails to colocalize with *Aspergillus fumigatus* containing phagosomes, and has a reduced response to CpG DNA (87,107). These data support the hypothesis that the hinge region (aa 441-470) is itself important for proper intracellular trafficking of TLR9. Co-immunoprecipitations from $TLR9^{-/-}$ macrophages retrovirally transduced with either full length TLR9 or mature TLR9 would determine whether or not mature TLR9 retains the ability to bind to gp96, PRAT4A and UNC93B1. These experiments would address whether the TLR9 N-ter is necessary for binding to accessory proteins, and would illuminate the role that the TLR9 N-ter plays in TLR9 biology.

REFERENCES

1. Ozinsky, A., Underhill, D. M., Fontenot, J. D., Hajjar, A. M., Smith, K. D., Wilson, C. B., Schroeder, L., and Aderem, A. (2000) *Proc Natl Acad Sci U S A* **97**(25), 13766-13771

2. Takeuchi, O., Kawai, T., Sanjo, H., Copeland, N. G., Gilbert, D. J., Jenkins, N. A., Takeda, K., and Akira, S. (1999) *Gene* **231**(1-2), 59-65

3. Latz, E., Visintin, A., Lien, E., Fitzgerald, K. A., Espevik, T., and Golenbock, D. T. (2003) *J Endotoxin Res* **9**(6), 375-380

4. Hayashi, F., Smith, K. D., Ozinsky, A., Hawn, T. R., Yi, E. C., Goodlett, D. R., Eng, J. K., Akira, S., Underhill, D. M., and Aderem, A. (2001) *Nature* **410**(6832), 1099-1103

5. Alexopoulou, L., Holt, A. C., Medzhitov, R., and Flavell, R. A. (2001) *Nature* **413**(6857), 732-738

6. Heil, F., Hemmi, H., Hochrein, H., Ampenberger, F., Kirschning, C., Akira, S., Lipford, G., Wagner, H., and Bauer, S. (2004) *Science* **303**(5663), 1526-1529

7. Hemmi, H., Takeuchi, O., Kawai, T., Kaisho, T., Sato, S., Sanjo, H., Matsumoto, M., Hoshino, K., Wagner, H., Takeda, K., and Akira, S. (2000) *Nature* **408**(6813), 740-745

8. Xu, Y., Tao, X., Shen, B., Horng, T., Medzhitov, R., Manley, J. L., and Tong, L. (2000) *Nature* **408**(6808), 111-115

9. Bell, J. K., Mullen, G. E., Leifer, C. A., Mazzoni, A., Davies, D. R., and Segal, D. M. (2003) *Trends Immunol* **24**(10), 528-533

10. Bell, J. K., Botos, I., Hall, P. R., Askins, J., Shiloach, J., Segal, D. M., and Davies, D. R. (2005) *Proc Natl Acad Sci U S A* **102**(31), 10976-10980

11. Choe, J., Kelker, M. S., and Wilson, I. A. (2005) *Science* **309**(5734), 581-585

12. Jin, M. S., Kim, S. E., Heo, J. Y., Lee, M. E., Kim, H. M., Paik, S. G., Lee, H., and Lee, J. O. (2007) *Cell* **130**(6), 1071-1082

13. Kang, J. Y., Nan, X., Jin, M. S., Youn, S. J., Ryu, Y. H., Mah, S., Han, S. H., Lee, H., Paik, S. G., and Lee, J. O. (2009) *Immunity* **31**(6), 873-884

14. Park, B. S., Song, D. H., Kim, H. M., Choi, B. S., Lee, H., and Lee, J. O. (2009) *Nature* **458**(7242), 1191-1195

15. Bell, J. K., Askins, J., Hall, P. R., Davies, D. R., and Segal, D. M. (2006) *Proc*

Natl Acad Sci U S A **103**(23), 8792-8797

16. Takeda, K., Kaisho, T., and Akira, S. (2003) *Annu Rev Immunol* **21**, 335-376

17. Krieg, A. M. (2002) *Annu Rev Immunol* **20**, 709-760

18. Cardon, L. R., Burge, C., Clayton, D. A., and Karlin, S. (1994) *Proc Natl Acad Sci U S A* **91**(9), 3799-3803

19. Klinman, D. M., Yi, A. K., Beaucage, S. L., Conover, J., and Krieg, A. M. (1996) *Proc Natl Acad Sci U S A* **93**(7), 2879-2883

20. Krieg, A. M., Yi, A. K., Matson, S., Waldschmidt, T. J., Bishop, G. A., Teasdale, R., Koretzky, G. A., and Klinman, D. M. (1995) *Nature* **374**(6522), 546-549

21. Gursel, I., Gursel, M., Yamada, H., Ishii, K. J., Takeshita, F., and Klinman, D. M. (2003) *J Immunol* **171**(3), 1393-1400

22. Verthelyi, D., Ishii, K. J., Gursel, M., Takeshita, F., and Klinman, D. M. (2001) *J Immunol* **166**(4), 2372-2377

23. Klinman, D. M., Zeuner, R., Yamada, H., Gursel, M., Currie, D., and Gursel, I. (2003) *Ann N Y Acad Sci* **1002**, 112-123

24. Krieg, A. M., Wu, T., Weeratna, R., Efler, S. M., Love-Homan, L., Yang, L., Yi, A. K., Short, D., and Davis, H. L. (1998) *Proc Natl Acad Sci U S A* **95**(21), 12631-12636

25. Lenert, P., Yi, A. K., Krieg, A. M., Stunz, L. L., and Ashman, R. F. (2003) *Antisense Nucleic Acid Drug Dev* **13**(3), 143-150

26. Avalos, A. M., and Ploegh, H. L. (2011) *Eur J Immunol* **41**(10), 2820-2827

27. Lenert, P., Yasuda, K., Busconi, L., Nelson, P., Fleenor, C., Ratnabalasuriar, R. S., Nagy, P. L., Ashman, R. F., Rifkin, I. R., and Marshak-Rothstein, A. (2009) *Arthritis Res Ther* **11**(3), R79

28. Vollmer, J., Weeratna, R., Payette, P., Jurk, M., Schetter, C., Laucht, M., Wader, T., Tluk, S., Liu, M., Davis, H. L., and Krieg, A. M. (2004) *Eur J Immunol* **34**(1), 251-262

29. Manzel, L., and Macfarlane, D. E. (1999) *Antisense Nucleic Acid Drug Dev* **9**(5), 459-464

30. Hacker, H., Mischak, H., Miethke, T., Liptay, S., Schmid, R., Sparwasser, T., Heeg, K., Lipford, G. B., and Wagner, H. (1998) *Embo J* **17**(21), 6230-6240

31. Ahmad-Nejad, P., Hacker, H., Rutz, M., Bauer, S., Vabulas, R. M., and Wagner, H. (2002) *Eur J Immunol* **32**(7), 1958-1968

32. Tian, J., Avalos, A. M., Mao, S. Y., Chen, B., Senthil, K., Wu, H., Parroche, P., Drabic, S., Golenbock, D., Sirois, C., Hua, J., An, L. L., Audoly, L., La Rosa, G., Bierhaus, A., Naworth, P., Marshak-Rothstein, A., Crow, M. K., Fitzgerald, K. A., Latz, E., Kiener, P. A., and Coyle, A. J. (2007) *Nat Immunol* **8**(5), 487-496

33. Lande, R., Gregorio, J., Facchinetti, V., Chatterjee, B., Wang, Y. H., Homey, B., Cao, W., Wang, Y. H., Su, B., Nestle, F. O., Zal, T., Mellman, I., Schroder, J. M., Liu, Y. J., and Gilliet, M. (2007) *Nature* **449**(7162), 564-569

34. Leadbetter, E. A., Rifkin, I. R., Hohlbaum, A. M., Beaudette, B. C., Shlomchik, M. J., and Marshak-Rothstein, A. (2002) *Nature* **416**(6881), 603-607

35. Honda, K., Ohba, Y., Yanai, H., Negishi, H., Mizutani, T., Takaoka, A., Taya, C., and Taniguchi, T. (2005) *Nature* **434**(7036), 1035-1040

36. Guiducci, C., Ott, G., Chan, J. H., Damon, E., Calacsan, C., Matray, T., Lee, K. D., Coffman, R. L., and Barrat, F. J. (2006) *J Exp Med* **203**(8), 1999-2008

37. Avalos, A. M., Latz, E., Mousseau, B., Christensen, S. R., Shlomchik, M. J., Lund, F., and Marshak-Rothstein, A. (2009) *J Immunol* **183**(10), 6262-6268

38. Yakubov, L. A., Deeva, E. A., Zarytova, V. F., Ivanova, E. M., Ryte, A. S., Yurchenko, L. V., and Vlassov, V. V. (1989) *Proc Natl Acad Sci U S A* **86**(17), 6454-6458

39. Beltinger, C., Saragovi, H. U., Smith, R. M., LeSauteur, L., Shah, N., DeDionisio, L., Christensen, L., Raible, A., Jarett, L., and Gewirtz, A. M. (1995) *J Clin Invest* **95**(4), 1814-1823

40. Sano, H., and Morimoto, C. (1982) *J Immunol* **128**(3), 1341-1345

41. Boule, M. W., Broughton, C., Mackay, F., Akira, S., Marshak-Rothstein, A., and Rifkin, I. R. (2004) *J Exp Med* **199**(12), 1631-1640

42. Ishii, K. J., Suzuki, K., Coban, C., Takeshita, F., Itoh, Y., Matoba, H., Kohn, L. D., and Klinman, D. M. (2001) *J Immunol* **167**(5), 2602-2607

43. Yasuda, K., Yu, P., Kirschning, C. J., Schlatter, B., Schmitz, F., Heit, A., Bauer, S., Hochrein, H., and Wagner, H. (2005) *J Immunol* **174**(10), 6129-6136

44. Guiducci, C., Tripodo, C., Gong, M., Sangaletti, S., Colombo, M. P., Coffman, R. L., and Barrat, F. J. (2010) *J Exp Med* **207**(13), 2931-2942

45. Sato, T., Yamamoto, M., Shimosato, T., and Klinman, D. M. (2010) *Wound Repair Regen* **18**(6), 586-593

46. Gregorio, J., Meller, S., Conrad, C., Di Nardo, A., Homey, B., Lauerma, A., Arai, N., Gallo, R. L., Digiovanni, J., and Gilliet, M. (2010) *J Exp Med* **207**(13), 2921-

2930

47. Garcia-Romo, G. S., Caielli, S., Vega, B., Connolly, J., Allantaz, F., Xu, Z., Punaro, M., Baisch, J., Guiducci, C., Coffman, R. L., Barrat, F. J., Banchereau, J., and Pascual, V. (2011) *Sci Transl Med* **3**(73), 73ra20

48. Lande, R., Ganguly, D., Facchinetti, V., Frasca, L., Conrad, C., Gregorio, J., Meller, S., Chamilos, G., Sebasigari, R., Riccieri, V., Bassett, R., Amuro, H., Fukuhara, S., Ito, T., Liu, Y. J., and Gilliet, M. (2011) *Sci Transl Med* **3**(73), 73ra19

49. Villanueva, E., Yalavarthi, S., Berthier, C. C., Hodgin, J. B., Khandpur, R., Lin, A. M., Rubin, C. J., Zhao, W., Olsen, S. H., Klinker, M., Shealy, D., Denny, M. F., Plumas, J., Chaperot, L., Kretzler, M., Bruce, A. T., and Kaplan, M. J. (2011) *J Immunol* **187**(1), 538-552

50. Napirei, M., Karsunky, H., Zevnik, B., Stephan, H., Mannherz, H. G., and Moroy, T. (2000) *Nat Genet* **25**(2), 177-181

51. Yasutomo, K., Horiuchi, T., Kagami, S., Tsukamoto, H., Hashimura, C., Urushihara, M., and Kuroda, Y. (2001) *Nat Genet* **28**(4), 313-314

52. Latz, E., Schoenemeyer, A., Visintin, A., Fitzgerald, K. A., Monks, B. G., Knetter, C. F., Lien, E., Nilsen, N. J., Espevik, T., and Golenbock, D. T. (2004) *Nat Immunol* **5**(2), 190-198

53. Leifer, C. A., Kennedy, M. N., Mazzoni, A., Lee, C., Kruhlak, M. J., and Segal, D. M. (2004) *J Immunol* **173**(2), 1179-1183

54. Barton, G. M., Kagan, J. C., and Medzhitov, R. (2006) *Nat Immunol* **7**(1), 49-56

55. Chockalingam, A., Brooks, J. C., Cameron, J. L., Blum, L. K., and Leifer, C. A. (2009) *Immunol Cell Biol* **87**(3), 209-217

56. Tabeta, K., Hoebe, K., Janssen, E. M., Du, X., Georgel, P., Crozat, K., Mudd, S., Mann, N., Sovath, S., Goode, J., Shamel, L., Herskovits, A. A., Portnoy, D. A., Cooke, M., Tarantino, L. M., Wiltshire, T., Steinberg, B. E., Grinstein, S., and Beutler, B. (2006) *Nat Immunol* **7**(2), 156-164

57. Kim, Y. M., Brinkmann, M. M., Paquet, M. E., and Ploegh, H. L. (2008) *Nature* **452**(7184), 234-238

58. Fukui, R., Saitoh, S., Matsumoto, F., Kozuka-Hata, H., Oyama, M., Tabeta, K., Beutler, B., and Miyake, K. (2009) *J Exp Med* **206**(6), 1339-1350

59. Kiyokawa, T., Akashi-Takamura, S., Shibata, T., Matsumoto, F., Nishitani, C., Kuroki, Y., Seto, Y., and Miyake, K. (2008) *Int Immunol* **20**(11), 1407-1415

60. Takahashi, K., Shibata, T., Akashi-Takamura, S., Kiyokawa, T., Wakabayashi, Y., Tanimura, N., Kobayashi, T., Matsumoto, F., Fukui, R., Kouro, T., Nagai, Y., Takatsu, K., Saitoh, S., and Miyake, K. (2007) *J Exp Med* **204**(12), 2963-2976

61. Srivastava, P. K., DeLeo, A. B., and Old, L. J. (1986) *Proc Natl Acad Sci U S A* **83**(10), 3407-3411

62. Lee, A. S., Delegeane, A., and Scharff, D. (1981) *Proc Natl Acad Sci U S A* **78**(8), 4922-4925

63. Yang, Y., and Li, Z. (2005) *Mol Cells* **20**(2), 173-182

64. Kozutsumi, Y., Segal, M., Normington, K., Gething, M. J., and Sambrook, J. (1988) *Nature* **332**(6163), 462-464

65. Li, Z., and Srivastava, P. K. (1993) *Embo J* **12**(8), 3143-3151

66. Liu, B., and Li, Z. (2008) *Blood* **112**(4), 1223-1230

67. Liu, B., Yang, Y., Qiu, Z., Staron, M., Hong, F., Li, Y., Wu, S., Li, Y., Hao, B., Bona, R., Han, D., and Li, Z. (2010) *Nat Commun* **1**(6), doi:10 1038/ncomms1070

68. Melnick, J., Aviel, S., and Argon, Y. (1992) *J Biol Chem* **267**(30), 21303-21306

69. Melnick, J., Dul, J. L., and Argon, Y. (1994) *Nature* **370**(6488), 373-375

70. Muresan, Z., and Arvan, P. (1997) *J Biol Chem* **272**(42), 26095-26102

71. Stoilova D, D. J., de Crom R, van Haperen R, Li Z. (2000) *Cell Stress Chaperones* **5**(395)

72. Yang, Y., Liu, B., Dai, J., Srivastava, P. K., Zammit, D. J., Lefrancois, L., and Li, Z. (2007) *Immunity* **26**(2), 215-226

73. Randow, F., and Seed, B. (2001) *Nat Cell Biol* **3**(10), 891-896

74. Wakabayashi, Y., Kobayashi, M., Akashi-Takamura, S., Tanimura, N., Konno, K., Takahashi, K., Ishii, T., Mizutani, T., Iba, H., Kouro, T., Takaki, S., Takatsu, K., Oda, Y., Ishihama, Y., Saitoh, S., and Miyake, K. (2006) *J Immunol* **177**(3), 1772-1779

75. Sasai, M., Linehan, M. M., and Iwasaki, A. (2010) *Science* **329**(5998), 1530-1534

76. Bonifacino, J. S., and Traub, L. M. (2003) *Annu Rev Biochem* **72**, 395-447

77. Blasius, A. L., Arnold, C. N., Georgel, P., Rutschmann, S., Xia, Y., Lin, P., Ross, C., Li, X., Smart, N. G., and Beutler, B. (2010) *Proc Natl Acad Sci U S A* **107**(46), 19973-19978

78. Yamashita, T., Shimada, S., Guo, W., Sato, K., Kohmura, E., Hayakawa, T., Takagi, T., and Tohyama, M. (1997) *J Biol Chem* **272**(15), 10205-10211

79. Nishiya, T., and DeFranco, A. L. (2004) *J Biol Chem* **279**(18), 19008-19017

80. Leifer, C. A., Brooks, J. C., Hoelzer, K., Lopez, J., Kennedy, M. N., Mazzoni, A., and Segal, D. M. (2006) *J Biol Chem* **281**(46), 35585-35592

81. Rutz, M., Metzger, J., Gellert, T., Luppa, P., Lipford, G. B., Wagner, H., and Bauer, S. (2004) *Eur J Immunol* **34**(9), 2541-2550

82. Ewald, S. E., Engel, A., Lee, J., Wang, M., Bogyo, M., and Barton, G. M. (2011) *J Exp Med* **208**(4), 643-651

83. Brinkmann, M. M., Spooner, E., Hoebe, K., Beutler, B., Ploegh, H. L., and Kim, Y. M. (2007) *J Cell Biol* **177**(2), 265-275

84. Chockalingam, A., Rose, W. A., 2nd, Hasan, M., Ju, C. H., and Leifer, C. A. (2011) *J Immunol*

85. Chockalingam, A., Cameron, J. L., Brooks, J. C., and Leifer, C. A. (2011) *Eur J Immunol* **41**(8), 2176-2184

86. Ewald, S. E., Lee, B. L., Lau, L., Wickliffe, K. E., Shi, G. P., Chapman, H. A., and Barton, G. M. (2008) *Nature* **456**(7222), 658-662

87. Park, B., Brinkmann, M. M., Spooner, E., Lee, C. C., Kim, Y. M., and Ploegh, H. L. (2008) *Nat Immunol* **9**(12), 1407-1414

88. Sepulveda, F. E., Maschalidi, S., Colisson, R., Heslop, L., Ghirelli, C., Sakka, E., Lennon-Dumenil, A. M., Amigorena, S., Cabanie, L., and Manoury, B. (2009) *Immunity* **31**(5), 737-748

89. Viglianti, G. A., Lau, C. M., Hanley, T. M., Miko, B. A., Shlomchik, M. J., and Marshak-Rothstein, A. (2003) *Immunity* **19**(6), 837-847

90. Lau, C. M., Broughton, C., Tabor, A. S., Akira, S., Flavell, R. A., Mamula, M. J., Christensen, S. R., Shlomchik, M. J., Viglianti, G. A., Rifkin, I. R., and Marshak-Rothstein, A. (2005) *J Exp Med* **202**(9), 1171-1177

91. Christensen, S. R., Shupe, J., Nickerson, K., Kashgarian, M., Flavell, R. A., and Shlomchik, M. J. (2006) *Immunity* **25**(3), 417-428

92. Kono, D. H., Haraldsson, M. K., Lawson, B. R., Pollard, K. M., Koh, Y. T., Du, X., Arnold, C. N., Baccala, R., Silverman, G. J., Beutler, B. A., and Theofilopoulos, A. N. (2009) *Proc Natl Acad Sci U S A* **106**(29), 12061-12066

93. Taldone, T., and Chiosis, G. (2009) *Curr Top Med Chem* **9**(15), 1436-1446

94. He, H., Zatorska, D., Kim, J., Aguirre, J., Llauger, L., She, Y., Wu, N., Immormino, R. M., Gewirth, D. T., and Chiosis, G. (2006) *J Med Chem* **49**(1), 381-390

95. Llauger, L., He, H., Kim, J., Aguirre, J., Rosen, N., Peters, U., Davies, P., and Chiosis, G. (2005) *J Med Chem* **48**(8), 2892-2905

96. Bauer, S., Kirschning, C. J., Hacker, H., Redecke, V., Hausmann, S., Akira, S., Wagner, H., and Lipford, G. B. (2001) *Proc Natl Acad Sci U S A* **98**(16), 9237-9242

97. Pratt, W. B., and Toft, D. O. (2003) *Exp Biol Med (Maywood)* **228**(2), 111-133

98. Zhao, R., Davey, M., Hsu, Y. C., Kaplanek, P., Tong, A., Parsons, A. B., Krogan, N., Cagney, G., Mai, D., Greenblatt, J., Boone, C., Emili, A., and Houry, W. A. (2005) *Cell* **120**(5), 715-727

99. Picard, D. (2006) *Trends Endocrinol Metab* **17**(6), 229-235

100. De Nardo, D., Masendycz, P., Ho, S., Cross, M., Fleetwood, A. J., Reynolds, E. C., Hamilton, J. A., and Scholz, G. M. (2005) *J Biol Chem* **280**(11), 9813-9822

101. Moulick, K., Ahn, J. H., Zong, H., Rodina, A., Cerchietti, L., Gomes DaGama, E. M., Caldas-Lopes, E., Beebe, K., Perna, F., Hatzi, K., Vu, L. P., Zhao, X., Zatorska, D., Taldone, T., Smith-Jones, P., Alpaugh, M., Gross, S. S., Pillarsetty, N., Ku, T., Lewis, J. S., Larson, S. M., Levine, R., Erdjument-Bromage, H., Guzman, M. L., Nimer, S. D., Melnick, A., Neckers, L., and Chiosis, G. (2011) *Nat Chem Biol* **7**(11), 818-826

102. Obrig, T. G., Culp, W. J., McKeehan, W. L., and Hardesty, B. (1971) *J Biol Chem* **246**(1), 174-181

103. Schneider-Poetsch, T., Ju, J., Eyler, D. E., Dang, Y., Bhat, S., Merrick, W. C., Green, R., Shen, B., and Liu, J. O. (2010) *Nat Chem Biol* **6**(3), 209-217

104. Latz, E., Verma, A., Visintin, A., Gong, M., Sirois, C. M., Klein, D. C., Monks, B. G., McKnight, C. J., Lamphier, M. S., Duprex, W. P., Espevik, T., and Golenbock, D. T. (2007) *Nat Immunol* **8**(7), 772-779

105. Bandholtz, L., Guo, Y., Palmberg, C., Mattsson, K., Ohlsson, B., High, A., Shabanowitz, J., Hunt, D. F., Jornvall, H., Wigzell, H., Agerberth, B., and Gudmundsson, G. H. (2003) *Cell Mol Life Sci* **60**(2), 422-429

106. Moulick M, e. a. (2011) *Nature Chem Biol (In Press)*

107. Kasperkovitz, P. V., Cardenas, M. L., and Vyas, J. M. (2010) *J Immunol* **185**(12), 7614-7622

108. Janeway, C. A., Jr., and Medzhitov, R. (2002) *Annu Rev Immunol* **20**, 197-216

109. Takeshita, F., Leifer, C. A., Gursel, I., Ishii, K. J., Takeshita, S., Gursel, M., and Klinman, D. M. (2001) *J Immunol* **167**(7), 3555-3558

110. Roe, S. M., Prodromou, C., O'Brien, R., Ladbury, J. E., Piper, P. W., and Pearl, L. H. (1999) *J Med Chem* **42**(2), 260-266

111. Stebbins, C. E., Russo, A. A., Schneider, C., Rosen, N., Hartl, F. U., and Pavletich, N. P. (1997) *Cell* **89**(2), 239-250

112. Nishiya, Y., Shibata, K., Saito, S., Yano, K., Oneyama, C., Nakano, H., and Sharma, S. V. (2009) *Anal Biochem* **385**(2), 314-320

113. Taldone, T., Zatorska, D., Patel, P. D., Zong, H., Rodina, A., Ahn, J. H., Moulick, K., Guzman, M. L., and Chiosis, G. (2011) *Bioorg Med Chem* **19**(8), 2603-2614

114. Warger, T., Hilf, N., Rechtsteiner, G., Haselmayer, P., Carrick, D. M., Jonuleit, H., von Landenberg, P., Rammensee, H. G., Nicchitta, C. V., Radsak, M. P., and Schild, H. (2006) *J Biol Chem* **281**(32), 22545-22553

115. Peter, M. E., Kubarenko, A. V., Weber, A. N., and Dalpke, A. H. (2009) *J Immunol* **182**(12), 7690-7697

116. Hernandez, M. P., Chadli, A., and Toft, D. O. (2002) *J Biol Chem* **277**(14), 11873-11881

117. Cheung, J., and Smith, D. F. (2000) *Mol Endocrinol* **14**(7), 939-946

118. Pratt, W. B., Galigniana, M. D., Morishima, Y., and Murphy, P. J. (2004) *Essays Biochem* **40**, 41-58

119. Fan, M., Park, A., and Nephew, K. P. (2005) *Mol Endocrinol* **19**(12), 2901-2914

120. Segnitz, B., and Gehring, U. (1997) *J Biol Chem* **272**(30), 18694-18701

121. Fan, H., Kashi, R. S., and Middaugh, C. R. (2006) *Arch Biochem Biophys* **447**(1), 34-45

122. Whitesell, L., and Lindquist, S. L. (2005) *Nat Rev Cancer* **5**(10), 761-772

123. Usmani, S. Z., Bona, R. D., Chiosis, G., and Li, Z. (2010) *J Hematol Oncol* **3**, 40

124. Kamal, A., Thao, L., Sensintaffar, J., Zhang, L., Boehm, M. F., Fritz, L. C., and Burrows, F. J. (2003) *Nature* **425**(6956), 407-410

125. Okawa, Y., Hideshima, T., Steed, P., Vallet, S., Hall, S., Huang, K., Rice, J., Barabasz, A., Foley, B., Ikeda, H., Raje, N., Kiziltepe, T., Yasui, H., Enatsu, S., and Anderson, K. C. (2009) *Blood* **113**(4), 846-855

126. Breinig, M., Caldas-Lopes, E., Goeppert, B., Malz, M., Rieker, R., Bergmann, F., Schirmacher, P., Mayer, M., Chiosis, G., and Kern, M. A. (2009) *Hepatology* **50**(1), 102-112

127. Caldas-Lopes, E., Cerchietti, L., Ahn, J. H., Clement, C. C., Robles, A. I., Rodina, A., Moulick, K., Taldone, T., Gozman, A., Guo, Y., Wu, N., de Stanchina, E., White, J., Gross, S. S., Ma, Y., Varticovski, L., Melnick, A., and Chiosis, G. (2009) *Proc Natl Acad Sci U S A* **106**(20), 8368-8373

128. Cerchietti, L. C., Lopes, E. C., Yang, S. N., Hatzi, K., Bunting, K. L., Tsikitas, L. A., Mallik, A., Robles, A. I., Walling, J., Varticovski, L., Shaknovich, R., Bhalla, K. N., Chiosis, G., and Melnick, A. (2009) *Nat Med* **15**(12), 1369-1376

129. Rice, J. W., Veal, J. M., Fadden, R. P., Barabasz, A. F., Partridge, J. M., Barta, T. E., Dubois, L. G., Huang, K. H., Mabbett, S. R., Silinski, M. A., Steed, P. M., and Hall, S. E. (2008) *Arthritis Rheum* **58**(12), 3765-3775

130. Zhu, F. G., and Pisetsky, D. S. (2001) *Infect Immun* **69**(9), 5546-5552

131. Workman, P., Burrows, F., Neckers, L., and Rosen, N. (2007) *Ann N Y Acad Sci* **1113**, 202-216

132. Liu, B., Dai, J., Zheng, H., Stoilova, D., Sun, S., and Li, Z. (2003) *Proc Natl Acad Sci U S A* **100**(26), 15824-15829

133. Huang, Q. Q., Sobkoviak, R., Jockheck-Clark, A. R., Shi, B., Mandelin, A. M., 2nd, Tak, P. P., Haines, G. K., 3rd, Nicchitta, C. V., and Pope, R. M. (2009) *J Immunol* **182**(8), 4965-4973

134. Asagiri, M., Hirai, T., Kunigami, T., Kamano, S., Gober, H. J., Okamoto, K., Nishikawa, K., Latz, E., Golenbock, D. T., Aoki, K., Ohya, K., Imai, Y., Morishita, Y., Miyazono, K., Kato, S., Saftig, P., and Takayanagi, H. (2008) *Science* **319**(5863), 624-627

135. Shlomchik, M. J., Zharhary, D., Saunders, T., Camper, S. A., and Weigert, M. G. (1993) *Int Immunol* **5**(10), 1329-1341

136. Helin, H., Korpela, M., Mustonen, J., and Pasternack, A. (1986) *Ann Rheum Dis* **45**(6), 508-511

137. Howard, T. W., Iannini, M. J., Burge, J. J., and Davis, J. S. t. (1991) *J Rheumatol* **18**(6), 826-830

138. Pisitkun, P., Deane, J. A., Difilippantonio, M. J., Tarasenko, T., Satterthwaite, A. B., and Bolland, S. (2006) *Science* **312**(5780), 1669-1672

139. Stein, C. A., Subasinghe, C., Shinozuka, K., and Cohen, J. S. (1988) *Nucleic Acids Res* **16**(8), 3209-3221

140. Leifer, C. A., Verthelyi, D., and Klinman, D. M. (2003) *J Immunother* **26**(4), 313-319

141. Zhao, Q., Matson, S., Herrera, C. J., Fisher, E., Yu, H., and Krieg, A. M. (1993) *Antisense Res Dev* **3**(1), 53-66

142. Hartmann, G., Weiner, G. J., and Krieg, A. M. (1999) *Proc Natl Acad Sci U S A* **96**(16), 9305-9310

143. Samulowitz, U., Weber, M., Weeratna, R., Uhlmann, E., Noll, B., Krieg, A. M., and Vollmer, J. (2010) *Oligonucleotides* **20**(2), 93-101